

c1

**NACA**

RESEARCH MEMORANDUM

AN ANALYSIS OF AIR-TURBOROCKET ENGINE PERFORMANCE
INCLUDING EFFECTS OF COMPONENT CHANGES

By Roger W. Luidens and Richard J. Weber

Lewis Flight Propulsion Laboratory
Cleveland, Ohio

Declassified August 22, 1962

LIBRARY COPY
FEB 9 1963
LANGLEY RESEARCH CENTER
ARLINGTON, VIRGINIA

NATIONAL ADVISORY COMMITTEE
FOR AERONAUTICS

WASHINGTON

April 6, 1958

NACA RM E55H04a

NATIONAL ADVISORY COMMITTEE FOR AERONAUTICS

RESEARCH MEMORANDUMAN ANALYSIS OF AIR-TURBOROCKET ENGINE PERFORMANCE
INCLUDING EFFECTS OF COMPONENT CHANGES

By Roger W. Luidens and Richard J. Weber

SUMMARY

Analytical estimates of the thrust, efficiency, drag, and weight of the air-turborocket engine are presented. The effects of changes in the engine components on both design and off-design performance are emphasized.

Increasing the design compressor pressure ratio increases the maximum thrust at all speeds. When cruising at supersonic speeds, however, best efficiency is obtained with a windmilling compressor (for gasoline - nitric acid propellants). This favors a low-pressure-ratio engine, which was assumed to have the higher air flow and smaller pressure losses under windmilling operation. Use of a methyl acetylene - gasoline mixture improves the cruising specific impulse, particularly since it is then advantageous to drive the compressor at part-speed. Methyl acetylene is not always beneficial for full-power operation, however. Increasing the rocket chamber pressure improves the full-power specific impulse. Changes in chamber temperature have little effect on thrust or specific impulse (for gasoline - nitric acid propellants). Increasing afterburner temperature does not appreciably increase the take-off thrust; it does, however, provide large thrust gains at supersonic speeds.

Compared with a representative turbojet design, the air-turborocket generally has a higher thrust-to-weight ratio but poorer efficiency; cruising efficiency of the air-turborocket is especially poor at subsonic speeds. Maximum specific impulses in the order of 1500 pounds per pound per second (including drag) are obtainable at a flight Mach number of 2.3 with gasoline - nitric acid propellants.

INTRODUCTION

The increasing flight speeds and varied flight requirements of modern aircraft afford a widening field for the application of new types of power plants. One of these engines, which appears to be suitable for supersonic propulsion, is the air-turborocket. This engine is characterized by a mechanical air compressor driven by a turbine. The working

fluid of the turbine is supplied by a rocket, independently of the primary air cycle. The compressed air is ducted around the turbine and burned in an afterburner. Anticipated advantages of this engine are supersonic cruising efficiency equal to that of a ram jet coupled with high take-off thrust. The engine weighs somewhat more than a ram jet but appreciably less than a turbojet.

Some cycle analyses and performance estimates of the air-turbo-rocket engine have already appeared in the literature. A very generalized thermodynamic design-point study is made in reference 1. Also, the calculated performance of several specific engine designs is presented in references 2 and 3. The present report, prepared at the NACA Lewis laboratory, is intended to illustrate the effect of variations in component design on output of the air-turbo-rocket engine. The parameters studied include inlet pressure recovery, compressor pressure ratio, rocket combustion pressure and temperature, turbine type, turbine efficiency, afterburner-inlet Mach number and combustion temperature, and exhaust-nozzle force coefficient. Gasoline - nitric acid propellants are usually assumed, but the use of methyl acetylene is also considered. Both design and off-design performance of the cycle is emphasized. In addition, the report includes (1) the effect of engine drag, (2) the required variations in engine area ratios, and (3) estimates of the weight of typical configurations. Where possible, advanced component characteristics are assumed that have been shown by laboratory tests to be attainable. The calculations are particularly directed toward engines suitable for use in interceptor aircraft.

Thrust coefficients and specific impulses are given for full-power operation for flight Mach numbers from 0 to 4.0. Part-power performance is presented for a Mach number of 2.3, which is the cruising speed primarily studied, and at Mach numbers of 0.9, 2.8, 3.5, and 4.0. Finally, air-turbo-rocket and turbojet-engine performances are compared.

ANALYSIS

The symbols used in this report are defined in appendix A. Details of the methods of calculation are presented in appendix B.

Description of Engine

A schematic diagram of the air-turbo-rocket engine is shown in figure 1(a). Free-stream air enters the engine and is compressed by a diffuser (stations ∞ to 1). It is further compressed (1 to 2) by an axial-flow compressor, which is driven through a gearbox by a turbine. The air is bypassed around the turbine by a duct (2 to 3). The working fluid for the turbine is supplied by a rocket thrust chamber, or gas generator

(4). The turbine gases, which are fuel-rich, are mixed with the compressed air and burned between stations 5 and 6. Additional fuel is usually also injected between stations 2 and 3. (In fact, for cruising operation, this may be the only source of fuel.) The burned gases are discharged to the atmosphere through the exhaust nozzle (6 to 8). Figure 1(b) shows an alternate configuration that is discussed in a later section.

Choice of Performance Parameters

The influence of any propulsion system on airplane performance is a result of the engine thrust, fuel economy, weight, and size. These quantities are expressed in the present report in terms of the following:

$$(1) \text{ Net thrust coefficient, } C_{F,n} = \frac{F_n}{\frac{1}{2} \rho_\infty V_\infty^2 A}$$

$$(2) \text{ Specific impulse, } I_n = \frac{F_n}{\dot{w}_F + \dot{w}_O}$$

$$(3) \text{ Weight parameter, } W/A$$

The area A can be any engine reference area. In this analysis it is taken as the compressor blade-tip frontal area A_1 , which will also be used as a reference area for defining other engine areas.

For external engine installations, it is convenient to include nacelle drag in the performance calculations. The parameters then become

$$(1) \text{ Propulsive thrust coefficient, } C_{F,p} = C_{F,n} - C_D$$

$$(2) \text{ Specific impulse, } I_p = I_n \frac{C_{F,p}}{C_{F,n}}$$

where C_F and I describe the aerothermodynamic performance of the engine, and W/A_1 describes the weight.

Because the air-turborocket produces a finite amount of thrust at zero flight speed, the parameter C_F becomes infinite at this condition. In the present report, therefore, C_F is replaced by $C_F M_\infty^2$ for all subsonic flight speeds.

Component Assumptions

Inlet. - The diffuser configuration is normally considered to be a double wedge (two oblique shocks plus one normal shock) in a conical.

cowl. A single-wedge geometry is also considered (one oblique plus one normal shock). The over-all diffuser pressure recovery is taken as 0.95 times the recovery through the shock system. Figure 2 shows the assumed values of total-pressure ratio as a function of flight Mach number. The wedge angles are assumed to be varied throughout flight to maintain maximum pressure recovery at each speed.

The inlet is sized to pass the required air flow when operating at full compressor speed at the design Mach number (usually 2.3). At other conditions when the inlet might tend to operate subcritically, a variable bypass is assumed to spill the excess air. Reference 4 shows that use of a bypass incurs less drag than does subsonic spillage across a bow wave.

A sharp-lipped low-angle conical cowl is assumed for both inlet configurations. Blow-in doors (i.e., auxiliary inlets) are provided to maintain a pressure recovery of 0.95 at subsonic flight speeds. Reference 5 shows that severe inlet pressure losses may result without blow-in doors.

Compressor. - The compressor is designed for the take-off condition, at which point the equivalent air flow is 35 pounds per second per square foot and the adiabatic efficiency is 88 percent. Design pressure ratios of 1.45, 2.10, and 3.05 are considered. These are obtained by one-, two-, and three-stage compressors respectively, where all stages are transonic. Figure 3 shows a map of the assumed compressor characteristics. These characteristics are based on tests of a single-stage transonic compressor (ref. 6).

Figure 3 also shows the assumed steady-state compressor operating line. Except when the compressor is assumed to windmill, the rotor-tip speed is held constant at the design value of 1000 feet per second. The operating line for the air-turborocket may be chosen arbitrarily, because the turbine cycle is independent of the compressor. The full-power line shown passes through the peak-efficiency points and is approximately a constant distance from the surge line. For a few calculations it was necessary to choose part-power operating lines. These are arbitrarily drawn as straight lines connecting the full-power operating point at a flight Mach number of 2.3 and a point having a pressure ratio of 1.05 and the windmilling air flow given in the following table:

Number of stages	$\frac{w_a \sqrt{\theta_1}}{A_1 \delta_1}$	$\frac{P_2}{P_1}$
1	25.6	0.95
2	18.8	.90
3	13.6	.85

When cruising at supersonic flight speeds, the compressor may be allowed to windmill freely. Variable stators are assumed for use at this condition, to minimize pressure losses. The preceding values of equivalent air flow were estimated assuming a compressor designed for constant axial Mach number at rated conditions. The air flow at windmilling conditions was then determined by the minimum area at the compressor exit. The total-pressure loss was assumed to be 5 percent per stage. The variation of compressor speed with flight Mach number is shown in figure 4 for a one-stage compressor.

It is assumed that all the air flowing through the afterburner first passes through the compressor. During operation with a windmilling compressor (supersonic cruising) it would be possible, although with added complication, to bypass part or all of the air around the compressor. This procedure would allow higher air flow or alleviate the pressure losses through the compressor.

Gas generator. - The gas generator is essentially a small rocket motor. The number of rockets does not influence the cycle calculations except possibly through changes in turbine efficiency. In any given engine, the rocket combustion temperature and pressure are held constant at all flight conditions, while the nozzle throat area is varied to provide the correct mass flow. The rocket efficiency (ratio of actual enthalpy drop through rocket nozzle and turbine to theoretical enthalpy drop if the turbine efficiency were 100 percent) was taken as 0.92.

Propellants. - In the present analysis the fuel normally employed in the gas generator is gasoline with nitric acid as the oxidizer. More than the stoichiometric amount of gasoline is used in order to limit the turbine-inlet gas temperature to values that the turbine blades can withstand. In addition, some calculations were made using methyl acetylene, a monopropellant, as the rocket fuel. Gasoline is mixed with the methyl acetylene to maintain the turbine-inlet temperature limit. In both cases, more gasoline may be added directly to the compressed air to obtain the desired afterburner temperature.

The effect of combustion pressure and temperature on the fuel-oxidant ratio is shown in figure 5 for the gasoline - nitric acid system. For a constant combustion temperature, the ratio of gasoline to nitric acid must increase in order to increase the chamber pressure. A pressure of 32 atmospheres is selected for most of the calculations. For a constant pressure of 32 atmospheres, figure 5 shows that the ratio of gasoline to nitric acid must decrease in order to increase the turbine-inlet temperature. A ratio of 1.13 is required for the selected temperature of 2100° R.

The stoichiometric ratio for gasoline and nitric acid is 0.184; but, since the stoichiometric combustion temperature is higher than the

structure can withstand, excess fuel is added to limit the temperature to a lower value. The final fuel-oxidant ratio is much higher than stoichiometric and also is higher than the soot-formation ratio of 0.673. For ratios higher than this value, free carbon is present in the rocket exhaust. The presence of carbon is undesirable with respect to both turbine operation and combustion; however, no specific recognition of this problem is included in the study. The ratios of gasoline to methyl acetylene to obtain 2100° and 2500° R are 0.74 and 0.31, respectively (at a pressure of 32 atm).

Table I shows the physical characteristics of the various propellants. Methyl acetylene has a 5-percent-higher heating value than gasoline. However, methyl acetylene has a lower density and is more difficult to handle than either gasoline or nitric acid, as indicated by its lower boiling point and higher vapor pressure.

Turbine. - Two types of turbines were studied. One is the conventional bladed type driving the compressor through reduction gearing, as pictured in figure 1(a). In the other type, several rotating gas generators or rockets are mounted on radial arms that are directly connected to the compressor (fig. 1(b)). The driving torque is derived from the reaction of the gases emitted by the rockets. In both cases the rocket exhaust gases were normally limited to a temperature of 2100° R for structural reasons. Several other temperatures were also considered, however.

If a rotating-rocket turbine is used in the air-turbo-rocket, the problems of turbine design are entirely different from those encountered in turbojet engines. However, even the conventional bladed turbine has important differences from turbojet practice. Blade-tip diameter was taken as 50 percent of the compressor-tip diameter in order to allow space for the air to be ducted around the turbine. If the turbine were directly coupled to the compressor, the small turbine diameter would result in very low turbine blade-hub velocities. As many as 13 stages would then be required to extract the needed turbine work to drive the compressor (for the assumed ratio of turbine-to-compressor tip diameter). To avoid the difficulties of designing a turbine with many stages, the use of reduction gears between the turbine and compressor was assumed, thus allowing an increase in turbine speed. Designing the turbine for limiting blade loading and stress resulted in a two-stage design with a tip speed of 1400 feet per second; this required a reduction-gear ratio of 2.8. (For the turbine design chosen, blade stresses are a comparatively unimportant problem for moderate turbine-inlet temperatures because of short blade lengths.)

The high density of the rocket gases driving the turbine necessitates partial admission; that is, the gases enter the turbine at a limited number of points on the circumference. Otherwise, with normal

uniform admission, the required flow area is so small that the turbine blades would be prohibitively short. Boundary-layer effects at the hub and shroud would then cause very poor performance. The turbine adiabatic efficiency was taken as only 0.60 because of the partial admission (ref. 7). In addition, performance was calculated for efficiencies of 0.4 and 0.8.

No reduction gear is employed in the rotating-rocket configuration. The propulsive efficiency of the rocket can be increased by lengthening the rotating arm on which it is mounted. However, this raises the stress in the arms and may increase the nacelle frontal area. Therefore, the arm diameter was chosen equal to the compressor blade-tip diameter. The rocket exhaust is directed slightly downstream with respect to the plane of rotation. Straightening vanes are provided to remove the whirl and aid mixing. No pressure loss in the air due to mixing was assumed. Rocket-nozzle losses are assumed to be included in the rocket efficiency of 0.92.

Afterburner. - Pressure losses are suffered because of the ducting of the air from the compressor exit and because of the flameholders. This drop in total pressure is assumed to be defined by the following equation:

$$P_2 - P_5 = 3q_3$$

A further momentum-pressure loss due to the heat addition was included. The total-pressure ratio across a constant-diameter duct due to heat addition is illustrated in figure 6 for several afterburner-inlet Mach numbers.

A cylindrical liner was provided in the afterburner for cooling purposes. Approximately 10 percent of the compressor-discharge air flows through the annulus thus formed in order to keep the afterburner walls at a fairly low temperature. Combustion occurs only in the remaining air within the liner. The maximum afterburner temperature was normally limited to 3500° R, but the effect of choosing other limiting temperatures was investigated. It should be noted that all temperatures discussed in this report are bulk or average temperatures. For example, at take-off, if the nominal afterburner temperature is 3500° R and 10 percent of the air is diverted for cooling, the remaining 90 percent is raised to a temperature of about 3800° R. This temperature approaches the maximum available with a stoichiometric mixture at take-off.

The afterburner combustion efficiency was normally taken as 90 percent. (Combustion efficiency is defined as the ideal fuel-air ratio needed for a given temperature divided by the actual fuel-air ratio.) In some cases, so much excess gasoline is contained in the rocket exhaust gases that the selected afterburner temperature limit would be exceeded

even if no further gasoline were added in the afterburner. In this situation, it was assumed that additional air is bypassed around the combustion zone through the cooling annulus. The fuel-air mixture in the central core then becomes richer than stoichiometric, and some of the gasoline is not burned. Effectively, this results in a decrease of the combustion efficiency sufficiently below 90 percent to obtain the desired average afterburner temperature.

The afterburner length was varied as a function of the design compressor pressure ratio, as described in appendix B. The afterburner-nacelle frontal area was made 15 percent larger than the maximum nozzle-exit area to allow for a converging nozzle lip. For an engine with a limiting gas temperature of 3500°R , this resulted in an afterburner-inlet Mach number at take-off of 0.14. The effect of variations in this value was also calculated.

Exhaust nozzle. - A supersonic nozzle with a variable-throat area is required for satisfactory operation of the air-turborocket engine. In the present study the nozzle was assumed to be of the fixed-plug type, with an adjustable-iris cowl. The nozzle force coefficient C_N was taken as 0.96. The plug size was selected to expand the gases to twice ambient pressure under cruising conditions; this method of selecting plug size is found experimentally to yield values of C_N near 0.96, at least for flight Mach numbers near 2.3 (ref. 8). Reference 8 shows also that the plug nozzle maintains its high value of C_N at lower flight speeds. The annular throat area required to pass the mass flow was determined for each operating condition, the maximum requirement usually occurring at take-off. The sum of the plug area and the maximum annular throat area was increased by 15 percent to obtain the afterburner frontal area, as described in the preceding paragraph.

At low supersonic flight speeds this configuration would have a high boattail drag. To reduce the drag, a movable conical fairing was assumed to float on the exhaust jet with no adverse effect on nozzle performance. The length of the fairing is 0.7 of the maximum engine diameter.

Engine Weight

Fairly detailed scale drawings of representative air-turborocket engines were made, from which estimates of engine weight were derived. The design of the rotating components, such as the reduction gears, shaft, and turbine, was based on the maximum stresses encountered during flight. Other components such as the nacelle were specified through selection of a realistic minimum thickness. The parts of the engine subjected to high temperatures were constructed of steel, while titanium was used wherever else possible.

Engine weight was assumed to change with the number of compressor stages and the type of turbine. Further assumptions made for the weight calculations are given in appendix B.

Flight Path

Performance of the air-turbo-rocket engine is a function of altitude in the tropopause largely because of the variations in ambient temperature and the consequent effect on the cycle temperature ratio. In contrast to engines such as the turbojet and ram jet, the thrust coefficient and specific impulse of the air-turbo-rocket are also functions of altitude even in the isothermal region of the atmosphere. This is a result of the constant rocket chamber pressure, which causes the pressure ratio across the turbine to vary when the ambient pressure is changed.

A range of Mach numbers at several different altitudes was considered for two basic engines for which component variations were studied. However, for the majority of the data that illustrate the effect of these variations, it was believed adequate to make comparisons for a specific flight path. The selected schedule of altitude with flight Mach number is shown in figure 7. This schedule is representative of the path that might be flown by an interceptor airplane during climb and acceleration. Choice of a somewhat different flight path would not significantly affect the comparisons between similar engines. Also pictured in figure 7 is the flight path that would result in a constant pressure ratio across the turbine (equal to the design-point value). At all flight speeds, the selected schedule results in turbine pressure ratios no greater than the design value.

Procedure

An engine was designed for a cruise Mach number of 2.3 using the values of the various design parameters listed in table II. The effect on both design and off-design performance of changing one parameter at a time was then calculated. In general, the resulting data are presented in two forms:

- (1) Thrust coefficient C_F and specific impulse I as a function of flight Mach number, for full-power operation
- (2) C_F as a function of I for various power settings, at the design cruising Mach number

These data are shown with and without engine drag included. The no-drag case is based only on the air that passes through the cycle. The case with drag accounts for nacelle drag and also for any additive or bypass drag that may result from incorrect matching of the inlet and

the compressor at the given operating condition. The simplified method used for calculation of the nacelle pressure drag resulted in a discontinuity in drag at a Mach number of 1.0. In plotting the data, an arbitrary line is drawn connecting the performance curves at subsonic and supersonic flight speeds.

RESULTS AND DISCUSSION

The discussion, although directed at the engine performance with drag, is generally also applicable to the engine performance without drag. Where significant differences in performance occur, these differences are discussed.

Performance of Reference Engines

Table III(a) presents the full-power performance of an air-turborocket engine whose design is based on the reference values listed in table II. Net and propulsive thrust coefficients and specific impulses and area variations are given for a range of flight Mach numbers and altitudes with different afterburner temperatures. Table III(b) presents data for a similar engine, except that it has a two-stage compressor. The part-power performance of both engines at the design Mach number of 2.3 is given in table III(c).

Figure 8 shows the relative magnitude of the various types of drag for the reference engine over a range of flight speeds. At subsonic speeds, nacelle friction causes the only drag. At low supersonic speeds, pressure drags are about twice as large as friction drag. Drag due to air spillage, both across the oblique shock and through the bypass door, is quite small compared with the forces acting on the nacelle. The boat-tail drag becomes large at low supersonic speeds even with the floating fairing, because the exhaust jet is small at this flight condition. Both the angle and the projected area of the boat-tail fairing increase with decreasing size of the jet. Both of these factors cause greater boat-tail drag.

The full-power performance of the one-stage reference engine from table III(a) is illustrated in figure 9(a) for several different flight Mach numbers and altitudes. As explained in the ANALYSIS, the thrust parameter $C_F M_\infty^2$ is used for subsonic speeds, and C_F for supersonic speeds; the two are equal, of course, at a Mach number of 1.0. The values of thrust coefficient and specific impulse shown are obtained by operating the compressor at rated mechanical speed and by afterburning to a temperature of 3500° R. Both the thrust coefficient and the specific impulse improve as altitude is increased from sea level to 35,332 feet. This improvement is a result of the greater cycle temperature ratio and turbine pressure ratio as the ambient temperature and pressure decrease. Over 35,332 feet, the ambient temperature remains constant,

but the turbine pressure ratio continues to increase as the altitude is increased. The consequent reduction in the rocket propellant flow required to drive the turbine results in further gains in specific impulse as altitude is increased in the stratosphere. The reduced rocket mass flow, however, causes a slight reduction in the thrust coefficient.

Also indicated in figure 9(a) is the performance corresponding to a flight path that maintains a constant pressure ratio across the turbine equal to the sea-level design value. It is doubtful that the illustrated improvements in specific impulse for still higher altitudes could be realized in practice, because lowered adiabatic efficiency and choking of the flow are likely for turbine pressure ratios higher than the design value; whereas, for calculation purposes, the turbine efficiency was assumed to be constant for all pressure ratios.

Figure 9(b) presents the performance of the reference engine operating at full power over the particular flight path shown in figure 7. In succeeding parts of this report, components of this engine are varied one at a time in order to indicate the sensitivity of the air-turbo-rocket engine to changes in component design and operation. All comparisons are made for simplicity only for this one flight path. Other flight paths would not be expected to alter the relative positions of the various engine designs.

The performance of the engine over a range of reduced thrusts is shown in figure 9(c) for the design flight Mach number of 2.3. Starting at low thrust levels, the thrust coefficient is increased by raising the afterburner temperature as indicated, while the compressor is allowed to windmill. After reaching the limiting afterburner temperature of 3500°R , the thrust coefficient may be further increased by speeding up the compressor, which raises the air flow through the engine (fig. 3). Because fuel-rich gases from the rockets are then expanded through the turbine and discharged into the afterburner, the fuel added directly in the afterburner must be reduced to prevent exceeding the temperature limit. The maximum thrust coefficient is obtained when the compressor reaches rated speed.

It is significant that, when engine drag is neglected, the maximum values of specific impulse occur at low afterburner temperatures and hence at low values of thrust coefficient. Since the drag at these conditions is a relatively large fraction of the internal engine thrust, the specific impulse is appreciably lowered when drag is taken into account. The penalties due to drag are relatively less severe at high thrust levels, so that, when the drag is included, the peak specific impulse is not only lowered but also occurs at a higher afterburner temperature.

Throughout this report full- or part-power operation should be understood as follows:

(1) Full-power: operation at rated mechanical compressor speed and maximum afterburner temperature up to Mach 2.3; windmilling compressor and maximum afterburner temperature above Mach 2.3.

(2) Part-power: operation at reduced compressor speed, although there may be substantial amounts of afterburning. Normal cruising operation is with no rocket propellant flow so that the compressor windmills freely. The performance is then the same as for a ram jet except for the additional pressure loss through the compressor. Thrust coefficient and specific impulse in this case are independent of altitude variations in the stratosphere, since there is no rocket flow.

Effect of Design Parameters

Inlet. - Although a variable two-wedge inlet was assumed for most of the calculations, use of a variable single-wedge inlet would offer desirable reductions in operating complexity. Figure 10(a) compares the full-power performance of engine having one- and two-wedge inlets. At subsonic and low supersonic speeds, there is little difference in the engine thrust or specific impulse with the two inlet types. At the design Mach number of 2.3, the diffuser pressure recovery with the double wedge is 11.7 percent higher than with the single wedge. The consequent improvement in specific impulse is about 5 percent; however, the increased air flow due to the higher pressure levels raises the thrust coefficient by about 17 percent.

Figure 10(b) compares the engine performance at part-power operation. The compressor is windmilling with no gas flow through the turbine. Various amounts of gasoline are added to the air to vary the afterburner temperature. (Still higher thrusts are obtainable by speeding up the compressor, as shown in fig. 9(b).) The difference in maximum specific impulse with the two inlet types is 6 percent.

The illustrated differences in performance can be achieved only if the higher-recovery diffuser has the same low-drag cowl as the single-wedge inlet. This may not be possible in practice; the illustrated differences must be then evaluated in the light of any associated drag changes that may occur.

To reduce spillage, the inlet could have alternatively been designed for the cruising condition at Mach 2.3. This would improve the engine efficiency but would also reduce the maximum thrust.

The inlet-geometry variations required during flight are discussed in a later section.

Compressor. - The reference engine has a compressor pressure ratio at take-off of 1.45, which is achieved with a one-stage transonic compressor. Figure 11(a) shows how the full-power thrust coefficient and specific impulse at various flight speeds are affected by adding more stages of compression. Two and three stages correspond to take-off pressure ratios of 2.05 and 3.10, respectively. At all flight Mach numbers up to 2.3, adding more stages - at least up to three - increases the thrust at full power.

Increasing the number of stages affects the specific impulse through two opposing factors. Raising the compressor pressure ratio improves the thermal efficiency of the air cycle (at least for the comparatively low pressure ratios of interest here); this results in greater engine thrust. Higher pressure ratios also require more turbine work and consequently greater turbine mass flow. Both the oxidant and the gasoline flows increase. The oxidant and fuel burned in the rocket are of no aid to the air cycle. Also present in the rocket gases is unburned gasoline, which cannot be utilized in the air cycle after the limiting afterburner temperature is reached. (In the case shown, the limiting temperature is 3500° R.) At low flight speeds (and thus little ram pressure rise) the advantages of increased cycle pressure ratio outweigh the disadvantages of high propellant flow in going from one to two compressor stages. In all other cases, increasing the pressure ratio reduces the specific impulse. For those cases where the unburned gasoline in the rocket gases exceeds that required to attain the afterburner-temperature limit, the excess fuel is assumed to be discarded without burning as described in the ANALYSIS.

Figure 11(b) compares the engines with different numbers of compressor stages when operating at a Mach number of 2.3 with various power settings and with the compressor windmilling. Except at undesirably low levels of thrust where fixed losses (such as internal pressure losses or external drag) are relatively high, maximum specific impulse at any value of thrust coefficient is obtained with the fewest number of compressor stages (for windmilling compressor operation). This is true because the single-stage compressor has the highest windmilling air flow and lowest pressure drop. For the high thrust coefficients the preceding discussion at full power is applicable.

Figure 12(a) presents the performance of the one-stage-compressor engine over a range of flight Mach numbers when operating (1) at full power and (2) with windmilling compressor and 3500° R afterburner temperature. Although the thrust with the windmilling compressor is lower for all flight speeds, this operation provides the higher specific impulse for Mach numbers above 1.6. The poorer specific impulse at lower

speeds is a result of the low cycle pressure ratio. The windmilling compressor, of course, has a lower cycle pressure ratio at flight Mach numbers above 1.6, also, but this is more than offset by elimination of the high fuel and oxidant consumption required to drive the compressor at rated speed.

The effect of compressor operating pressure ratio for cruising flight is shown in figure 12(b), where specific impulse is plotted as a function of thrust coefficient at a flight Mach number of 2.3. Three lines of constant compressor pressure ratio are given (1.15, 1.05, and 0.95), which are obtained by driving the compressor at various fractions of rated speed (see fig. 3). Thrust is varied along each line by varying the afterburner temperature. For any value of thrust coefficient, highest specific impulse is obtained with the pressure ratio of 0.95, which corresponds to the case of windmilling operation and thus requires no oxidant in the gas generator.

If the windmilling compressor pressure ratio were less than 0.95, however, the cycle thermal efficiency and specific impulse would suffer accordingly. In this case it might then be advantageous to eliminate the pressure drop by driving the compressor at some higher speed. An alternative solution would be to bypass part or all of the air around the compressor. (Note that fig. 1, which illustrates a typical Mach 2.3 design engine, indicates that room is available for a bypass without enlarging the nacelle.)

An additional advantage of bypassing air around the compressor is to better match the inlet and engine air flows. In the present analysis the inlet was sized for flight at a Mach number of 2.3 with the compressor operating at rated mechanical speed. Consequently, when the compressor is allowed to windmill, its air-flow capacity is reduced and the excess air captured by the inlet must then be discharged through the inlet bypass. Figure 12(b) shows how the part-power thrust and specific impulse may be improved by ducting this excess air around the compressor and burning it in the afterburner. (The preceding discussion is based on the use of bipropellants in the rocket chamber. Somewhat different results are obtained when a monopropellant is used, as is discussed later.)

There are several other compressor parameters that may affect engine performance. The adiabatic efficiency assumed is fairly high (88 percent). Little improvement can be made by increasing this value, particularly when compared with the effect of the turbine efficiency. (The compressor and turbine efficiencies are multiplied together as shown in eq. (B9).) Compressor air flow is also not of major importance in the air-turbo-rocket engines studied. For all the cases considered, the external geometry, and hence the drag, of the engine was not affected by moderate changes in compressor air flow. Changing compressor size may

affect the compressor weight somewhat, but this is not a major factor for the air-turbo-rocket. Compressor design is eased by the assumption of reduction gears, since no compromises are needed to ensure good turbine operation.

The foregoing discussion of the compressor design and operation may be summarized as follows:

(1) Increasing the design compressor pressure ratio raises the maximum thrust of the engine at all flight speeds. Maximum thrust is achieved by running the compressor at rated speed.

(2) For cruise operation at the design Mach number, highest specific impulse is achieved by shutting off the gas generator and allowing the compressor to windmill freely (when propellants are gasoline and nitric acid).

(3) The single-stage compressor affords best windmilling performance, since adding more stages decreases the windmilling air flow and increases the pressure drop. There is thus a conflict in the compressor requirements between best economy and highest thrust.

Gas generator. - Two more or less independent thermodynamic cycles are present in the air-turbo-rocket engine, the air cycle and the rocket cycle. This section discusses how changes in the rocket cycle affect the over-all performance of the engine. The effect of rocket chamber pressure on full-power performance over a range of flight speeds is shown in figure 13(a). Values of chamber pressure of 16 and 64 atmospheres are presented; a value of 32 atmospheres was used in most other calculations. As the pressure is varied, the fuel-oxidant ratio is also changed to hold the chamber temperature constant (2100° R), as explained in the ANALYSIS. Raising the pressure from 16 to 64 atmospheres increases the rocket expansion ratio and so improves the rocket cycle efficiency. For the same amount of turbine work, therefore, less rocket exhaust gas is required. At the same time, the percentage of oxidant in the gas is decreased (fig. 5). This reduction is very desirable, since the oxidant contributes nothing to the heat release in the afterburner. The net result of this fourfold increase in chamber pressure is a 20-percent improvement in specific impulse over the range of flight speeds. Little change occurs in the thrust coefficient, however. Although high chamber pressures are thus beneficial to the thermodynamic cycle, they intensify the problems of structural design, efficient expansion, and formation of soot.

Increasing the combustion temperature at constant pressure is another means of improving the rocket cycle efficiency that permits a reduction in the flow of fuel and oxidant to the rocket. However, the percentage of oxidant increases (fig. 5). The net result is that the absolute amount of gasoline flowing into the rocket is reduced, but the

amount of oxidant is increased. This explains why figure 13(b) shows that raising the rocket chamber temperature from 2006° to 2398° R results in a decrease in specific impulse. (A value of 2100° was used in most of the other calculations.) The reduction in rocket gasoline flow is unimportant, since more fuel must be added in the afterburner to obtain a temperature of 3500° R. On the other hand, more oxidant is being used to supply the same amount of turbine power. Except for the slight effect of the different mass addition, the engine thrust is unaffected.

Low chamber temperatures are, therefore, beneficial to the thermodynamic cycle when a fuel-rich bipropellant is used in the rocket. Low temperatures are also desirable with regard to stress but have an adverse effect on the formation of soot (because of the increased fuel-oxidant ratio). For multistage compressors, low chamber temperatures also aggravate the previously mentioned problem of excess fuel in the afterburner.

Propellant. - The preceding section indicates that the need for an oxidant in the gas generator may be harmful to the over-all engine efficiency. Performance calculations were also made assuming that methyl acetylene, a monopropellant, is used in the gas generator. Gasoline is mixed with the methyl acetylene to maintain the specified turbine-inlet temperature. The decomposition products of methyl acetylene are mostly hydrogen and carbon. These, together with the cooling gasoline, are burned after passing through the turbine. As before, more gasoline may be added in the afterburner to obtain the desired exit temperature.

Figure 14(a) compares the full-power performance of one-stage-compressor engines using different propellants in the gas generator. Excess gasoline is added to both the nitric acid and the methyl acetylene to maintain the turbine-inlet temperature at 2100° R. As shown in the figure, there is little difference in thrust between the two propellants. However, by eliminating the oxidant, which is superfluous to the air cycle, the monopropellant is able to provide about a 30-percent improvement in specific impulse.

So much cooling gasoline is required to limit the combustion temperature to 2100° R that the available enthalpy drop per pound of propellants for methyl acetylene plus gasoline is less than that available with the gasoline - nitric acid system (see fig. 29, which is discussed in appendix B). More fuel from the rocket is therefore required to drive the turbine for the methyl-acetylene case; furthermore, all the turbine exhaust gases in this case are available for combustion in the afterburner. The result of using methyl acetylene plus gasoline in the rocket to drive the turbine at full speed is that an excess of fuel is passed into the afterburner. In order to restrict the afterburner temperature to 3500° R, this excess must be discarded without being burned, even without directly injecting any further gasoline. The excess is slight

for an engine with a single-stage compressor and does not outweigh the advantages of eliminating the oxidant from the cycle.

When a two-stage compressor is employed, approximately twice as much gas flow is needed to drive the turbine as for a single-stage compressor. Use of the methyl acetylene - gasoline mixture then results in a sizable fuel surplus in the afterburner, all of which must be discarded without being burned. (This is true to a much lesser degree with the gasoline - nitric acid system.) The result, as shown in figure 14(b), is that changing from gasoline - nitric acid to methyl acetylene - gasoline lowers the full-power specific impulse by 15 percent for the engine with a two-stage compressor.

This situation arises because of the large amount of gasoline that must be mixed with the methyl acetylene in order to restrict the rocket combustion temperature to 2100° R. If the temperature limit set by the rocket or the turbine could be raised to 2500° R, relatively less cooling gasoline would be required, and the available turbine work per pound of methyl acetylene and gasoline would rise. As shown in figure 14(b), such a temperature increase raises the full-power specific impulse with methyl acetylene above that for gasoline plus nitric acid. Still higher temperatures would be expected to improve the specific impulse even more. In contrast, it was previously explained that raising the turbine-inlet temperature was not profitable with the gasoline - nitric acid system because of the increased consumption of oxidant.

The preceding discussion has been concerned with full-power operation over a range of flight speeds. Figure 15 compares the two propellant systems under cruising conditions at a Mach number of 2.3 (with a one-stage compressor). With a windmilling compressor, use of methyl acetylene in the afterburner instead of gasoline gives specific impulses that are 5 percent higher because of its higher heating value (table I). The figure also shows that further gains may be realized by injecting a methyl acetylene - gasoline mixture into the gas generator and expanding through the turbine. The specific impulse improves because the higher pressure ratio affects the cycle thermal efficiency favorably (and also because the increased air flow through the engine reduces the ratio of drag to thrust). This gain is possible for the monopropellant because no oxidant is needed. It was previously shown that this method is not helpful for the gasoline - nitric acid system because of the oxidant that is consumed.

Calculations indicate that the illustrated part-power performance with methyl acetylene in the rocket is insensitive to changes in flight altitude and chamber temperature and pressure.

The major points of the preceding discussion of the rocket and its propellants may be summarized as follows:

(1) Increasing the chamber pressure improves the engine specific impulse, with little change in the thrust coefficient for full-power operation with gasoline - nitric acid.

(2) Increasing the chamber temperature is detrimental to the specific impulse for full-power operation with gasoline - nitric acid.

(3) Use of methyl acetylene plus gasoline instead of gasoline - nitric acid substantially improves the full-power specific impulse for the engine with a one-stage compressor. Methyl acetylene plus gasoline is inferior, however, for full-power operation of the engine with a two-stage compressor if the chamber and afterburner temperatures are limited to 2100° and 3500° R, respectively. If the chamber temperature is raised to 2500° R with methyl acetylene plus gasoline, the full-power specific impulse is higher than that for gasoline - nitric acid at a chamber temperature of 2100° R.

(4) Use of methyl acetylene in the afterburner when cruising with a windmilling compressor provides specific impulses 5 percent higher than those obtainable with gasoline. Further gains are possible when methyl acetylene plus gasoline is injected into the rocket and expanded through the turbine before burning.

Although methyl acetylene shows significant gains in specific impulse over gasoline, there are features that detract from its apparent advantages. These include its lower density, lower boiling point and higher vapor pressure, high cost, and low availability. Balancing of these considerations involves more than just an engine analysis and is not within the scope of this report.

Turbine. - The effect of increasing rocket chamber pressure on engine performance has already been discussed. The turbine is, of course, affected by the pressure ratio across it, which depends on the pressure at the turbine exhaust as well as the rocket chamber pressure. Figure 16 shows the pressure ratio across the turbine for the flight plan assumed (fig. 7). The highest turbine pressure ratio occurs at take-off. A turbine designed for this pressure ratio would be satisfactory for the entire flight.

Another important turbine parameter is its adiabatic efficiency. For a given turbine expansion ratio, the ratio of rocket-gas flow to engine-air flow varies inversely as the adiabatic efficiency (see eq. (B9)). The effect of changing turbine efficiency on the full-power performance of the engine is shown in figure 17. Thrust coefficient and specific impulse are given over a range of flight speeds for adiabatic

efficiencies of 0.4 and 0.8. This doubling of the efficiency permits a 50-percent reduction in the consumption of both rocket gasoline and oxidant. The total engine liquid consumption is not halved, however, because with the higher turbine efficiency more gasoline must be added in the afterburner (to maintain the 3500° R temperature) to make up for the lessened excess gasoline carried through the turbine. The 50-percent decrease in oxidant consumption results in a 23-percent increase in specific impulse. The thrust coefficient decreases slightly because of the lower rate of mass addition to the cycle.

The preceding figures relate to the use of a conventional bladed turbine. The performance of this engine is compared with that afforded by an engine with a rotating-rocket turbine in figure 18. An equivalent adiabatic efficiency may be defined for this device to enable comparison with the conventional type (see eq. (B12)). This factor varies with the rocket exhaust velocity, compressor rotative speed, and length of the rocket mounting arms. For the conditions of the present analysis, this value is of the order of 0.33. For engines having a single-stage compressor, if the assumed efficiency of 0.60 is obtainable with the conventional turbine, use of the rotating-rocket turbine causes a 17-percent reduction in specific impulse (fig. 18(a)). If the conventional turbine efficiency is only 0.4, then the rotating-rocket turbine is only 5 percent poorer in specific impulse.

The rotating-rocket turbine is even more inferior in engines with a two-stage compressor. The specific impulse is 37 percent lower than that with a bladed turbine having an adiabatic efficiency of 0.60 (fig. 18(b)). As before, the higher rocket oxidant consumption needed with the rotating-rocket turbine is a total loss. The rocket gasoline consumption is also higher in the same proportion, of course. For the single-stage compressor this higher rocket fuel flow is not too serious, because only a small part of it is burned with the oxidant and the remainder is available for combustion in the afterburner. Less additional fuel need then be added to the afterburner to maintain the temperature at 3500° R. This is not the case, however, when the rotating-rocket turbine drives a two-stage compressor. The low turbine efficiency results in the carrying over into the afterburner of an excessive amount of rocket fuel, which must then be discharged without burning. The specific impulse suffers accordingly.

Thermodynamically, the rotating-rocket turbine is thus inferior to the conventional bladed turbine. On the other hand, it possesses advantages of simplicity and low weight. (Engine weight is discussed in a later section.)

Afterburner. - The afterburner-inlet Mach number has two opposing effects on engine performance. Low inlet Mach numbers minimize the internal pressure losses of the engine that are due to wall friction, flameholder turbulence, and the effect of heat addition. These losses are

6679

CE-3 back

particularly important at take-off, where the cycle pressure ratio is low and the temperature ratio is large (about 6, for a peak temperature of 3500°R ; fig. 6 indicates the importance of the latter effect). On the other hand, high inlet Mach numbers reduce the diameter of the afterburner. Because this is the largest component of the engine, the reduction in frontal area results in substantially lower nacelle drag, an important factor during transonic and supersonic flight. The afterburner-inlet Mach number must be chosen to balance properly the internal pressure losses and the external drag.

Still another consideration is the necessity of achieving satisfactory performance from the exhaust nozzle. The ANALYSIS describes how the afterburner diameter is nominally related to the nozzle throat area. The method results in a nominal inlet Mach number at take-off of 0.144. Figure 19(a) shows how the full-power take-off performance is influenced by changes in this value. Reducing inlet Mach number improves both the thrust and specific impulse at take-off. As shown in figure 19(b), this is also true for supersonic, part-power operation if engine drag is neglected. When drag is included, however, the low inlet Mach number engine is penalized, particularly at low thrust levels. The figure indicates that, at a flight Mach number of 2.3, an afterburner-inlet Mach number higher than 0.144 may be of some advantage. An alternative way to accomplish this during windmilling operation (other than by decreasing afterburner diameter) is to bypass some additional air around the compressor. A 16-percent increase in air flow with the given inlet is possible; this procedure raises the thrust and permits the inlet to operate nearer its design air flow (as discussed in connection with fig. 12(b)).

The foregoing discussion refers to the afterburner-inlet Mach number at take-off as the design value. This value does not remain constant throughout flight; it varies with flight speed, engine design, and mode of compressor operation, as illustrated in figure 19(c). The variations during flight are not great in any of the cases.

The other major afterburner design parameter is the exit temperature. High afterburner temperatures tend to increase the available enthalpy drop through the nozzle (see fig. 28, which is discussed in appendix B). This results in higher thrust, which is particularly desirable at take-off, for acceleration, and for high maneuverability. However, high temperature ratios also increase the pressure loss due to combustion (fig. 6). The resulting decrease in the nozzle pressure ratio tends to reduce the available enthalpy drop and hence the thrust. This situation is especially serious at take-off (similarly to the previously described effect of raising the afterburner-inlet Mach number). The net effect of these factors is that the thrust at take-off increases very little for an increase of the afterburner temperature from 3000° to 4000°R , as shown in figure 20(a) for the engine with a one-stage compressor. As indicated, the required fuel flow increases faster than the thrust, which

decreases the specific impulse. For the engine with a two-stage compressor, there is similarly only a small gain in thrust at take-off when the afterburner temperature is raised from 3500° to 4000° R (fig. 20(b)).

At higher flight Mach numbers, appreciable thrust gains may be achieved by raising the afterburner temperature. However, the higher jet velocity decreases the engine propulsive efficiency, so that the specific impulse is reduced, if nacelle drag is neglected. Figure 20(a) shows the effect on full-power performance of raising the afterburner temperature from 3000° to 4000° R when engine drag is accounted for. It is possible in some instances to obtain an increase in specific impulse as afterburner temperature is raised, because the drag at the high temperatures is a smaller proportion of the net engine thrust. For the two-stage compressor, however, there is practically no penalty in specific impulse, even in the no-drag case. The reason is related to the higher requirements for rocket gas flow in order that the turbine supply the increased power for compression. The excess gasoline contained in the fuel-rich rocket gases creates a surplus of gasoline in the afterburner, even when the secondary fuel flow is entirely turned off. The surplus gasoline cannot be burned without exceeding the afterburner temperature limit. To prevent this, the present analysis assumed that the unneeded fuel is discharged without burning, effectively resulting in a decrease in afterburner combustion efficiency, as previously discussed. (The beneficial effect of raising the afterburner temperature with the methylacetylene fuel is indicated in fig. 15.)

The effective combustion efficiency for full-power operation over a range of flight speeds is shown in figure 20(c). With a one-stage compressor, a 3500° R limit requires no reduction in effective efficiency. At all speeds some additional fuel must be added in the afterburner with the nominal combustion efficiency of 90 percent. With the two-stage compressor, however, the rocket gas flow is so high that no additional fuel is required. And, in fact, it is necessary to lower the combustion efficiency to as low as 77 percent to prevent overtemperature. As shown, the problem is much worse if three stages are used.

The previous discussion points out that this same problem exists in most of the variations of the two- and three-stage engines considered. It is aggravated by factors that tend to increase the amount of rocket gases needed to drive the turbine. In addition to increases in the compressor pressure ratio, these include decreases in compressor, gear, or turbine efficiency (eq. (B9)). The difficulty does not exist at cruising conditions, since the gas generator is ordinarily not in operation then.

High allowable afterburner temperatures are ineffective in producing high thrusts at take-off, and they have an adverse effect on specific impulse. At higher Mach numbers, high temperatures yield high

thrusts, in some cases with no specific-impulse penalty; but the structural cooling problems may be more critical at the higher Mach numbers because of the increased temperature of the compressor-discharge air used for cooling.

Exhaust nozzle. - Losses due to the exhaust nozzle are from two different sources, internal pressure losses caused by friction or shocks and external losses caused by failure to expand the gases completely. Experimental data show that the plug-type nozzle assumed in the present report is capable of reducing the sum of these losses to about 4 percent of the ideal isentropic thrust; that is, the nozzle force coefficient is 0.96. Figure 21(a) shows the improvement in full-power performance to be gained by raising the force coefficient to 1.0. The differences in thrust and specific impulse are about 8 percent. As shown in figure 21(b), the improvement at cruising operation is slightly greater. For both full- and part-power operation, the exit-jet momentum is not much larger than the inlet momentum, and the drag is a significant percentage of the thrust. Thus, the engine propulsive thrust, which is the difference between two large numbers (exit momentum minus inlet momentum and drag), is quite sensitive to variations in the exit-jet momentum. The variations required in nozzle throat area throughout flight are discussed in another section.

Design flight Mach number. - Only engines designed for a flight Mach number of 2.3 have been discussed up to this point. An engine designed for a different flight Mach number will now be considered. This engine has an inlet sized for operation with a windmilling compressor at a Mach number of 2.8, which eliminates the inlet-bypass drag at cruising conditions and also reduces the inlet drag at lower flight speeds. Such a design does, however, limit the full-power thrust at a Mach number of 2.8. Despite being sized for the windmilling condition, the inlet of the Mach 2.8 engine is larger than that of the Mach 2.3 engine (which was designed for compressor operation at rated speed). Also, the nozzle plug of the Mach 2.8 engine is enlarged to take advantage of the higher cruising nozzle pressure ratio. Although the external size of the engine is increased, the afterburner internal size is maintained the same as for the reference one-stage-compressor engine. This choice was made from a qualitative consideration of afterburner weight.

The full-power performance of the two engines is compared in figure 22(a). Subsonic performance is essentially the same for both engines. At supersonic flight Mach numbers below 2.3, the Mach 2.8 engine yields poorer performance because of its higher additive, bypass, and nacelle drags, particularly boattail drag. At higher flight speeds, however, the maximum thrust of the Mach 2.3 engine is inferior because of the inability of its inlet to supply enough air to the engine (not shown). (Between flight Mach numbers of 2.3 and 2.8, there is a gradual transition of compressor speed from rated to windmilling, as discussed a little later in this section.)

Figure 22(b) shows the part-power performance of the Mach 2.8 engine cruising at a Mach number of 2.8. The specific impulse is comparatively constant over a wide range of afterburner temperatures. Increasing the compressor speed would add very little to the thrust and would appreciably lower the specific impulse, because the inlet then would be forced into supercritical operation. Similar part-power performance at a flight Mach number of 2.8 is possible for the Mach 2.3 engine; the specific impulse is somewhat lower for any given value of thrust coefficient, because the exhaust nozzle is not designed for the higher pressure ratio existing at the Mach number of 2.8.

Some design-point calculations for flight Mach numbers of 3.5 and 4.0 were also carried out. Figures 22(c) and (d) present the performance at these speeds for the part-power case (with windmilling compressors). When the inlet and exhaust nozzle are designed for these speeds using the previously stated procedure, the drags during lower-speed operation ($M \approx 1.2$) become very large. It is believed, however, that some other approach to the inlet and exhaust problems would yield smaller drags, on the order of those calculated for the Mach 2.3 or 2.8 engines. For the data of figures 22(c) and (d), the right end represents the maximum-thrust point as explained in the discussion of figure 22(b).

At high flight Mach numbers, it is anticipated that an air-turbo-rocket will be operated with a windmilling compressor even if the rocket fuel is a monopropellant. This will minimize the compressor blade stresses by reducing compressor speed. The lower blade strength due to the increased air total temperature might otherwise cause difficulty. Figure 4 shows the mechanical and aerodynamic speed of the compressor as a function of flight Mach number. Under the present assumptions for the one-stage compressor, the mechanical speed at a Mach number of 4.0 is about 20 percent less than the design speed. This results in nearly 40-percent reduction in blade stress. In the present calculations all air flowing through the afterburner must first pass through the compressor. Ducting all or part of the air around the compressor was previously mentioned as a possible method of improving the supersonic cruising performance of the engine. This would also relieve the compressor blade stress problem when the air total temperature is high.

Effect of Subsonic Cruising Mach Number

Cruising has been discussed only at the design flight Mach number up to this point. It is frequently proposed to cruise at subsonic flight speeds to take advantage of the high airplane lift-drag ratios obtainable there. This would provide longer interceptor range and endurance, provided the engine efficiency were not adversely affected. Figure 23 presents the performance of the Mach 2.3 engine when flying at an altitude of 35,332 feet and a flight Mach number of 0.9. Data are given for a

range of compressor pressure ratios from 0.95 (windmilling) to 1.527 (rated mechanical compressor speed). The parameter varied for each line of constant pressure ratio is the afterburner temperature. Contrary to the case of supersonic cruising (fig. 12(b)), it is desirable to derive some pressure ratio from the compressor. Even with the best compressor pressure ratio, however, the maximum specific impulse is extremely low, about 900 pounds per pound per second with drag, compared with 1500 at Mach 2.3.

Geometry Variations

The engine performance presented in this report can be achieved only with the use of variable-geometry components. The angles of the diffuser wedges must be varied with flight speed to maintain maximum pressure recovery. The reason for selecting the wedge-type inlet was to facilitate this geometry variation. Similar performance would be available from a conical inlet, except for the difficulty in varying the angles. In order to match the compressor air flow efficiently, an auxiliary inlet or blow-in doors are needed at take-off. The size of the blow-in doors to maintain a pressure recovery of 0.95 is shown in figure 24. The opposite problem is encountered at supersonic flight speeds. The oblique shocks from the compression wedges lie forward of the diffuser lip, so that some air is therefore spilled around the inlet. Nevertheless, the air-flow capacity of the inlet is still larger than that of the compressor. To avoid subcritical operation, the excess air is captured by the inlet and discharged in a downstream direction through a convergent nozzle or bypass. The amount of air spilled across the oblique shocks and through the bypass is also shown in the figure. There is no spillage at the inlet design point of rated compressor speed and flight Mach number of 2.3. Some spillage is necessary, however, when the compressor is allowed to windmill. More spillage is required for the two-stage compressor because of its lower windmilling air flow. The figure shows that, at take-off, the blow-in doors must increase the effective inlet size by 38 percent. On the other hand, at a Mach number of slightly over 1.0, the bypass must be large enough to discharge up to 37 percent of the air entering the inlet if no subcritical operation is permitted. Even greater variations are required if the inlet is sized for a Mach number of 2.8.

The required variations in nozzle throat area are shown in figure 25. For an engine with a one-stage compressor, the area needed for cruising at a Mach number of 2.3 at maximum specific impulse is 35 percent smaller than the area needed for maximum thrust at take-off. The corresponding value with two compressor stages is 25 percent. Figures 20(a) and (b) show that very little thrust loss occurs at subsonic speeds if the afterburner temperatures are reduced. A possible exhaust-nozzle operating line is shown for the one-stage compressor that would reduce the area variation required to 31 percent with little sacrifice in thrust.

Engine Weight Estimates

The weight of an aircraft engine is fully as important as the thrust. Some estimates of the probable weight of typical air-turborocket designs were therefore made in order to determine which components contribute most to the weight of the engine, to enable prediction of the effect of component changes on engine thrust-weight ratio and permit comparisons with the turbojet-engine weight calculated by the same method.

Table IV(a) presents the results of the weight study for the reference one- and two-stage-compressor engines, which employ a conventional bladed turbine. For the single-stage engine, the nacelle is estimated to comprise about half the total engine weight. The gearbox is the next heaviest component. Adding another stage to the compressor increases the engine weight mostly through the larger gearbox needed to transmit the higher horsepower. The horsepower required to drive the compressor varies both with design compressor pressure ratio and flight path, as shown in figure 26. The values shown will change if a different schedule of altitude with flight speed is used, with a consequent effect on gear size. Refinements in gear design can appreciably affect the weight of this engine type. Changes in turbine size or the reduction-gear ratio are not expected to appreciably affect engine weight (unless the gearing can be eliminated altogether).

Since the gearbox is such a heavy component, its elimination, even at the expense of poorer cycle efficiency, may be desirable. Table IV(b) presents an estimated weight-breakdown of the air-turborocket engine when using a rotating-rocket turbine. The weights of the rotating parts are quite small, and the nacelle is then more than half of the total weight. Elimination of the bladed turbine and its gearbox results in a weight reduction of 20 and 28 percent for the one- and two-stage-compressor engines, respectively.

Because of the lightness of the internal components, the nacelles are comparatively heavy, particularly for the one-stage-compressor engine. This is true despite the thin gages assumed and liberal use of titanium. Probably the most satisfactory way to further reduce the nacelle weight is to shorten the afterburner.

Comparison with Turbojet Engine

Development of a new engine type is warranted only if it promises significant improvement over existing types. Figure 27 compares the performance of the air-turborocket engine with that of a turbojet engine with afterburning. The design of the air-turborocket is based on the reference values of table II. To make the comparison, the design assumptions for the turbojet are fairly optimistic by present-day production

6293

CE-4

standards. The turbine-inlet temperature is 2500° R, and the maximum afterburner temperature is 3500° R. Equivalent compressor air flow at take-off is 35 pounds per second per square foot, with a take-off design pressure ratio of 7. The compressor is operated at a constant mechanical speed. Design-point adiabatic efficiency for both compressor and turbine is 87 percent. Other comparable parameters are the same for the two engines.

The full-power performance of the engines over a range of flight speeds is shown in figure 27(a). At all speeds the specific impulse of the turbojet is appreciably greater than that of the air-turborocket. At take-off, the air-turborocket specific impulse is 34 percent that of the turbojet; at a Mach number of 2.3, it is 65 percent. The turbojet also produces more thrust per unit compressor frontal area than the air-turborocket with one compressor stage at all except the highest speeds. The turbojet thrust advantage exists only at low speeds when compared with the two-stage-compressor air-turborocket, however. Figure 27(b) compares the part-power performance of the engines at a flight Mach number of 2.3. At any given value of thrust coefficient, the turbojet is the more efficient engine. The maximum specific impulse of the air-turborocket is 70 percent that of the turbojet. Figure 27(c) shows the part-power performance at a flight Mach number of 0.9. The data for the air-turborocket is the envelope of the curves of figure 23. At this flight condition the air-turborocket is about one-third as efficient as the turbojet.

Despite its poorer efficiency, the air-turborocket may compete with the turbojet because of its lighter weight. The estimated weights of the two engine types are compared in table IV(c), the weight of the turbojet being estimated on the same basis as that of the air-turborocket. The weight of the air-turborocket is about half that of the turbojet. (The value in the table for the turbojet, 615 lb/sq ft, is optimistic by present-day standards; e.g., a recent production turbojet engine designed for supersonic flight has a weight of 680 lb/sq ft of compressor-tip area without including the extra weight of the inlet and outer shell.)

From the calculated data, engine thrust-weight ratios were computed for full-power operation with afterburning to 3500° R. These and the corresponding specific impulses are presented in table V. At a flight Mach number of 2.3 the thrust-weight ratio of the air-turborocket is between 2.2 and 3.4 times that of the turbojet. At take-off the air-turborocket thrust-weight ratio is 1 to 2 times that of turbojet. At take-off the air-turborocket engines with two compressor stages have a higher thrust-weight ratio than the one-stage engines. However, the one-stage engines have comparable thrust-weight ratios and also are more efficient than the two-stage engines at a Mach number of 2.3.

3679

Balancing the high thrust-weight ratio of the air-turborocket against the high specific impulse of the turbojet requires an airplane performance study, which is beyond the scope of the present report. It appears reasonable, however, that the air-turborocket will show to best advantage where high ratios of engine thrust to airplane gross weight are needed. Such airplanes might feature vertical take-off or high combat ceilings and maneuverability. The air-turborocket converts with ease to a ram-jet mode of operation (i.e., by windmilling the compressor). This fact, together with its light weight, makes it attractive for attaining higher flight Mach numbers and altitudes than the turbojet can be expected to provide.

CONCLUDING REMARKS

The present report is intended to illustrate the principal design characteristics of the air-turborocket engine and to indicate the importance to engine performance of changes in the various components.

1. At a flight Mach number of 2.3, use of a two-wedge rather than a one-wedge inlet, which raises the diffuser pressure recovery from 0.775 to 0.866, results in a 6-percent increase in maximum specific impulse.
2. The compressor pressure ratio is one of the major engine design parameters. Increasing the design pressure ratio from 1.45 to 3.10 increases the thrust at take-off 2.5 times with only minor effects on specific impulse. Allowing the compressor to windmill yields the highest specific impulse at supersonic cruising conditions (when the rocket propellants are gasoline and nitric acid). Low design compressor pressure ratios give best windmilling operation and hence highest specific impulses for supersonic cruising.
3. Increasing the rocket chamber pressure improves the full-power specific impulse. Changes in chamber temperature have little effect on thrust or specific impulse for gasoline - nitric acid propellants.
4. Use of the rocket monopropellant methyl acetylene (mixed with gasoline) increases full-power specific impulse by 27 percent (compared with gasoline plus nitric acid) for an engine with a one-stage compressor. The improvement for the multistage-compressor engine depends on the chamber temperature. Driving the turbine (and compressor) at part speed with the monopropellant improves the peak specific impulse at Mach 2.3 by 11 percent over that obtainable with gasoline - nitric acid and a windmilling compressor.

5. The full-power specific impulse is quite sensitive to changes in turbine efficiency when gasoline - nitric acid propellants are used. This is also true when methyl acetylene is used with a two-stage compressor. The use of a rotating-rocket turbine affords savings in engine weight but at a sacrifice in full-power specific impulse.

6. Increasing afterburner temperature does not appreciably aid take-off thrust but does increase thrust at supersonic speeds.

The engine weight estimates show that the nacelle and afterburner comprise about half the weight of the air-turbo-rocket. Shortening or other lightening of these components thus would have a very beneficial effect on total engine weight. In air-turbo-rocket engines with bladed turbines, the gearing represents a large part of the remaining weight. This is particularly true of the engines with multistage compressors. Refined gear design is therefore important.

The turbine will probably be one of the major problems in developing an air-turbo-rocket engine. For the bladed turbine, a high-pressure-ratio multistage partial-admission design is indicated, having a high blade hub-tip ratio. The gearing associated with this type is also a major problem. For the rotating-rocket turbine, a rocket chamber of low volume and efficient operation in a centrifugal field is required.

At take-off conditions, some forms of the air-turbo-rocket can provide up to twice as much thrust for a given engine weight than can the turbojet. At full power and a flight Mach number of 2.3, the thrust is from 2.2 to 3.4 times that of the turbojet (for a given engine weight). The efficiency of the air-turbo-rocket is inferior to that of the turbojet, however. Full-power specific impulse of the air-turbo-rocket is about 34 and 65 percent of that of the turbojet at flight Mach numbers of 0 and 2.3, respectively. The maximum specific impulse of the air-turbo-rocket is 70 and 33 percent that of the turbojet at Mach numbers of 2.3 and 0.9, respectively.

Lewis Flight Propulsion Laboratory
National Advisory Committee for Aeronautics
Cleveland, Ohio, August 19, 1955

APPENDIX A

SYMBOLS

A	cross-sectional area, sq ft
C_D	drag coefficient
C_F	thrust coefficient, F/qA (for supersonic flight speeds)
C_{FM}^2	thrust parameter, $F/\frac{\gamma}{2} pA$ (for subsonic flight speeds)
C_N	nozzle force coefficient (see eq. (B4))
c_p	heat capacity at constant pressure, Btu/(lb)(°R)
d	diameter, ft
E	power, ft-lb/sec
F	thrust, lb
g	acceleration due to gravity, 32.2 ft/sec ²
H	total enthalpy per unit weight, Btu/lb
h	static enthalpy per unit weight, Btu/lb
I	specific impulse, lb/(lb/sec)
J	mechanical equivalent of heat, 778 ft-lb/Btu
l	length, ft
M	Mach number
N	compressor mechanical speed, rpm
n	flameholder drag parameter
P	total pressure, lb/sq ft or atm, as indicated
p	static pressure, lb/sq ft
q	incompressible dynamic pressure, $\frac{1}{2} \rho V^2$, lb/sq ft
Re	Reynolds number

S	nacelle surface area, sq ft
T	total temperature, °R
U	tip speed, ft/sec
V	velocity, ft/sec
v	rocket jet velocity, ft/sec
W	installed engine weight, lb
w	weight flow, lb/sec
γ	ratio of specific heats
δ	pressure-correction factor, P/2116
η	efficiency
θ	temperature-correction factor, T/519
ρ	density, slugs/cu ft

Subscripts:

a	compressor air
ab	afterburner
B	rocket combustor
C	compressor
f	rocket fuel
fr	friction
ft	rocket plus afterburner fuel
g	gear
i	inlet
is	isentropic
m	cylindrical, maximum-diameter section of nacelle

n net (not including drag)
o rocket oxidant
p propulsive (including drag)
pl exhaust-nozzle plug
r rocket propellants, fuel plus oxidant
rt rotating-rocket turbine
T turbine
x forward conical section of nacelle
y rear conical exhaust fairing of nacelle
∞ free-stream
1 compressor inlet
2 compressor exit
3 afterburner inlet
4 rocket combustion chamber
5 afterburner (downstream of flameholder)
6 afterburner exit
7 exhaust-nozzle throat
8 exhaust-nozzle exit

APPENDIX B

METHOD OF CALCULATION

Internal Performance

The internal or net thrust produced by the engine is equal to the difference in momentum of the fluid which passes through the engine cycle entering and leaving the engine:

$$F_n = \frac{w_a}{g} \left(\frac{w_8}{w_a} V_8 - V_\infty \right) \quad (B1)$$

For convenience, the momentum of the entering air is measured in the free stream ahead of the inlet. This requires that the external air forces on the streamtube ahead of the inlet be included as a drag term (additive drag). Also, not all the air in the streamtube flows through the engine, part may be discharged through an auxiliary nozzle instead. The effect of this discharge on thrust has also been treated as a drag term (bypass drag). The calculation of these two drags and of nacelle drag is described in a following section.

Equation (B1) may be rewritten as a net thrust coefficient in the following manner:

$$C_{F,n} = \frac{F_n}{q_\infty A_1} = \frac{F_n}{w_a} \left(\frac{1}{\frac{\gamma}{2} M_\infty^2} \right) \left(\frac{w_a \sqrt{\theta}}{A_8} \right)_1 \frac{\left(\frac{P_1}{P_\infty} \right) \left(\frac{P_\infty}{P_8} \right)}{2116} \frac{1}{\sqrt{\frac{T_1}{519}}} \quad (B2)$$

The net specific impulse may also be expressed using the terms of equation (B1):

$$I_n = \frac{F_n}{w_{ft} + w_o} = \frac{\frac{F_n}{w_a}}{\frac{w_8}{w_a} - 1} \quad (B3)$$

The exit velocity needed for equation (B1) is given by

$$V_8 = C_N \sqrt{2gJ(H_6 - h_\infty)_{is}} \quad (B4)$$

in which h_∞ is the enthalpy that would be obtained by an isentropic expansion of the exhaust gas to ambient pressure. The enthalpy difference $H_6 - h_\infty$ is a function of the gas properties, the nozzle pressure

ratio, and the gas temperature T_6 . It is plotted in figure 28, which was calculated using the method of reference 9. (The data are very similar to those for gasoline and air.) The nozzle force coefficient C_N accounts both for the internal nozzle losses and any thrust loss due to underexpansion or overexpansion.

The nozzle pressure ratio is calculated from the expression

$$\frac{P_{\infty}}{P_6} = \frac{\frac{P_{\infty}}{P_1} \frac{P_1}{P_2} \frac{P_2}{P_3} \frac{P_3}{P_5} \frac{P_5}{P_6}}{\frac{P_{\infty}}{P_1} \frac{P_1}{P_2} \frac{P_2}{P_3} \frac{P_3}{P_5} \frac{P_5}{P_6}} \quad (B5)$$

where P_1/P_{∞} is the inlet pressure recovery given by figure 2, and P_2/P_1 is the compressor pressure ratio given by figure 3. The friction and turbulence losses across the afterburner flameholder are defined by

$$P_3 - P_5 = nq_3 = n \frac{\gamma_3}{2} P_3 M_3^2$$

It is assumed that the losses in the air duct around the turbine are also included in this quantity if n is taken as 3, giving

$$\frac{P_5}{P_2} = 1 - 3 \frac{\gamma_3}{2} \frac{P_3}{P_2} M_3^2 \quad (B6)$$

The momentum-pressure loss due to heat addition P_6/P_5 is calculated from the equations of conservation of mass and momentum. It is a function of M_5 and T_6/T_5 (fig. 6), where

$$T_5 = \frac{t_{\infty}}{t_{\infty}} \frac{T_1}{T_{\infty}} \frac{T_2}{T_1} \frac{T_5}{T_2} \quad (B7)$$

and it is assumed that

$$\frac{T_1}{T_{\infty}} = \frac{T_5}{T_2} = \frac{T_8}{T_6} = 1.0$$

3679

CE-5

$$\frac{T_2}{T_1} = \left[\frac{\left(\frac{P_2}{P_1} \right)^{\frac{\gamma_1 - 1}{\gamma_1}}}{\eta_C} \right] + 1$$

where the compressor adiabatic efficiency η_C is determined from figure 3.

The Mach numbers M_3 and M_5 , which are functions of the compressor air flow and the engine area ratios, are found by use of the continuity equation.

The ratio of exit to entrance mass flow w_8/w_a in equations (B1) and (B3) may be written

$$\frac{w_8}{w_a} = 1 + \frac{w_o}{w_a} + \frac{w_{ft}}{w_a} = 1 + \frac{\frac{w_r}{w_a}}{\frac{w_f}{w_o} + 1} + \frac{w_{ft}}{w_a} \quad (B8)$$

The quantity w_r/w_a is determined by the turbine work requirements:

$$\frac{w_r}{w_a} = \frac{c_{p,l} T_1 \left[\left(\frac{P_2}{P_1} \right)^{\frac{\gamma_1 - 1}{\gamma_1}} - 1 \right]}{\eta_C \eta_g \eta_T \eta_B \Delta h_T} \quad (B9)$$

The ideal enthalpy drop across the turbine Δh_T is given in figure 29 as a function of the turbine pressure ratio p_3/p_4 and the rocket chamber temperature T_4 . Data for the gasoline-nitric acid system were taken from reference 10. The gasoline - methyl acetylene data were calculated by the method of reference 9. The pressure ratio is given by

$$\frac{p_3}{p_4} = \frac{\frac{P_1}{P_\infty} \frac{P_2}{P_1} \frac{P_3}{P_2} \frac{P_3}{P_3} \frac{P_\infty}{P_3}}{\frac{P_\infty}{P_4} P_4} \quad (B10)$$

in which P_3/P_2 is taken equal to unity.

The rocket fuel-oxidant ratio w_f/w_o needed for equation (B8) is determined as a function of chamber pressure and temperature (fig. 5).

The over-all fuel-air ratio w_{ft}/w_a may be written in the following manner:

$$\frac{w_{ft}}{w_a} = \frac{1}{\eta_{ab}} \left(\frac{\eta_{ab} w_{ft}}{w_o + w_a} \right) \left(1 + \frac{\frac{w_r}{w_a}}{\frac{w_f}{w_o} + 1} \right) \quad (B11)$$

The first quantity in parentheses may be obtained from figure 30 as a function of the temperature before combustion T_2 and the total-temperature rise $T_6 - T_1$. The figure is taken from references 1 and 11 and is actually intended only for the combustion of gasoline in air. Although not exact, this method yields sufficiently accurate results as checked by more detailed calculations.

The foregoing discussion must be modified slightly when a rotating-rocket turbine is used instead of the conventional bladed turbine. The useful power E produced by a rocket rotating at a tip speed U with jet velocity v is

$$E = \frac{w_r}{g} (Uv - U^2)$$

Substituting $\eta_B \sqrt{2gJ\Delta h_T}$ for v , an equivalent turbine efficiency can be written as

$$\eta_{rt} = \frac{E}{Jw_r\Delta h_T} = \frac{U\eta_B \sqrt{2gJ\Delta h_T} - U^2}{gJ\Delta h_T} \quad (B12)$$

For the rotating-rocket turbine, equation (B9) can be then rewritten as

$$\frac{w_r}{w_a} = \frac{c_{p,1} T_1 \left[\left(\frac{P_2}{P_1} \right)^{\frac{\gamma_1 - 1}{\gamma_1}} - 1 \right]}{\eta_C \eta_{rt} \Delta h_T} \quad (B13)$$

Engine Geometry

In order to calculate the drag and weight of the air-turborocket, it is necessary to specify the dimensions of the engine. The various internal area ratios are determined from the cycle analysis. The method described in the ANALYSIS resulted in the following exhaust-nozzle plug sizes:

Number of compressor stages	$\frac{A_{pl}}{A_1}$
1	0.41
2	.39
3	.30

The annular nozzle-throat area is given by

$$\frac{A_7}{A_1} = \frac{\left(\frac{w_a \sqrt{\theta}}{A_8}\right)_1 \sqrt{\frac{T_7}{T_1}} w_8}{\left(\frac{w_a \sqrt{\theta}}{A_8}\right)_7 \frac{P_7}{P_1}} \quad (B14)$$

The afterburner frontal area is specified by

$$\frac{A_m}{A_1} = (1.1)(1.15) \left(\frac{A_{pl}}{A_1} + \frac{A_7}{A_1} \right) \quad (B15)$$

This is also the maximum engine frontal area in the cases studied. The value of A_7/A_1 used in equation (B15) is the maximum required during flight with a 3500° afterburner temperature (see fig. 25(a)). The factor 1.15 is required to ensure efficient operation of the nozzle.

The diffuser plus rotating parts was assumed to have a length of 3.5 compressor diameters. The afterburner length was taken as 4 times the diameter that would provide an afterburner-inlet Mach number of 0.20 at take-off. This imaginary diameter varies with the compressor pressure ratio but is independent of the actual afterburner diameter (which is fixed by the nozzle design). The length of the floating exit-fairing is 0.7 of the maximum engine diameter.

Table VI lists the major length and diameter ratios calculated for the various engine designs. (The dimensions referred to in the table are depicted in fig. 1.) At the higher design flight speed the compressor is relatively small compared with both the inlet and afterburner.

Raising the compressor pressure ratio decreases both the afterburner diameter and length. Use of the rotating-rocket turbine not only eliminates the weight of the gears but also shortens the engine.

External Drag

As previously stated, the internal thrust of the engine is defined as the change in momentum of the gases passing through the engine cycle entering and leaving the engine. All other forces acting on the exterior of this streamtube of gas are drags. These drags are composed of the following parts:

- (1) Forces due to inlet spillage:
 - (a) Additive drag due to spillage before inlet
 - (b) Bypass drag due to spillage after air enters inlet
- (2) Forces on the engine nacelle:
 - (a) Friction drag parallel to flow direction
 - (b) Pressure drag normal to local nacelle surface

The net thrust F_n accounts for none of the drag terms. The propulsive thrust F_p is obtained by subtracting all the above drag terms from F_n .

Nacelle friction drag. - The friction drag coefficient based on compressor frontal area is given by the following equation (from ref. 12) assuming a turbulent boundary layer:

$$C_{D,fr} = \frac{0.0306 \frac{S}{A_1}}{(Re)^{1/7} \left(1 + \frac{\gamma-1}{4} M_\infty^2\right)^{5/7}} \quad (B16)$$

where Re is the Reynolds number based on free-stream conditions and was calculated for an assumed nominal engine length of 20 feet.

The ratio of nacelle-skin area to compressor frontal area for Mach 2.3 is given by

$$\frac{S}{A_1} = 4 \left[\frac{1}{2} \left(\frac{d_i}{d_1} + \frac{d_m}{d_1} \right) \frac{l_x}{d_1} + \frac{d_m}{d_1} \left(\frac{l_m}{d_1} + \frac{l_y}{d_1} \right) \right] \quad (B17)$$

For higher Mach numbers conical nacelles were assumed.

Nacelle pressure drag. - The pressure drag is composed of the axial projection of the forces on the diverging forward part of the nacelle and the converging boattail at the rear. The drag coefficients were obtained from reference 13.

Additive drag. - The additive drag, which is the integrated axial component of the static-pressure forces acting on the diverging streamline entering the inlet, was evaluated from simple two-dimensional flow theory.

Bypass drag. - In cases when the inlet captures more air than is needed by the compressor, the excess is assumed to be discharged to the rear through an auxiliary sonic nozzle. Full free-stream momentum is not regained because of inlet losses and incomplete expansion. The calculation is essentially the same as for a ram jet with no heat-addition.

Engine Weight

Weight of the air-turborocket engine was considered in three parts:

- (1) Nacelle, including inlet, afterburner, exhaust nozzle, and all external fairings
- (2) Compressor and turbine unit
- (3) Engine accessories

The weight was calculated for an engine with a 28-inch compressor-tip diameter.

The outer shell of the nacelle was assumed to be of double-walled construction. Both walls are made of sheet titanium with a thickness of 0.02 inch. The walls are separated and stiffened by rings and stringers, which were assumed to weigh 38 percent of the weight of the walls. A cylindrical steel liner is placed in the afterburner; it too has a thickness of 0.02 inch and is supported by stringers that add 64 percent to its weight. The ratio of liner to nacelle cross-sectional area is nominally 0.90. The nozzle plug and exhaust fairing are built of 0.032-inch-thick steel.

Weights of the compressor, gears, gas generators, and turbine were estimated with the aid of large-scale preliminary lay-outs of the engines. Figure 31 illustrates the relative proportions of the components of this section for representative engines. The materials are titanium and steel (see table IV). A weight of 10 pounds per square foot of compressor frontal area was assumed for the engine accessories.

The foregoing assumptions wherever applicable and similar design procedures were used for estimating the turbojet-engine weight. The accessory weight was increased to 15 pounds per square foot of compressor frontal area to account for a larger starter.

REFERENCES

1. Charyk, Joseph V., and Sutherland, George S.: A Performance Study of the Ram Rocket Power Plant and Related Problems. Tech. Rep. No. 36, Princeton Univ., Mar. 25, 1952. (Contract N6 ori-105, Task Order III, NR 220-038.)
2. House, William C.: The Air-TurboRocket Engine and Its Place in the Flight Propulsion Spectrum. Aerojet-General Corp. (Paper presented at Meeting Inst. Aero. Sci., Cleveland (Ohio), Mar. 13, 1953.)
3. Anon.: Preliminary Performance Data for a 26-Inch Diameter Air-TurboRocket Engine (Model No. ATR-1001). Rep. No. 839, Aerojet-General Corp., June 1954.
4. Allen, J.L., and Beke, Andrew: Performance Comparison at Supersonic Speeds of Inlets Spilling Excess Flow by Means of Bow Shock, Conical Shock, or Bypass. NACA RM E53H11, 1953.
5. Fradenburgh, Evan A., and Wyatt, DeMarquis D.: Theoretical Performance Characteristics of Sharp-Lip Inlets at Subsonic Speeds. NACA Rep. 1193, 1954. (Supersedes NACA TN 3004.)
6. Serovy, George K., Robbins, William H., and Glaser, Frederick W.: Experimental Investigation of a 0.4 Hub-Tip Diameter Ratio Axial-Flow Compressor Inlet Stage at Transonic Inlet Relative Mach Numbers. I - Rotor Design and Over-All Performance at Tip Speeds from 60 to 100 Percent of Design. NACA RM E53I11, 1953.
7. Kohl, Robert C., Herzig, Howard Z., and Whitney, Warren J.: Effects of Partial Admission on Performance of a Gas Turbine. NACA TN 1807, 1949.
8. Krull, H. George, and Beale, William T.: Effect of Plug Design on Performance Characteristics of Convergent-Plug Exhaust Nozzles. NACA RM E54H05, 1954.
9. Huff, Vearl N., Gordon, Sanford, and Morrell, Virginia E.: General Method and Thermodynamic Tables for Computation of Equilibrium Composition and Temperature of Chemical Reactions. NACA Rep. 1037, 1951. (Supersedes NACA TN's 2113 and 2161.)

10. Weymouth, F. R.: Thermodynamic Properties of the Product of Combustion of Aviation Gasoline and White Fuming Nitric Acid at Rich and Extremely Rich Mixtures. Rep. No. 56-982-011, Bell Aircraft Corp., Jan. 15, 1951. (Contract NOrd 9876 and W33-038 ac 14169.)
11. Turner, L. Richard, and Bogart, Donald: Constant-Pressure Combustion Charts Including Effects of Diluent Addition. NACA Rep. 937, 1949. (Supersedes NACA TN's 1086 and 1655.)
12. Tucker, Maurice: Approximate Calculation of Turbulent Boundary-Layer Development in Compressible Flow. NACA TN 2337, 1951.
13. Fraenkel, L. E.: The Theoretical Wave Drag of Some Bodies of Revolution. Rep. No. Aero 2420, British R.A.E., May 1951.

TABLE I. - PHYSICAL CHARACTERISTICS OF PROPELLANTS

	Gasoline	Nitric acid	Methyl acetylene
Heating value in air, Btu/lb	18,700	----	19,631
Specific gravity at 100° F	0.76	1.47	0.60
Vapor pressure at 100° F, lb/sq in.	2.3	2.2	119
Boiling point, °F	155	187	-10

TABLE II. - REFERENCE VALUES OF ENGINE PARAMETERS

Design flight Mach number	2.3
Inlet type	Two-wedge, variable
Compressor:	
Number of stages	1
Take-off pressure ratio	1.45
Take-off equivalent air flow, (lb/sec)/sq ft	35
Adiabatic efficiency, percent	88
Gas generator:	
Propellants	Gasoline - nitric acid
Chamber temperature, °R	2100
Chamber pressure, atm	32
Turbine:	
Type	Bladed, with reduction gear
Adiabatic efficiency, percent	60
Afterburner:	
Inlet Mach number	0.14
Maximum exit temperature, °R	3500
Combustion efficiency, percent	90
Exhaust nozzle:	
Type	Variable convergent-divergent
Force coefficient	0.96
Flight altitude	Scheduled with M_∞ (fig. 7)

TABLE III. - PERFORMANCE OF AIR TURBOROCKET ENGINES

(a) Full-power operation; one-stage compressor

Flight Mach number, M_∞	Altitude, ft	Compressor total-pressure ratio, P_2/P_1	Afterburner-exit temperature, $T_6, ^\circ R$	Net thrust coefficient, $C_{F,n}$	Net specific impulse, I_n	Propulsive thrust coefficient, $C_{F,p}$	Propulsive specific impulse, I_p	Area ratios		
								A_6/A_1	A_7/A_1	A_8/A_1
0	0	1.450	3000	1.063	693.2	1.063	693.2	↓	1.447	1.765
			3500	1.097	613.5	1.097	613.5		1.613	2.028
			4000	1.152	524.9	1.152	524.9		1.802	2.379
0.5	2,188	1.436	3000	1.182	662.1	1.144	640.8	↓	1.425	1.495
			3500	1.263	604.9	1.225	586.7		1.591	1.686
			4000	1.385	543.0	1.345	528.1		1.774	1.907
	35,332	1.600	3000	1.660	825.7	1.624	607.8	↓	1.524	1.544
			3500	1.729	731.6	1.693	716.4		1.706	1.738
			4000	1.939	661.2	1.903	648.9		1.863	1.898
0.9	35,332	1.528	3500	2.720	856.8	2.592	816.5	0.6945	1.678	1.706
1.0	0	1.353	3000	2.137	837.6	{2.006 1.472}	{786.4 577.1}	↓	1.323	1.389
			3500	2.185	732.4	{2.054 1.692}	{688.5 567.1}		1.476	1.504
			4000	3.030	698.2	{2.899 2.604}	{859.4 771.9}		1.617	1.787
	8,750	1.390	3000	2.133	799.8	{1.997 1.481}	{748.8 555.3}	↓	1.370	1.406
			3500	2.378	764.9	{2.242 1.828}	{721.2 588.0}		1.524	1.559
			4000	2.681	705.9	{2.545 2.223}	{668.2 583.7}		1.697	1.729
	35,332	1.508	3000	2.787	941.2	{2.634 2.216}	{889.5 748.4}	↓	1.489	1.555
			3500	3.090	887.7	{2.937 2.693}	{843.7 773.6}		1.661	1.726
			4000	3.275	764.0	{3.122 3.003}	{728.3 700.5}		1.860	1.920
	0	1.273	3000	1.670	869.1	1.233	641.5	↓	1.173	1.571
			3500	1.854	832.9	1.499	673.3		1.292	1.645
			4000	2.188	905.0	1.854	766.6		1.422	1.881
	19,680	1.331	3000	1.963	952.0	1.558	755.8	↓	1.287	1.674
			3500	2.259	938.2	1.942	806.4		1.430	1.846
			4000	2.568	870.9	2.259	766.3		1.587	2.031
	35,332	1.403	3000	2.352	1045	1.992	885.4	↓	1.385	1.839
			3500	2.690	1020	2.404	911.5		1.543	2.032
			4000	2.926	901.3	2.696	830.4		1.717	2.236
2.0	55,000	1.298	3000	2.343	1087	2.115	981.2	↓	1.214	2.315
			3500	2.750	1089	2.525	999.9		1.344	2.544
			4000	3.145	1015	2.920	948.4		1.488	2.790
2.3	46,288	1.252	3000	2.378	1146	2.174	1048	↓	1.093	2.660
			3500	2.819	1153	2.614	1069		1.208	2.922
			4000	3.251	1086	3.047	1018		1.332	3.195

7070

TABLE III. - Concluded. PERFORMANCE OF AIR-TURBOROCKET ENGINES

(b) Full-power operation; two-stage compressor

Flight Mach number, M_∞	Altitude, ft	Compressor total-pressure ratio, P_2/P_1	Afterburner-exit temperature, $T_6, ^\circ R$	Net thrust coefficient, $C_{F,n}$	Net specific impulse, I_n	Propulsive thrust coefficient, $C_{F,p}$	Propulsive specific impulse, I_p	Area ratios		
								A_6/A_1	A_7/A_1	A_8/A_1
0	0	2.103	3500	1.902	748.2	1.902	748.2	-	1.133	1.133
			4000	2.059	686.2	2.059	686.2	-	1.263	1.264
0.5	2,188	2.062	3500	2.007	663.2	1.976	653.0	0.8974	1.133	1.144
			4000	2.207	629.8	2.176	621.0	.8974	1.259	1.268
	35,332	2.560	3500	2.721	852.3	2.685	841.0	0.9311	1.049	1.120
			4000	3.024	758.2	2.988	749.2	.9311	1.172	1.245
1.0	0	1.831	3500	2.847	610.9	{ 2.716 2.505 3.488 3.362	{ 582.8 537.5 688.1 663.2	0.6389	1.170	1.287
			4000	3.619	713.9			↓	1.226	1.493
	8,750	1.932	3500	3.152	662.1	{ 3.043 2.832 3.404 3.252	{ 658.5 612.9 648.7 619.8	0.6546	1.137	1.288
			4000	3.513	669.5			↓	1.261	1.417
	35,332	2.274	3500	3.939	831.3	{ 3.786 3.657 4.245 4.175	{ 799.0 771.8 741.4 729.2	0.6847	1.101	1.341
			4000	4.398	768.1			↓	1.229	1.483
1.5	0	1.621	3500	2.247	563.8	1.819	456.4	0.6913	1.138	1.590
			4000	2.730	684.9	2.529	634.6	.6913	1.184	1.865
	19,680	1.772	3500	2.698	748.4	2.504	694.5	0.7359	1.125	1.673
			4000	3.030	748.5	2.847	703.1	.7359	1.247	1.856
	35,332	1.968	3500	3.100	847.8	2.885	789.1	0.7735	1.125	1.774
			4000	3.516	806.9	3.312	760.1	.7735	1.253	1.956
2.0	35,000	1.685	3500	3.138	832.8	2.980	791.0	0.9796	1.090	2.396
			4000	3.548	843.5	3.390	805.9	.9796	1.203	2.617
2.3	46,288	1.568	3500	3.123	896.9	3.008	863.8	1.141	1.013	2.796
			4000	3.575	899.3	3.459	870.5	1.141	1.118	3.055

(c) Part-power operation; flight Mach number, 2.3

Stages	Compressor total-pressure ratio, P_2/P_1	Afterburner-exit temperature, $T_6, ^\circ R$	Net thrust coefficient, $C_{F,n}$	Net specific impulse, I_n	Propulsive thrust coefficient, $C_{F,p}$	Propulsive specific impulse, I_p	Area ratios			
							A_7/A_1	A_8/A_1	A_9/A_1	A_{10}/A_1
1	0.95	3500	2.125	1486	1.917	1341	1.368	2.755	0.9835	2.51
		3000	1.774	1591	1.566	1404	1.228	2.500	↓	↓
		2500	1.427	1736	1.215	1478	1.098	2.211	↓	↓
		2000	1.015	1832	.7815	1410	.9582	1.914	↓	↓
		1500	.5773	1871	.3040	985.1	.8090	1.603	↓	↓
2	0.90	3500	1.525	1456	1.331	1271	1.063	2.064	0.7205	1.89
		3000	1.265	1550	1.071	1312	.9586	1.878	↓	↓
		2500	1.020	1694	.8216	1564	.8518	1.657	↓	↓
		2000	.7157	1762	.5026	1237	.7433	1.435	↓	↓
		1500	.4072	1801	.1631	721.6	.6268	1.202	↓	↓

TABLE IV. - ESTIMATED WEIGHT OF AIR-TURBOROCKET ENGINES

(a) Engine with bladed turbine

Component	Material	Weight, W/A_1 , lb/sq ft	
		One-stage compressor	Two-stage compressor
Compressor-turbine unit:			
Compressor rotors and stators	Ti	17.7	38.0
Shaft	Steel	6.7	10.0
Gearbox	Ti, Steel	51.0	101.0
Rocket-turbine assembly	Steel	39.0	39.0
Nonrotating parts	Ti, Steel	44.6	53.8
		158.0	241.5
Nacelle:			
Inlet section	Ti	53.5	50.0
Afterburner section	Ti, Steel	71.6	63.1
Exhaust-nozzle group	Steel	36.8	32.6
		161.9	145.7
Accessories		10.0	10.0
Total		329.9	397.2

(b) Engine with rotating-rocket turbine

Component	Material	Weight, W/A_1 , lb/sq ft	
		One-stage compressor	Two-stage compressor
Compressor-turbine unit:			
Compressor rotors and stators	Ti	17.7	38.0
Shaft	Steel	7.9	12.0
Rotating-rocket turbine	Steel	17.1	26.3
Nonrotating parts	Ti, Steel	49.5	54.4
		92.2	130.7
Nacelle:			
Inlet section	Ti	50.5	43.5
Afterburner section	Ti, Steel	71.6	63.1
Exhaust-nozzle group	Steel	36.8	32.6
		158.9	139.2
Accessories		10.0	10.0
Total		261.1	279.9

(c) Comparison with turbojet engine

Component	Weight, W/A_1 , lb/sq ft				
	Air-turborocket engine				Turbojet engine
	Bladed turbine		Rotating-rocket turbine		
	One-stage compressor	Two-stage compressor	One-stage compressor	Two-stage compressor	
Compressor-turbine unit	158	241	92	131	450
Nacelle	162	146	159	139	150
Accessories	10	10	10	10	15
Total	330	397	261	280	615

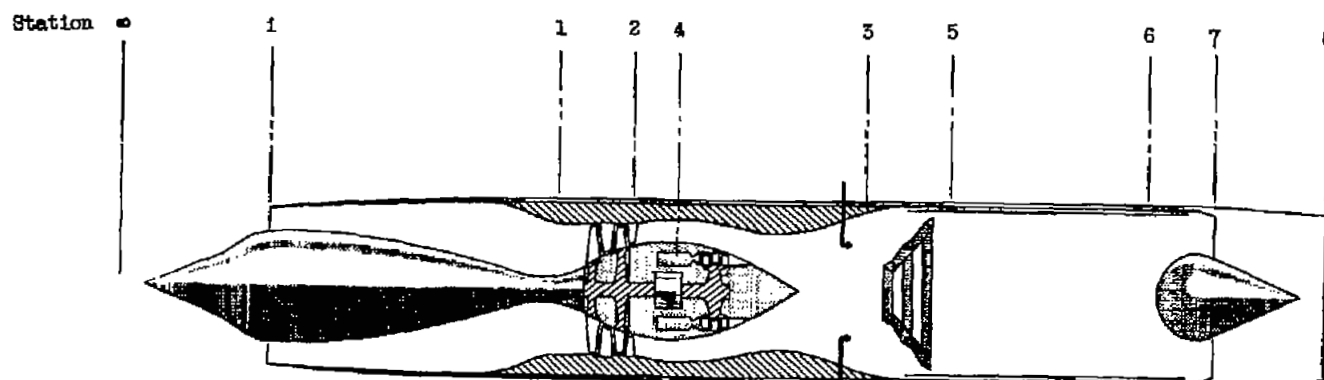
TABLE V. - PERFORMANCE COMPARISON OF AIR-TURBOROCKET AND TURBOJET ENGINES (INCLUDING DRAG)

	Air-turborocket				Turbojet
	Bladed turbine		Rotating-rocket turbine		
	One-stage compressor	Two-stage compressor	One-stage compressor	Two-stage compressor	Six-stage compressor
Maximum thrust:					
$M_\infty = 0$, $\left\{ \begin{array}{l} \text{F/W} \\ \text{Sea level} \end{array} \right. \text{I}$	4.92	7.17	6.26	10.8	5.23
	615	750	505	468	1815
$M_\infty = 2.3$, $\left\{ \begin{array}{l} \text{F/W} \\ 50,000 \text{ ft} \end{array} \right. \text{I}$	13.4	12.8	17.5	20.4	5.84
	1082	865	897	575	1670
Maximum efficiency:					
I ($M_\infty = 2.3$; 46,000 ⁺ ft)	1480	1363	1480	1363	2115
I ($M_\infty = 0.9$; 35,332 ⁺ ft)	900				2720

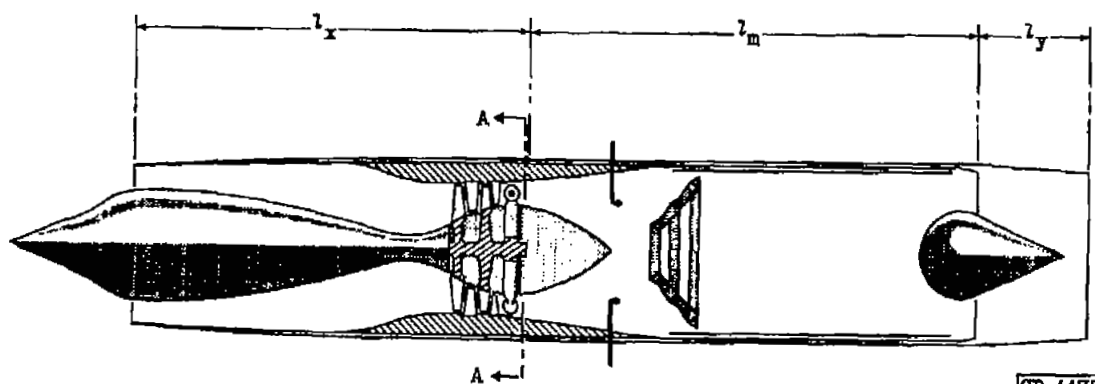
TABLE VI. - AIR-TURBOROCKET ENGINE PROPORTIONS

	Design flight Mach number			
	2.3			2.8
	One-stage compressor	Two-stage compressor	Three-stage compressor	One-stage compressor
Diameter ratios:				
Inlet, d_1/d_1	1.07	1.07	1.07	1.21
Maximum nacelle, d_m/d_1	1.58	1.38	1.20	1.82
Exhaust-nozzle plug, d_{pl}/d_1	.64	.62	.55	.85
Length-to-diameter ratios:				
Forebody, l_x/d_1	3.50	3.50	3.50	3.50
Midsection, l_m/d_1	$\left\{ \begin{array}{l} {}^a 4.96 \\ {}^b 4.56 \end{array} \right.$	$\left\{ \begin{array}{l} {}^a 4.25 \\ {}^b 3.25 \end{array} \right.$	${}^a 3.63$	${}^a 4.84$
Afterbody, l_y/d_1	1.11	.96	.84	1.27

^aBladed turbine.^bRotating-rocket turbine.



(a) Engine with bladed turbine.



CD-4475



Section A-A

(b) Engine with rotating-rocket turbine.

Figure 1. - Schematic drawing of typical air-turborocket engines.

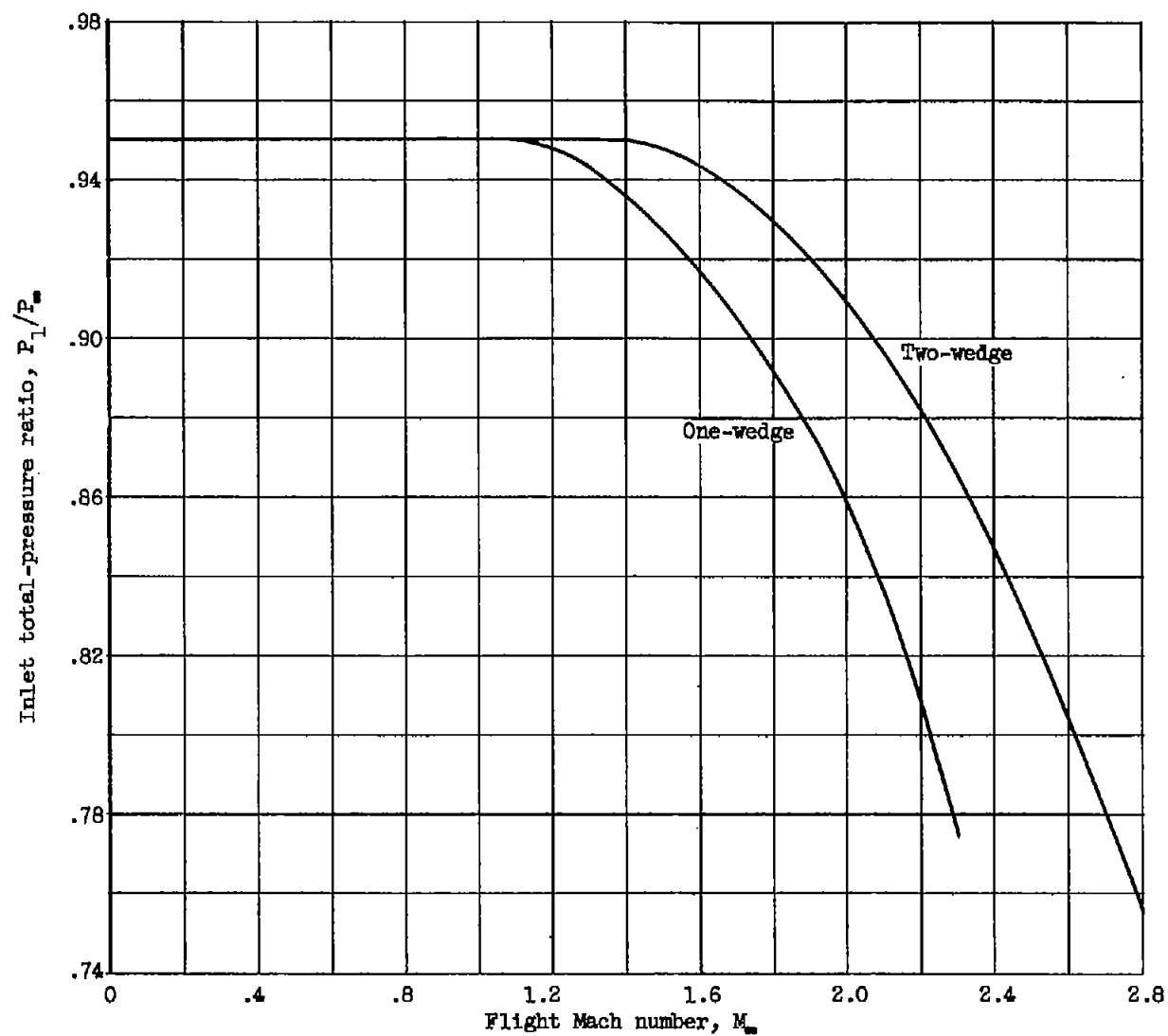


Figure 2. - Inlet-diffuser pressure recovery with one- and two-wedge centerbodies.

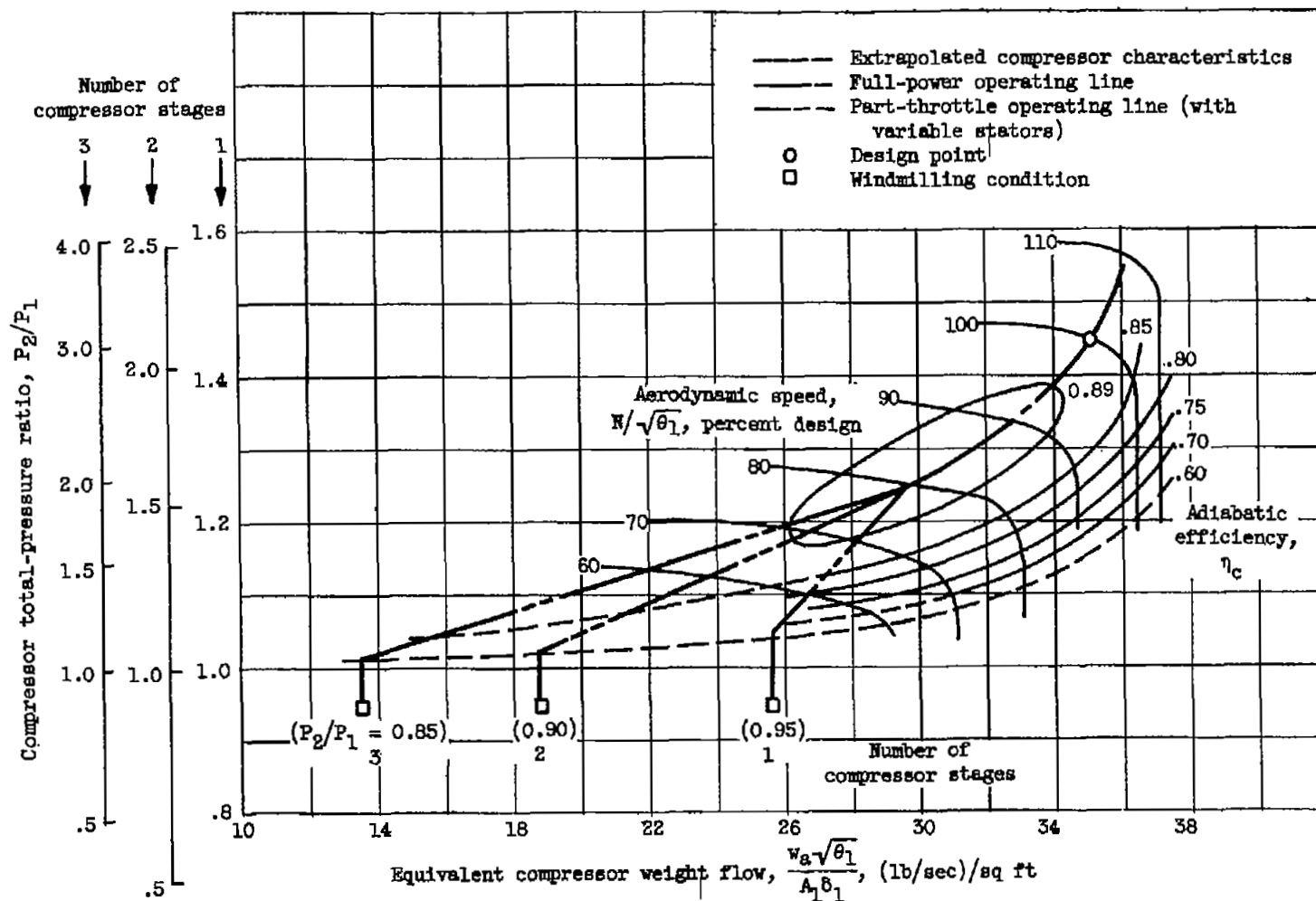


Figure 3. - Compressor performance map.

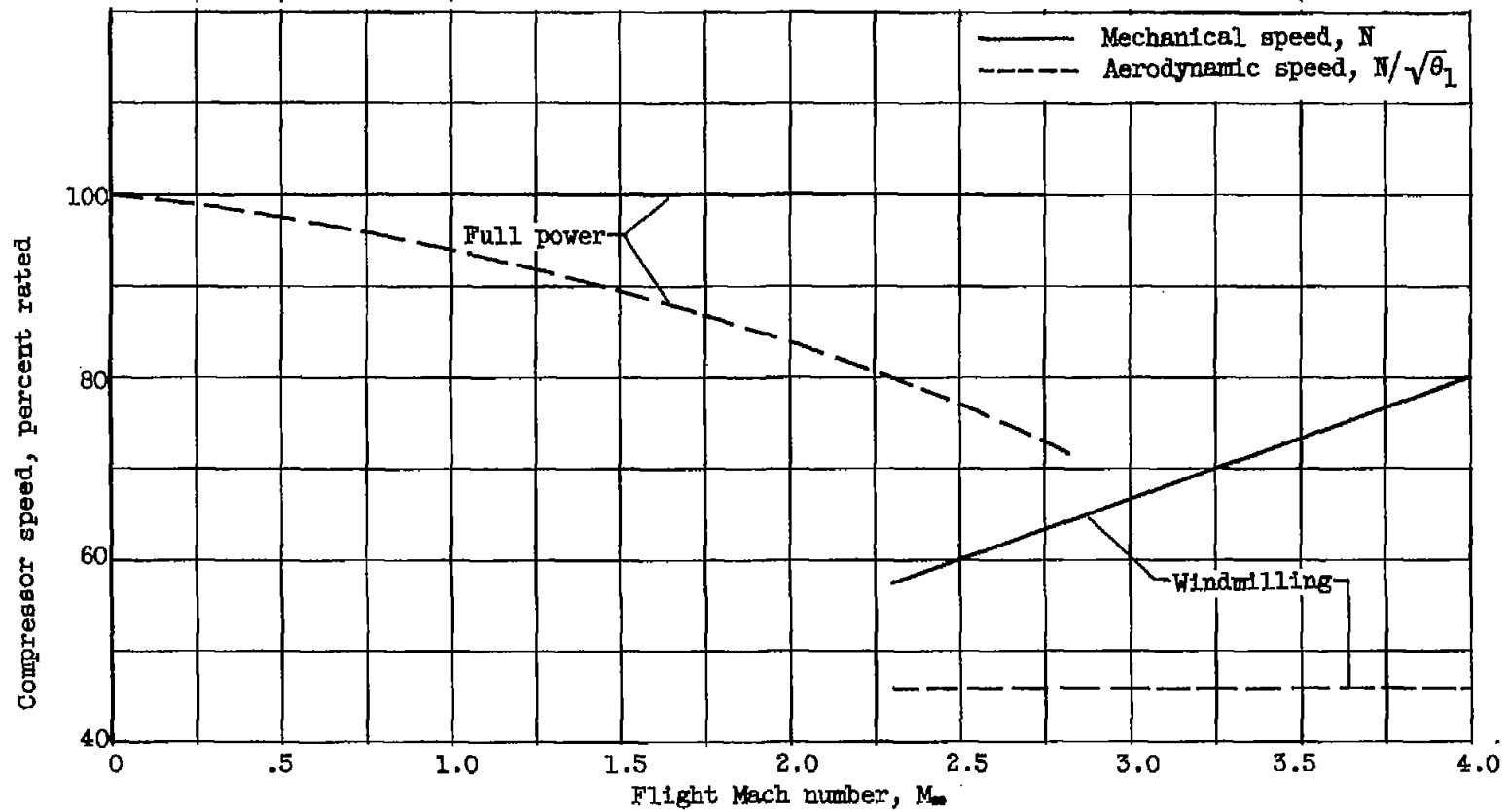


Figure 4. - Variation of one-stage compressor speed with flight Mach number. Altitude scheduled with Mach number (fig. 7).

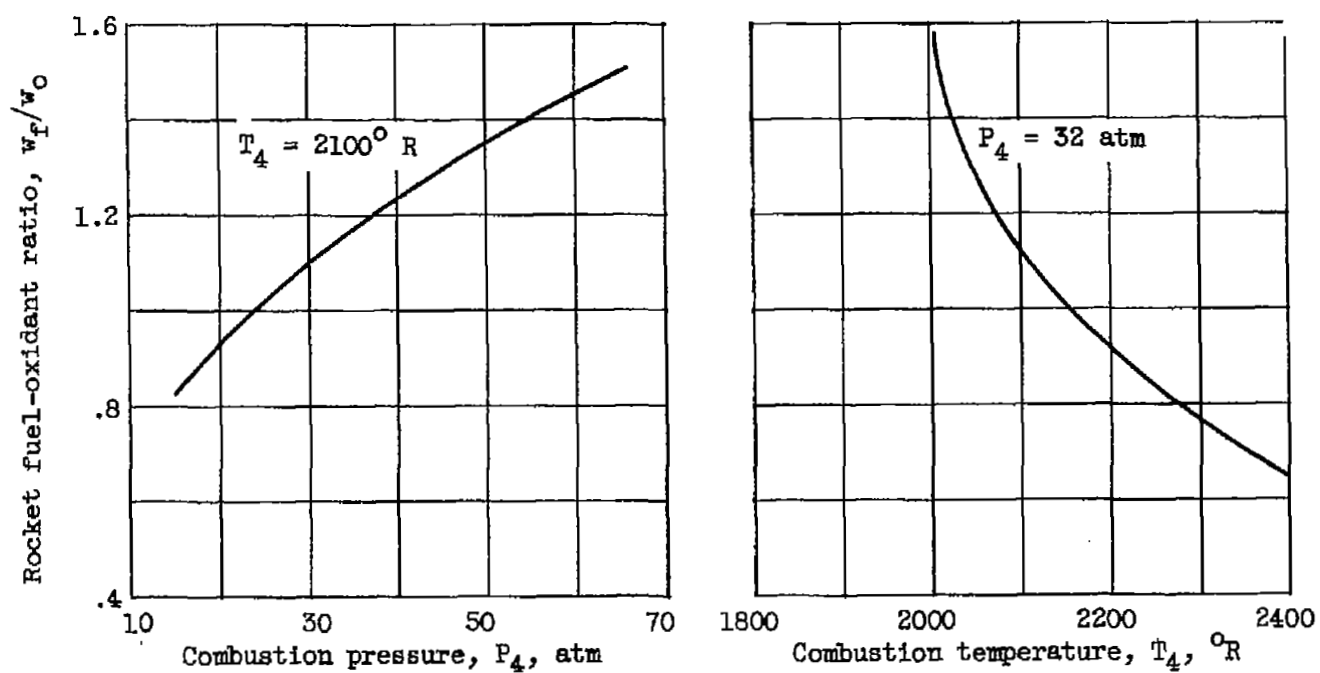


Figure 5. - Effect of chamber conditions on rocket fuel-oxidant ratio. Propellants, gasoline and nitric acid.

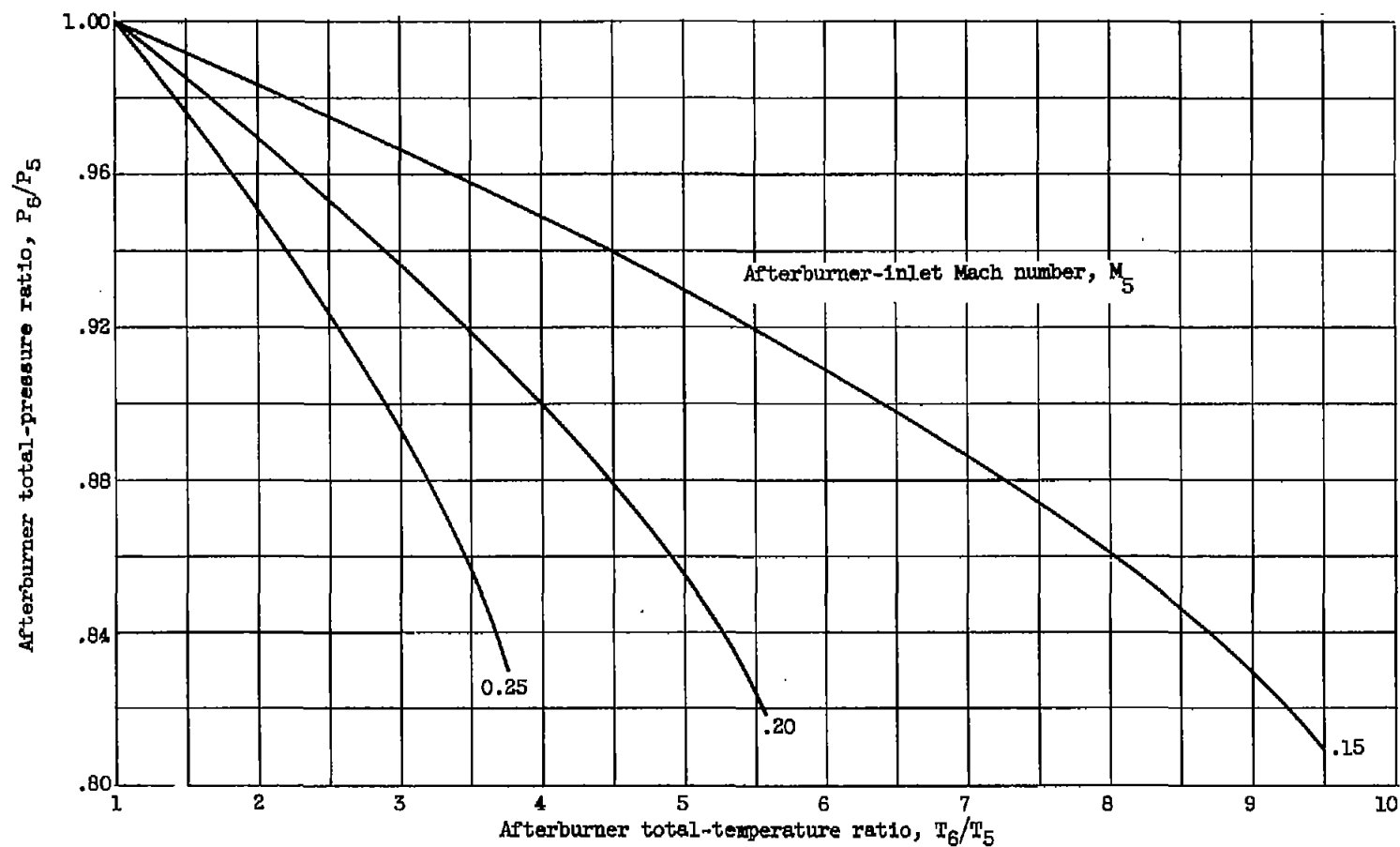


Figure 6. - Effect of afterburner-inlet Mach number and temperature ratio on momentum-pressure drop.

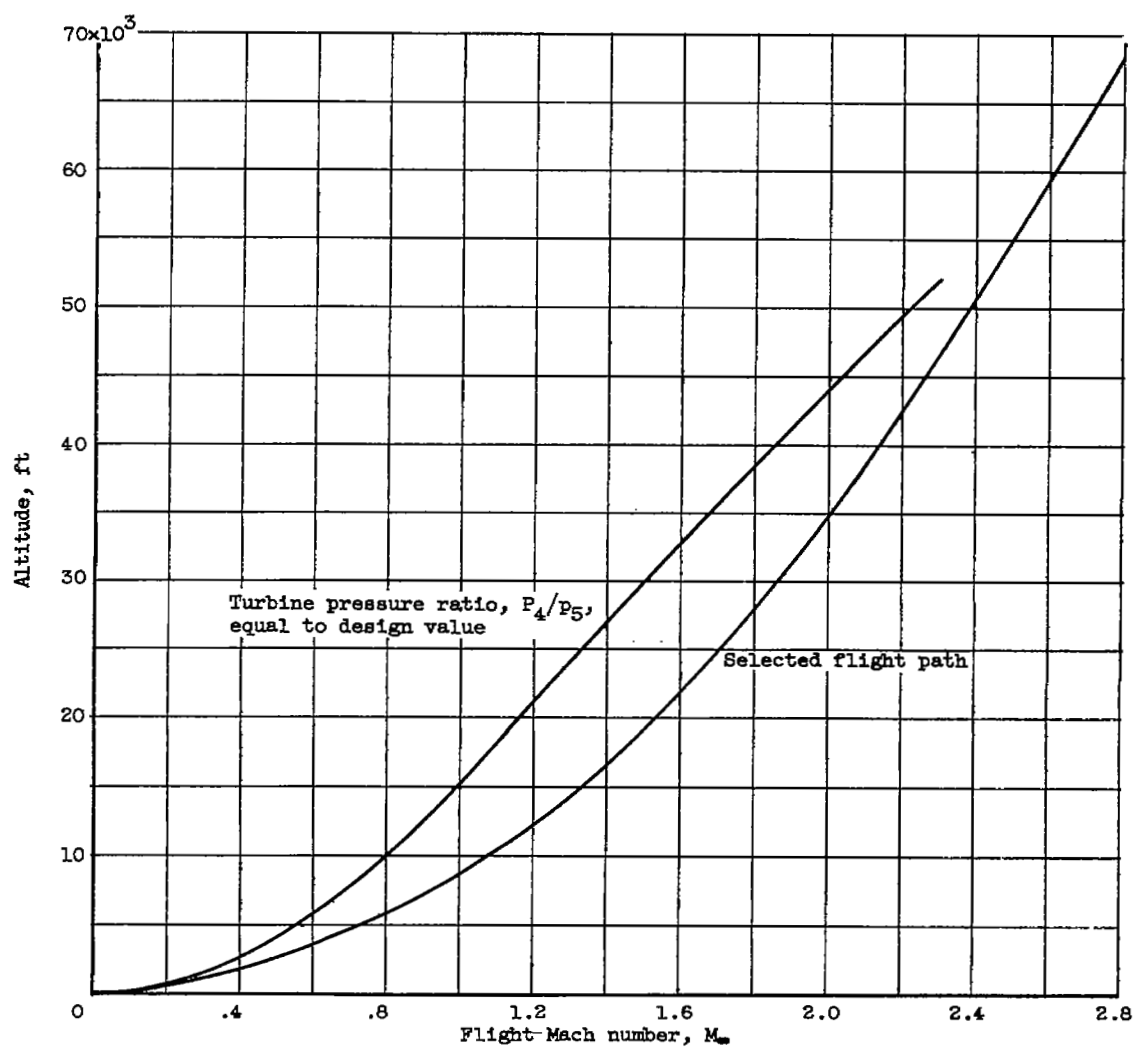


Figure 7. - Assumed schedule of altitude with flight Mach number.

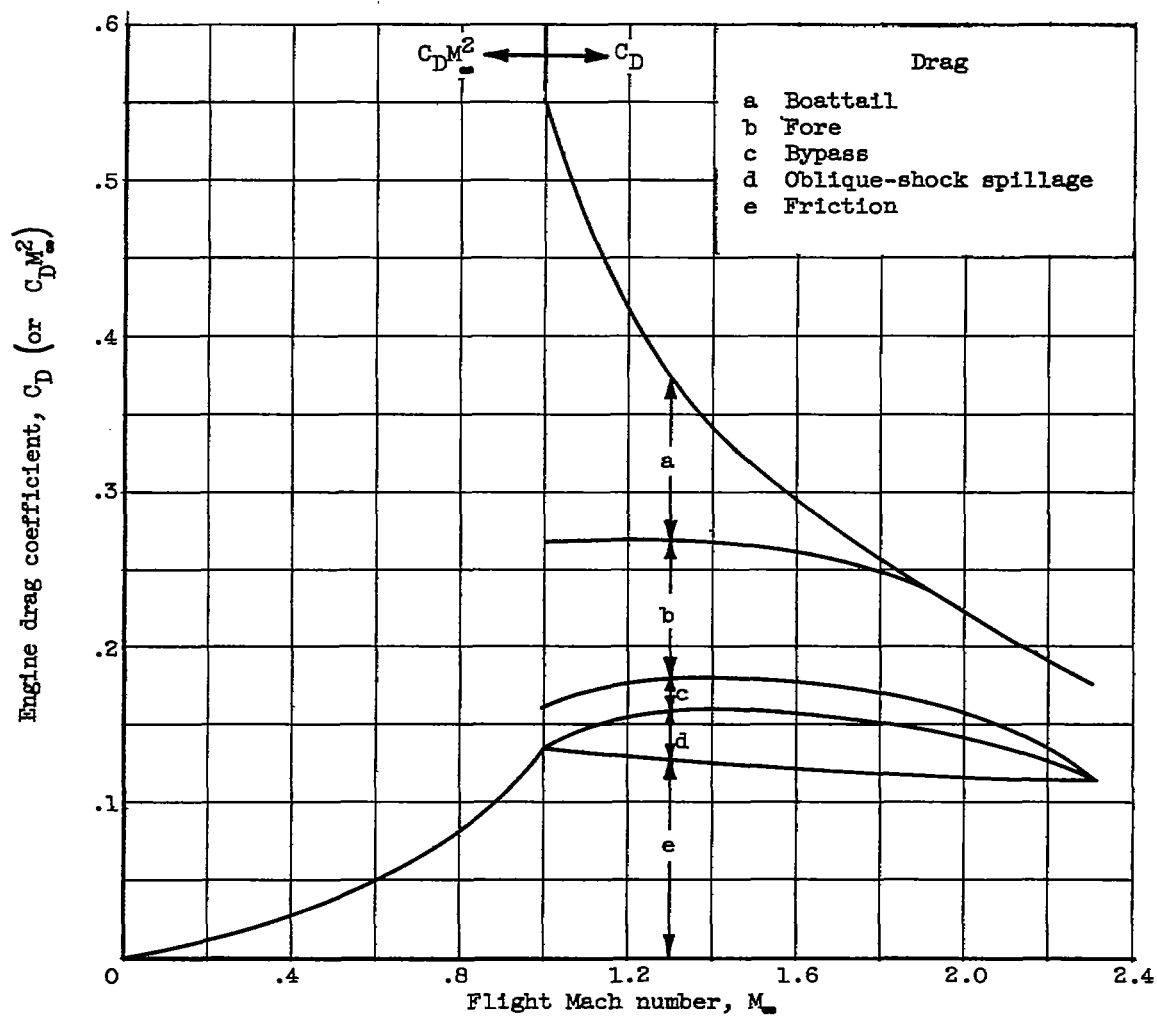
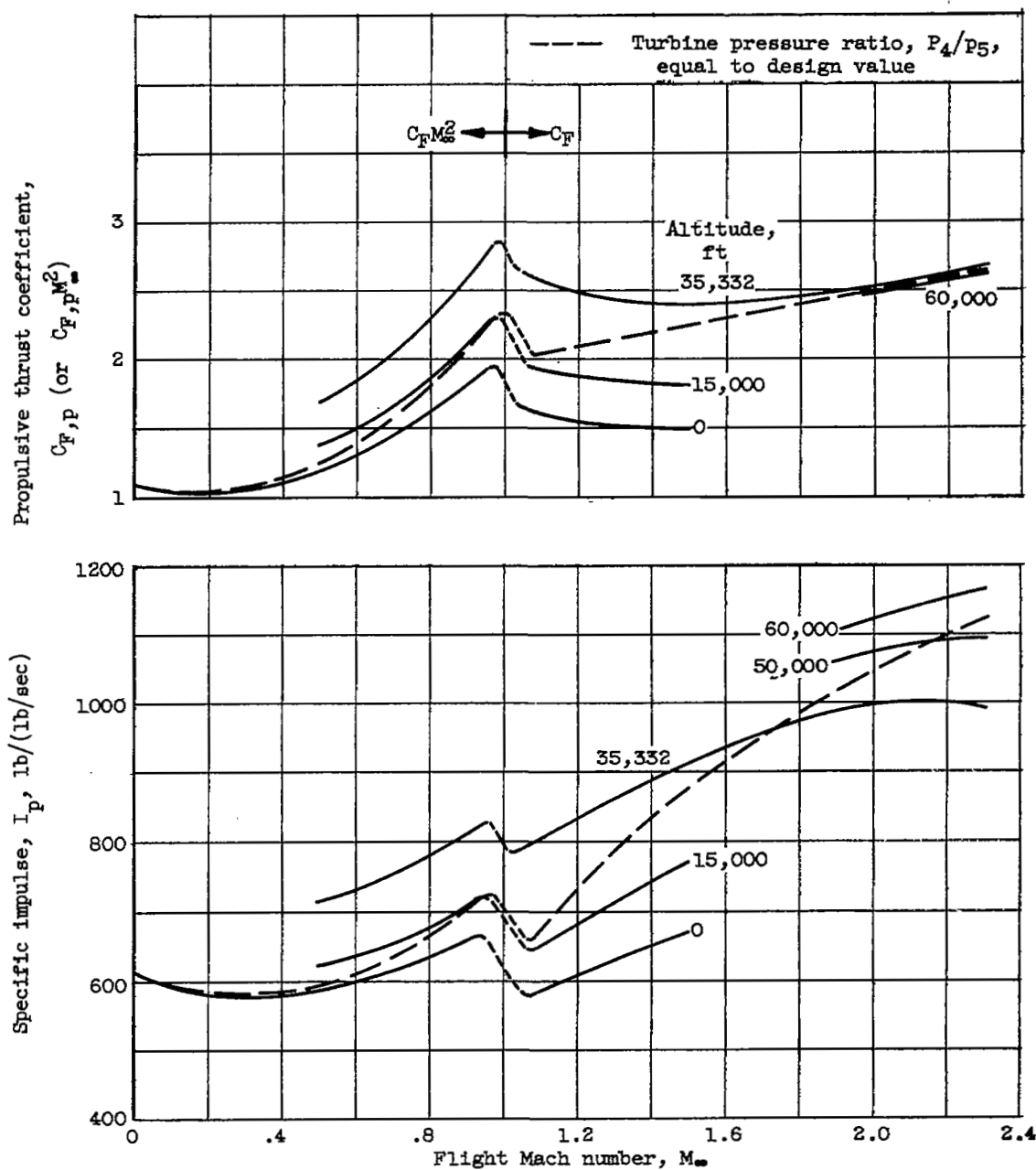


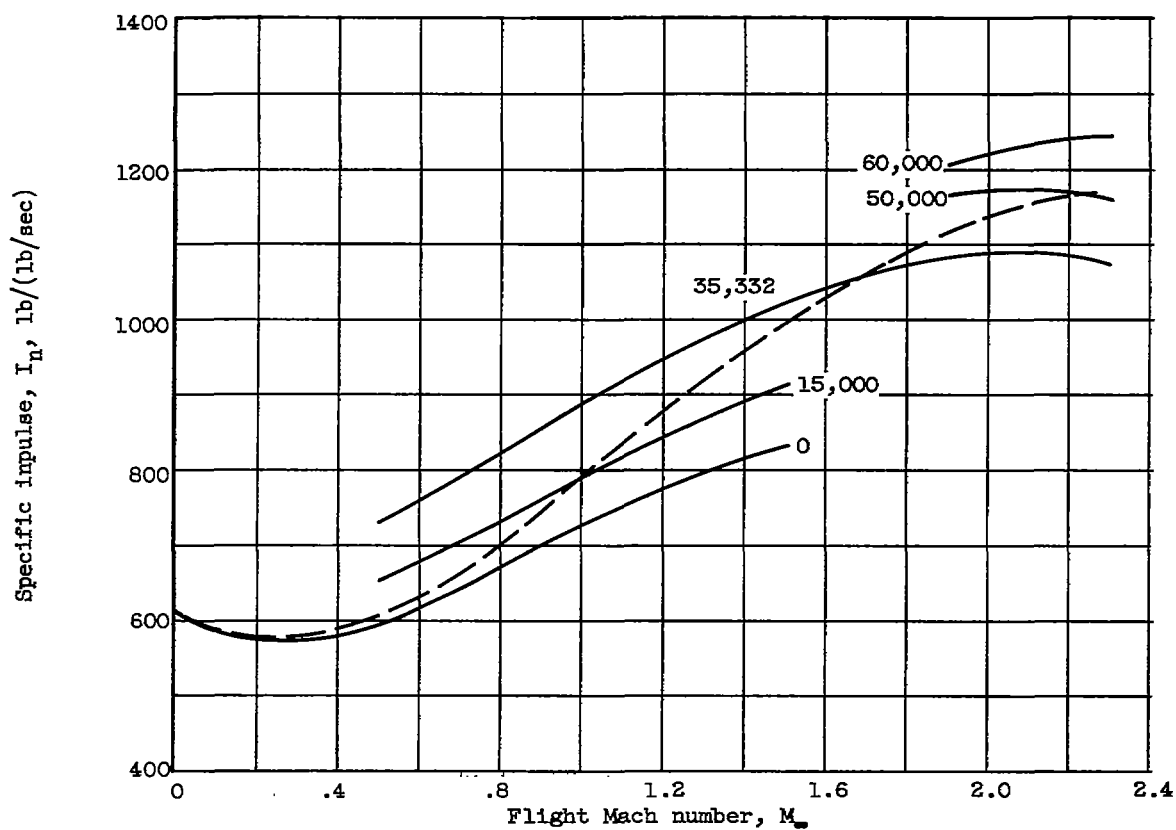
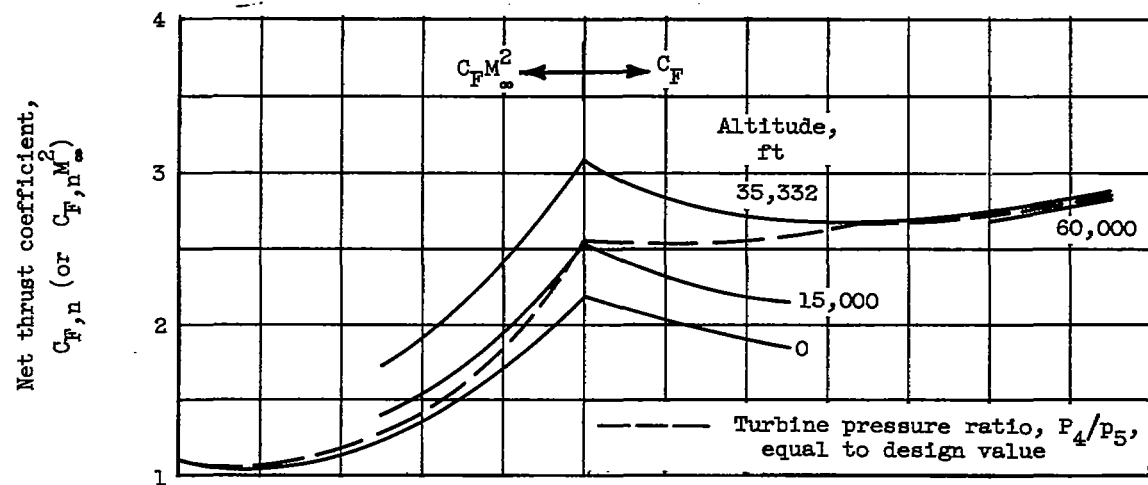
Figure 8. - Distribution of engine drags over a range of flight Mach numbers. Engine with one-stage compressor operating at full power; design flight Mach number, 2.3.



(1) With drag.

(a) Full-power operation at several altitudes.

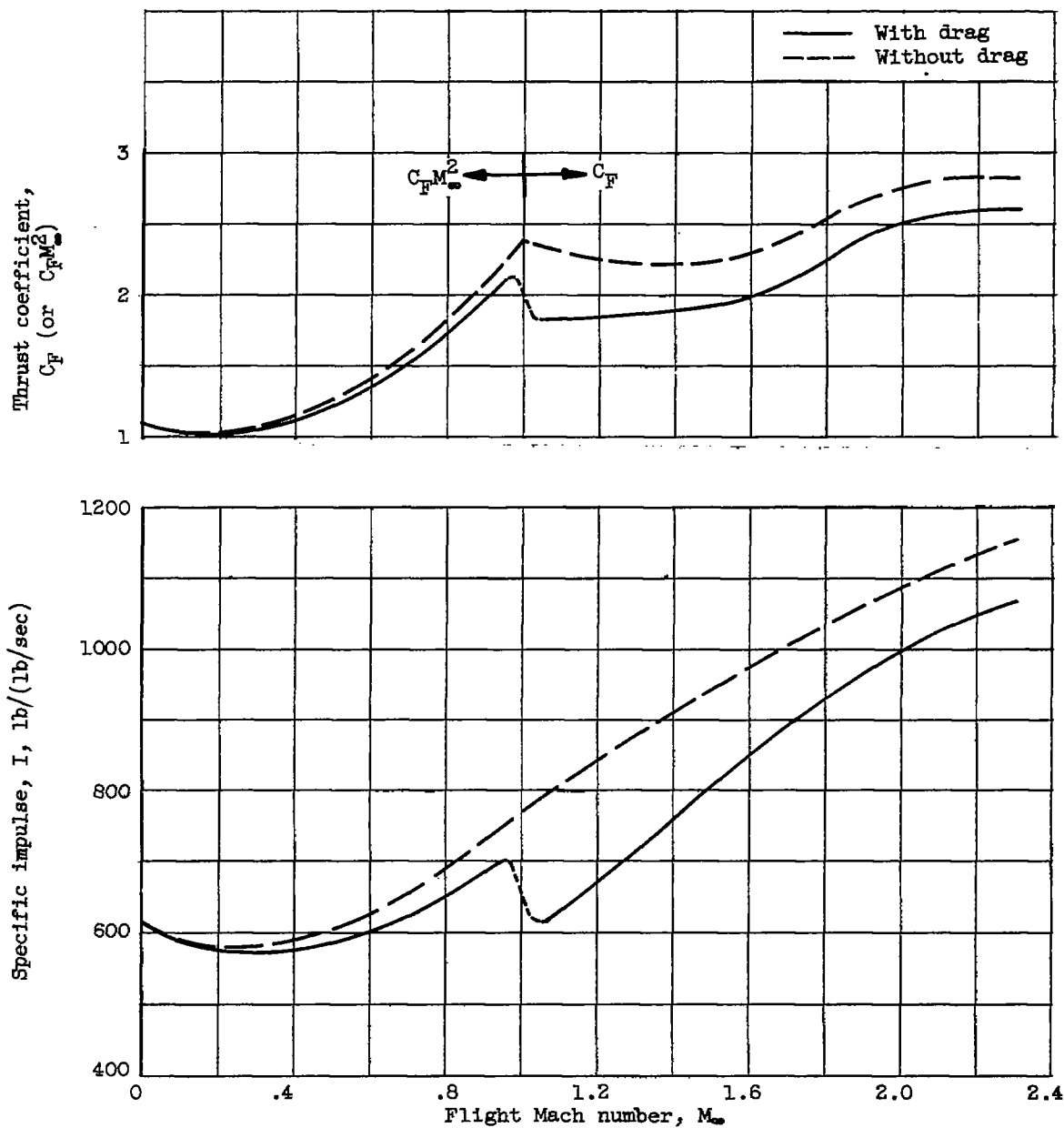
Figure 9. - Performance of reference engine with one-stage compressor.



(2) Without drag.

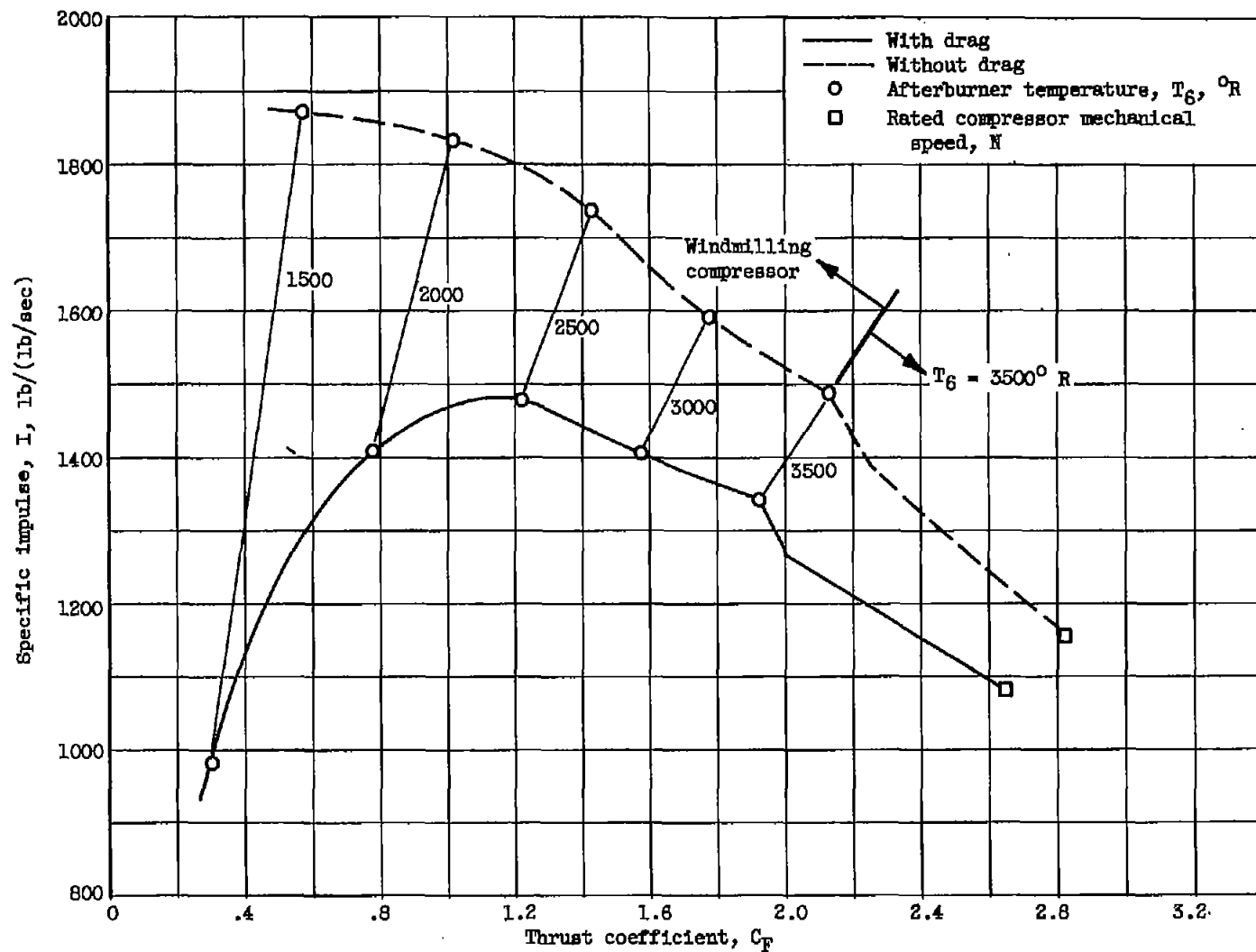
(a) Concluded. Full-power operation at several altitudes.

Figure 9. - Continued. Performance of reference engine with one-stage compressor.



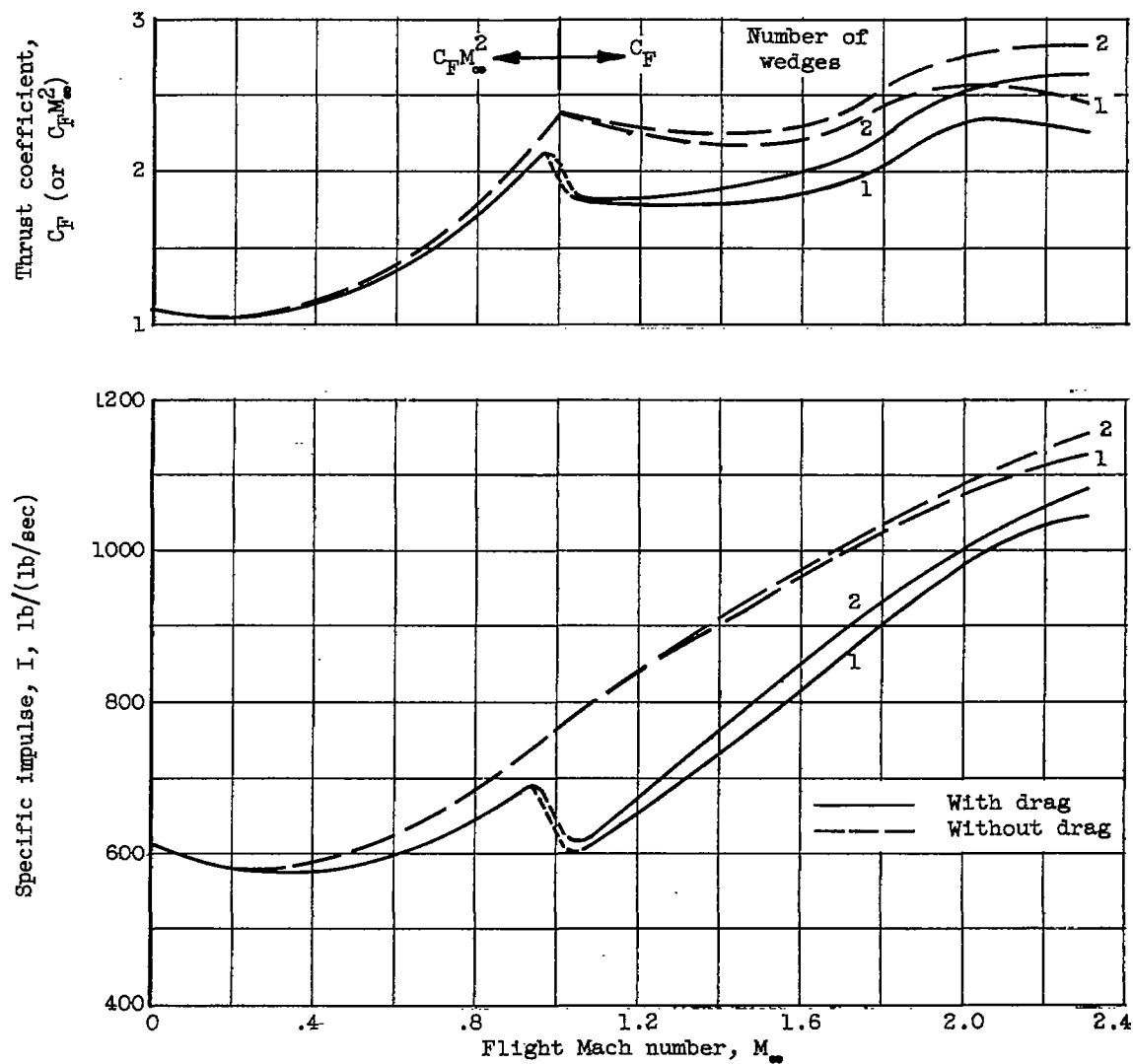
(b) Full-power operation for selected flight path.

Figure 9. - Continued. Performance of reference engine with one-stage compressor.



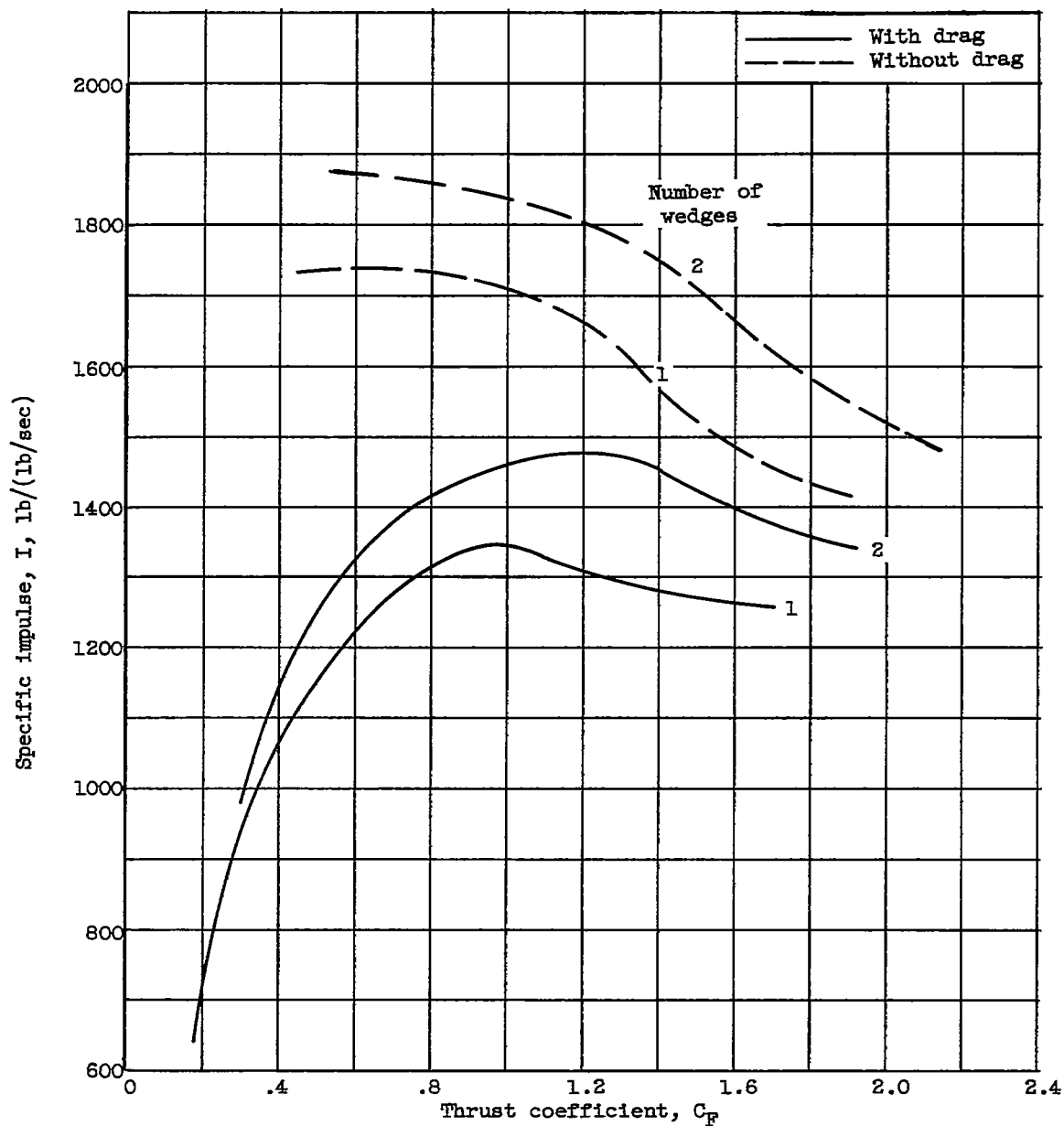
(c) Part-power operation; flight Mach number, 2.3.

Figure 9. - Concluded. Performance of reference engine with one-stage compressor.



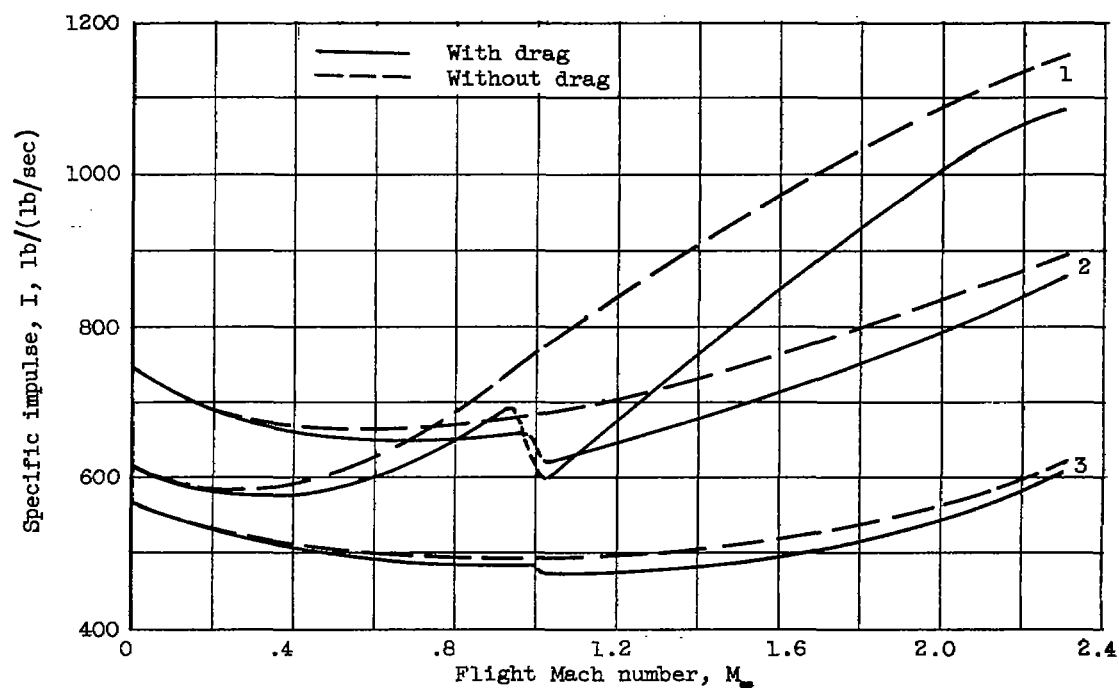
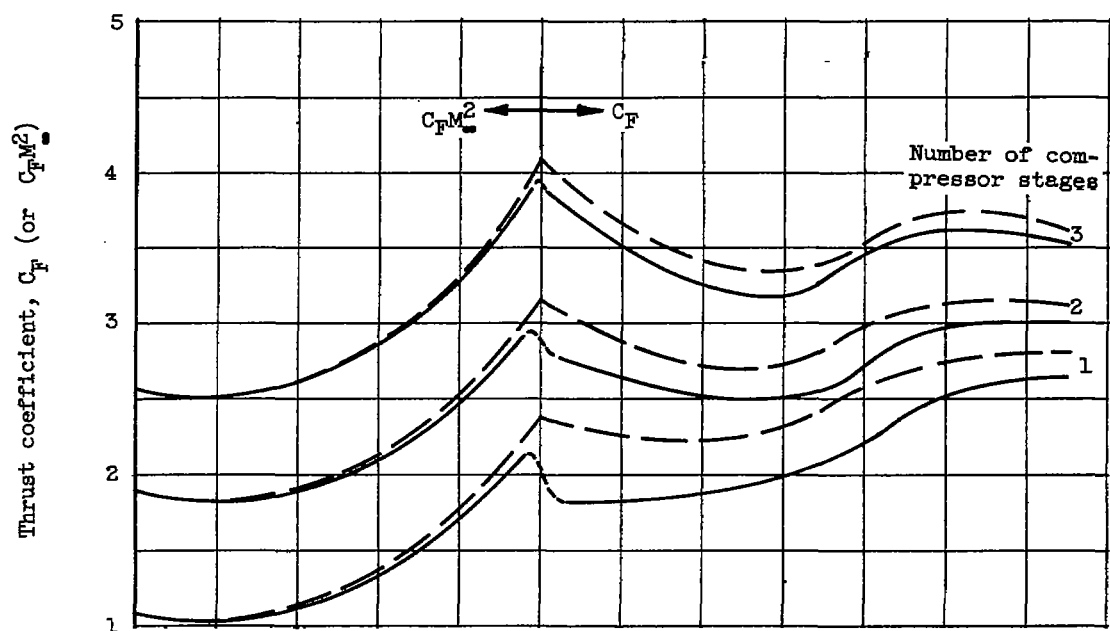
(a) Full-power operation.

Figure 10. - Effect of inlet type on engine performance. Design flight Mach number, 2.3.



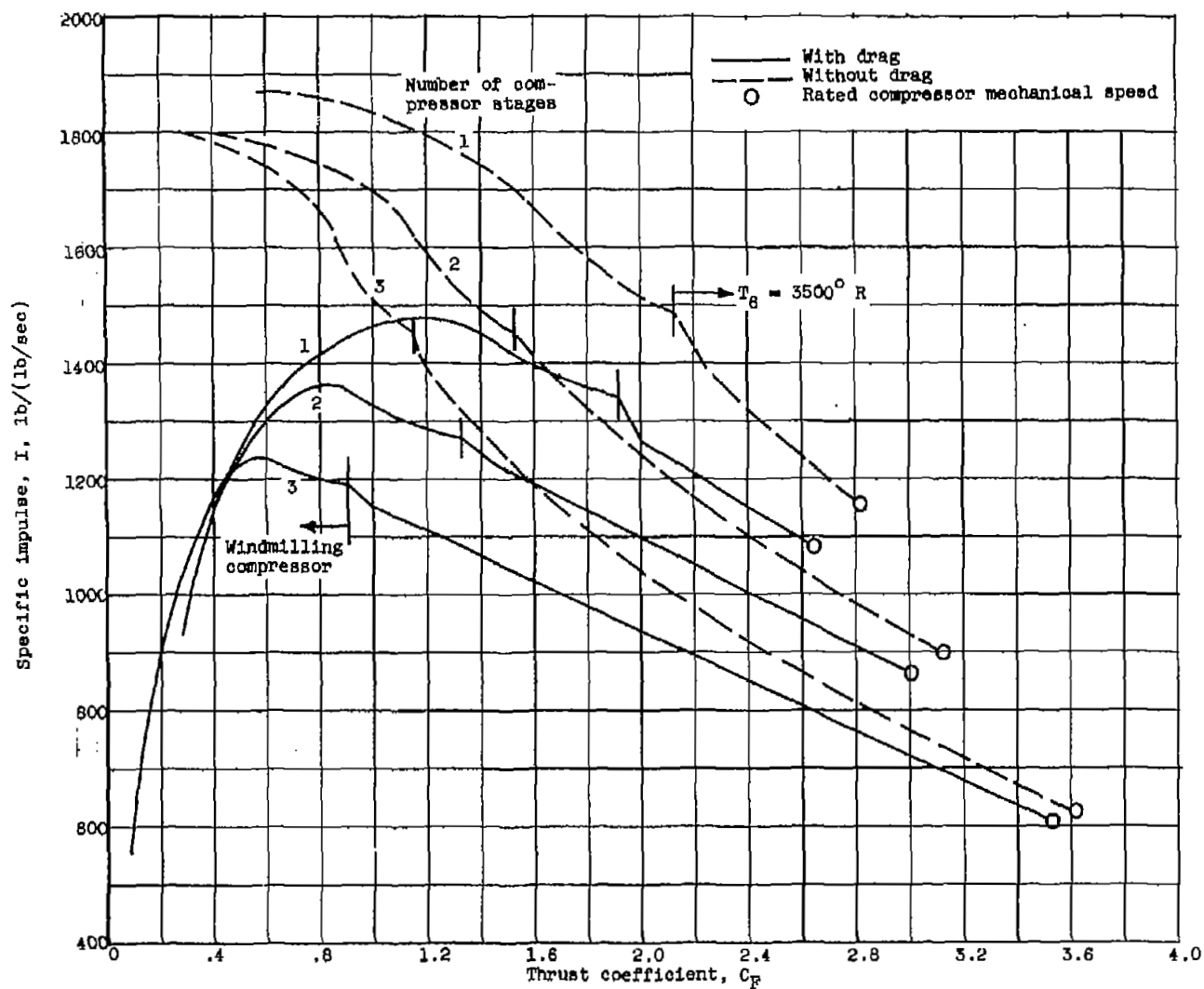
(b) Part-power operation; flight Mach number, 2.3.

Figure 10. - Concluded. Effect of inlet type on engine performance.
Design flight Mach number, 2.3.



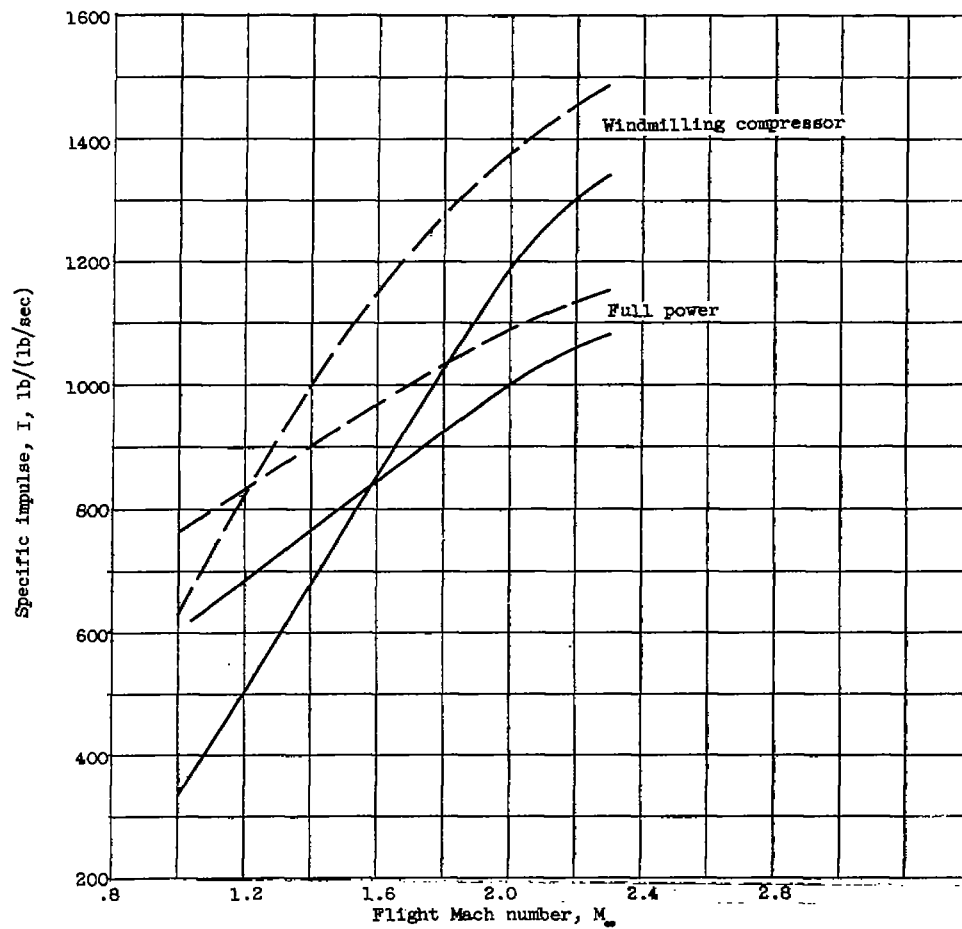
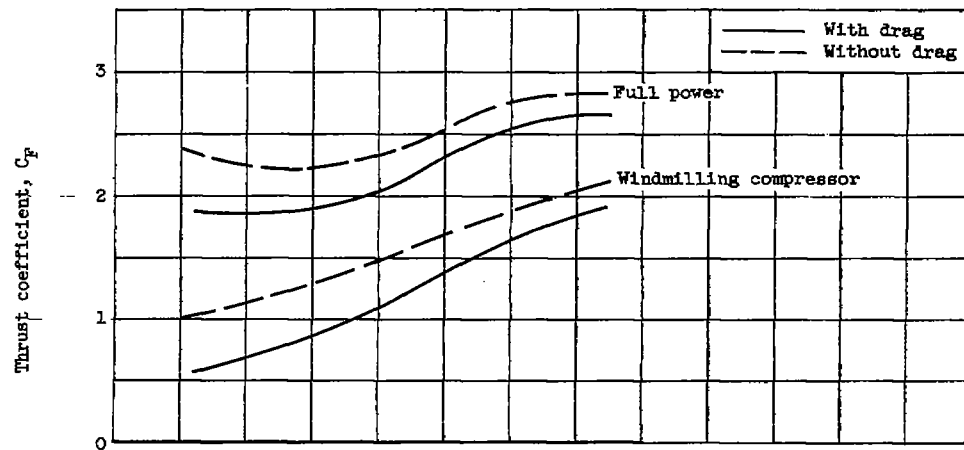
(a) Full-power operation.

Figure 11. - Effect of design compressor pressure ratio on engine performance. Design flight Mach number, 2.3.



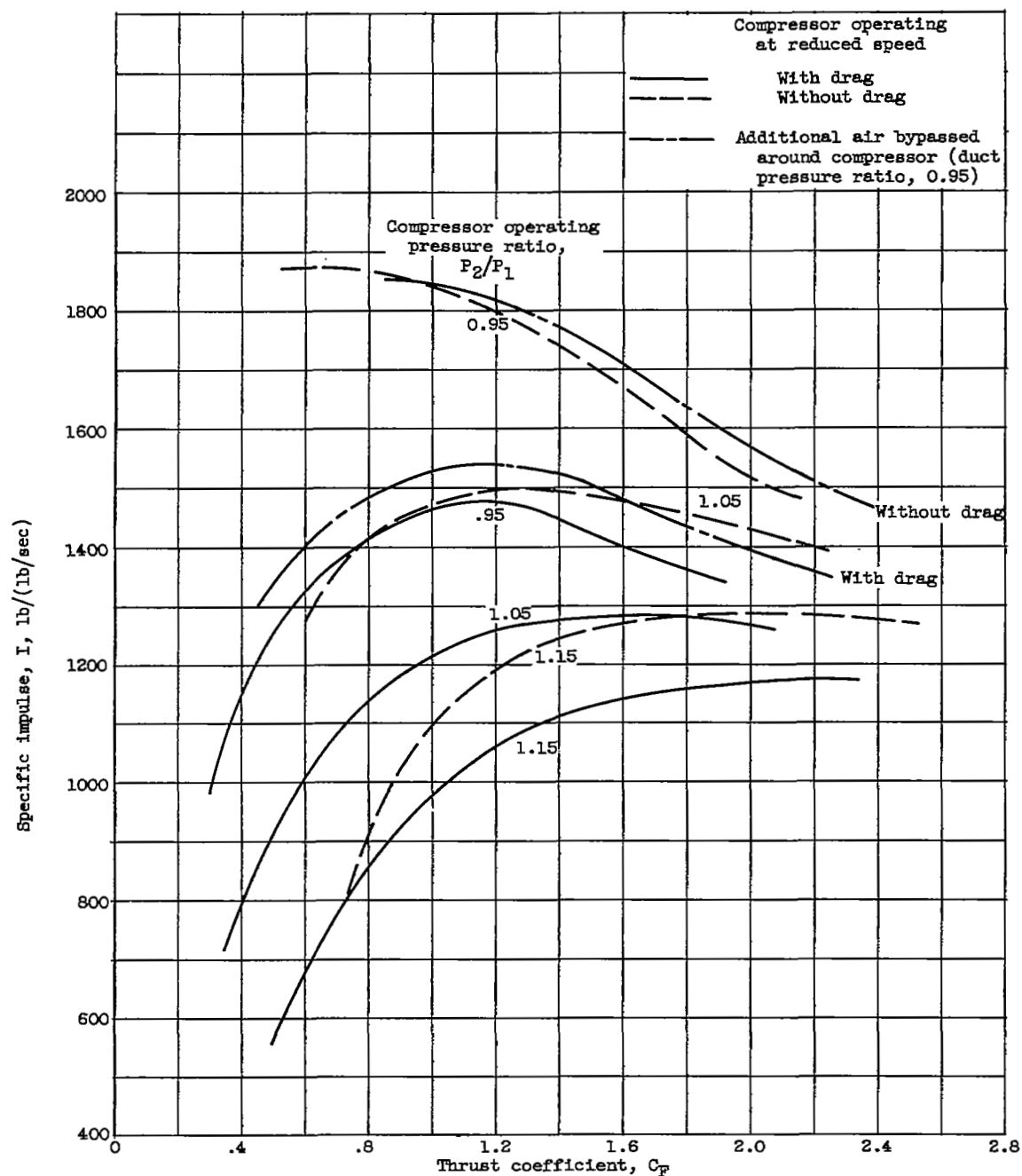
(b) Part-power operation; flight Mach number, 2.3.

Figure 11. - Concluded. Effect of design compressor pressure ratio on engine performance. Design flight Mach number, 2.3.



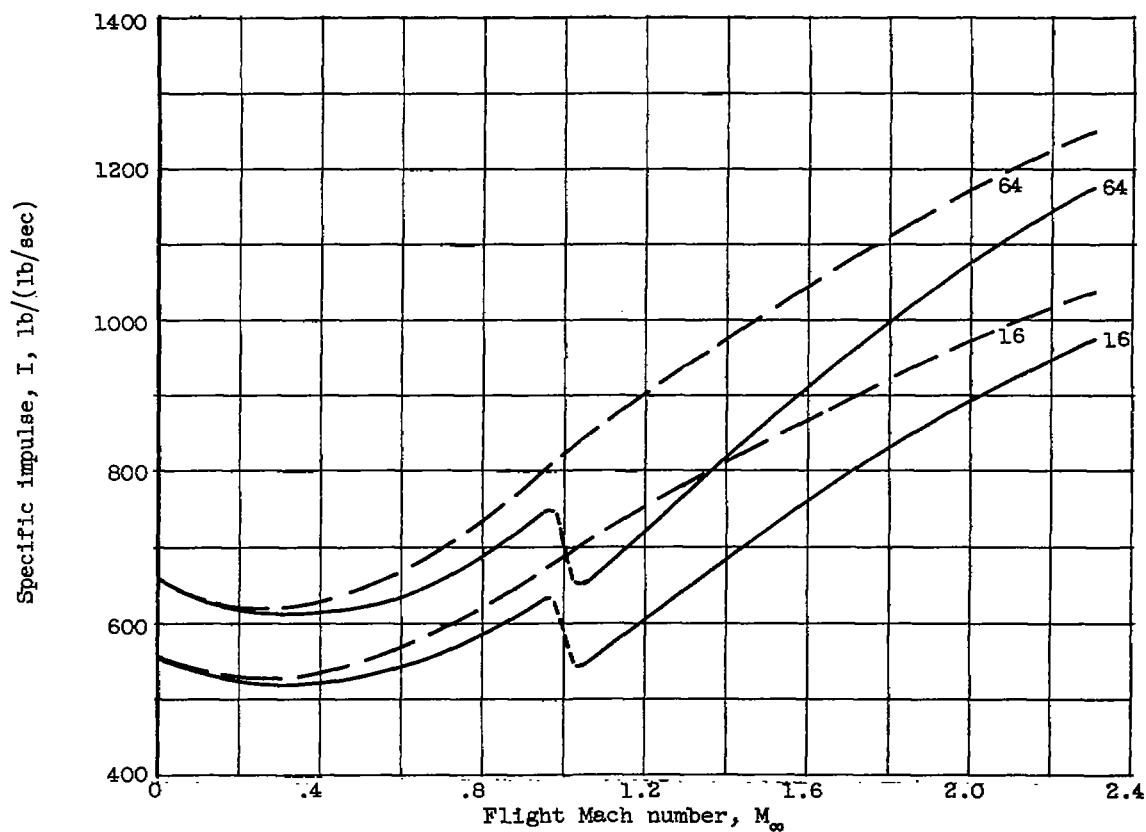
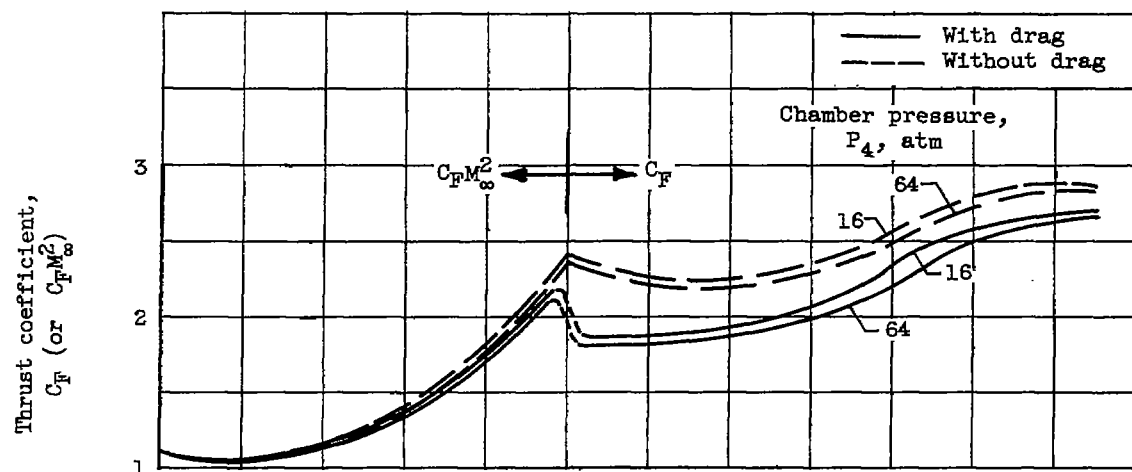
(a) Full-power operation.

Figure 12. - Effect of compressor operation on engine performance. Design flight Mach number, 2.3.



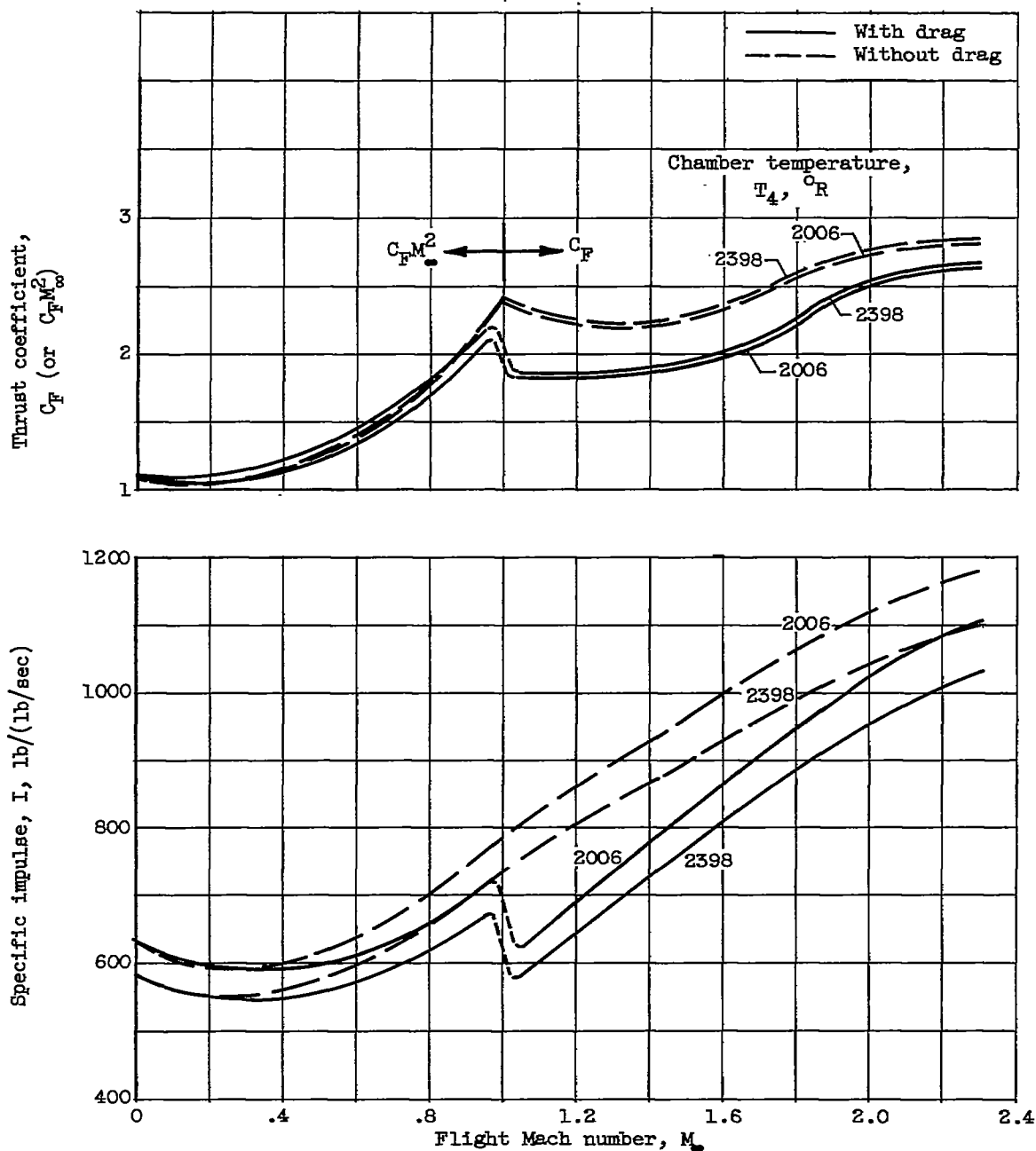
(b) Part-power operation; flight Mach number, 2.3.

Figure 12. - Concluded. Effect of compressor operation on engine performance. Design flight Mach number, 2.3.



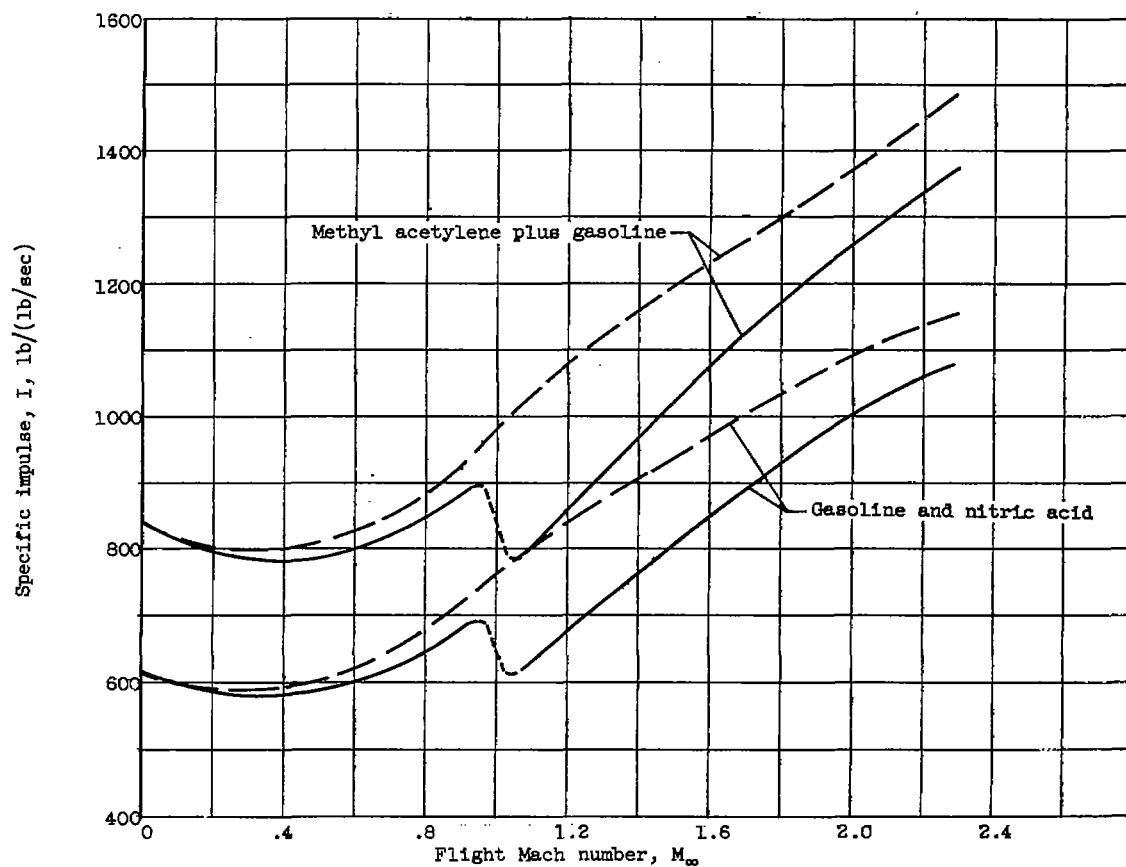
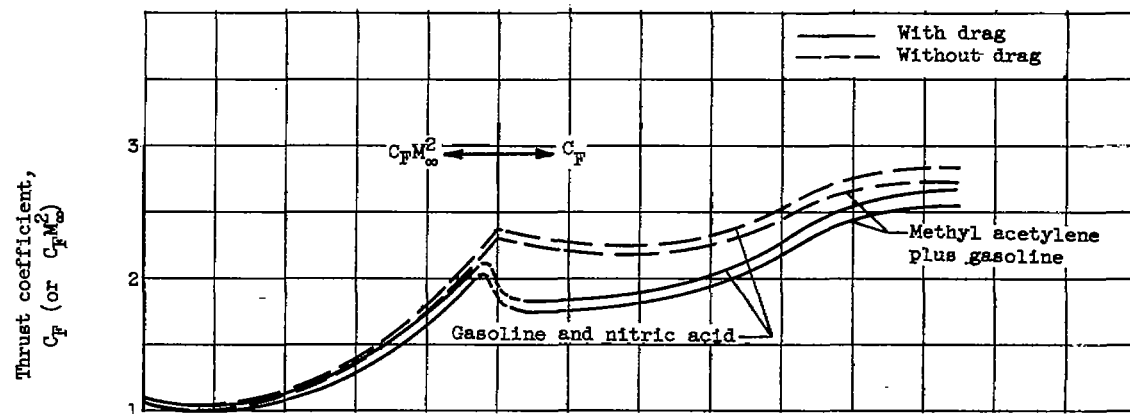
(a) Chamber pressure.

Figure 13. - Effect of gas-generator variables on full-power engine performance. Design flight Mach number, 2.3.



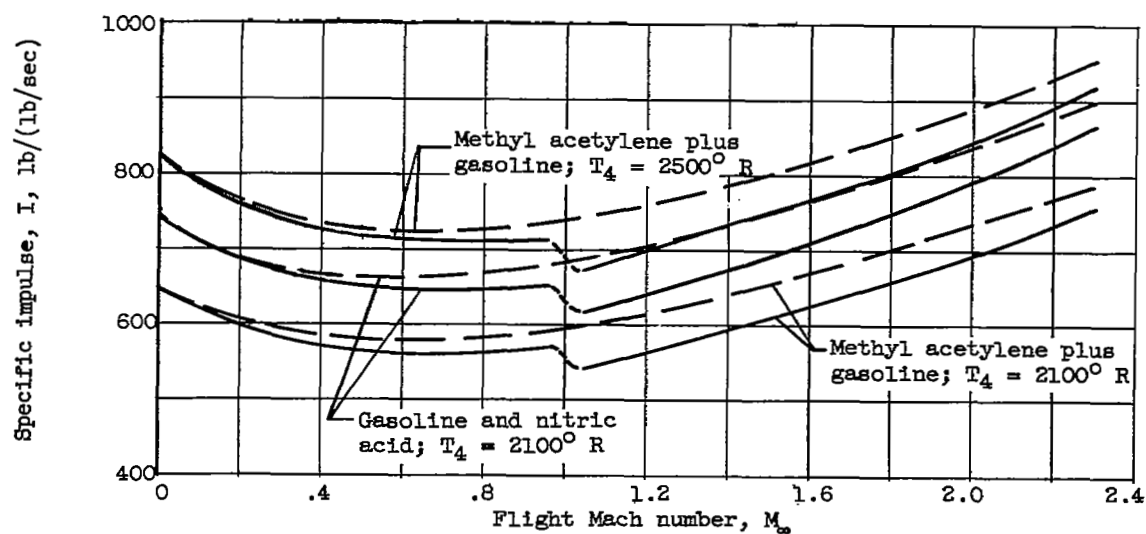
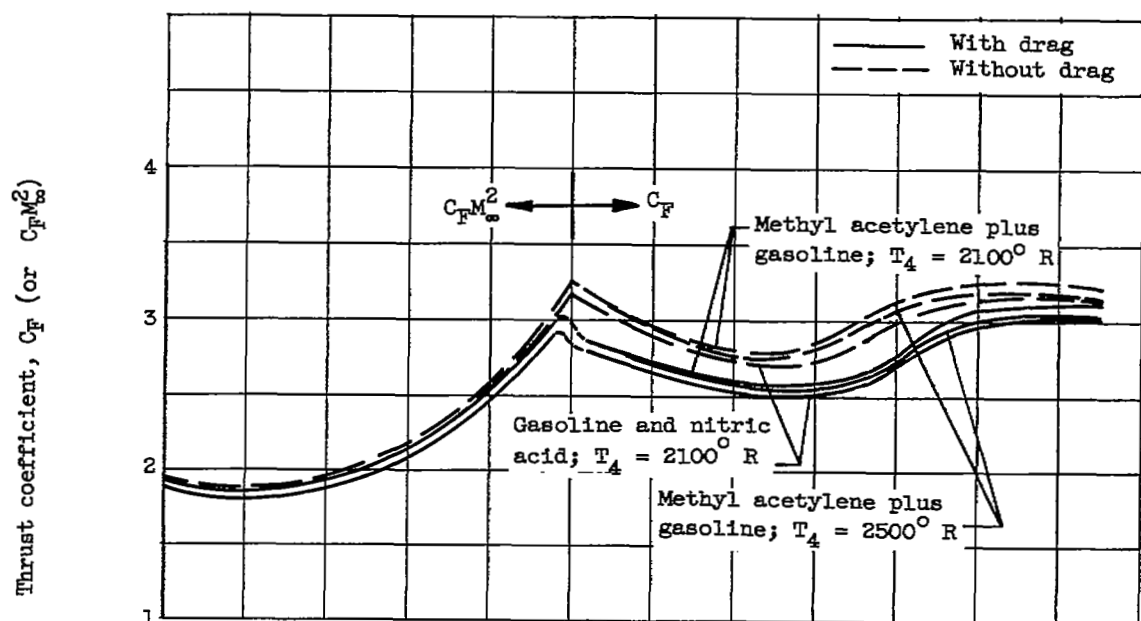
(b) Chamber temperature.

Figure 13: - Concluded. Effect of gas-generator variables on full-power engine performance. Design flight Mach number, 2.3.



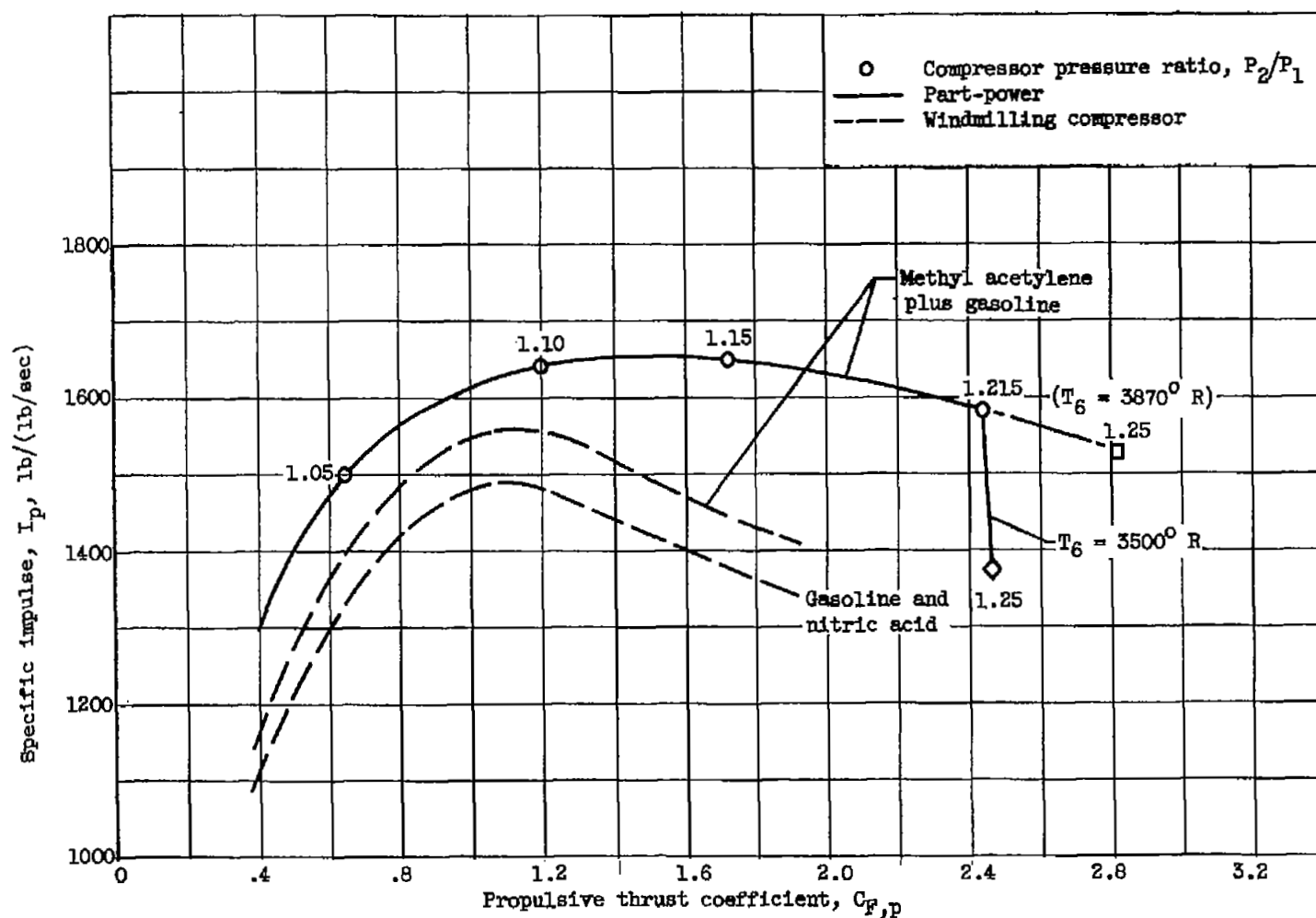
(a) Engine with one-stage compressor.

Figure 14. - Effect of propellant type on full-power engine performance. Design flight Mach number, 2.3.



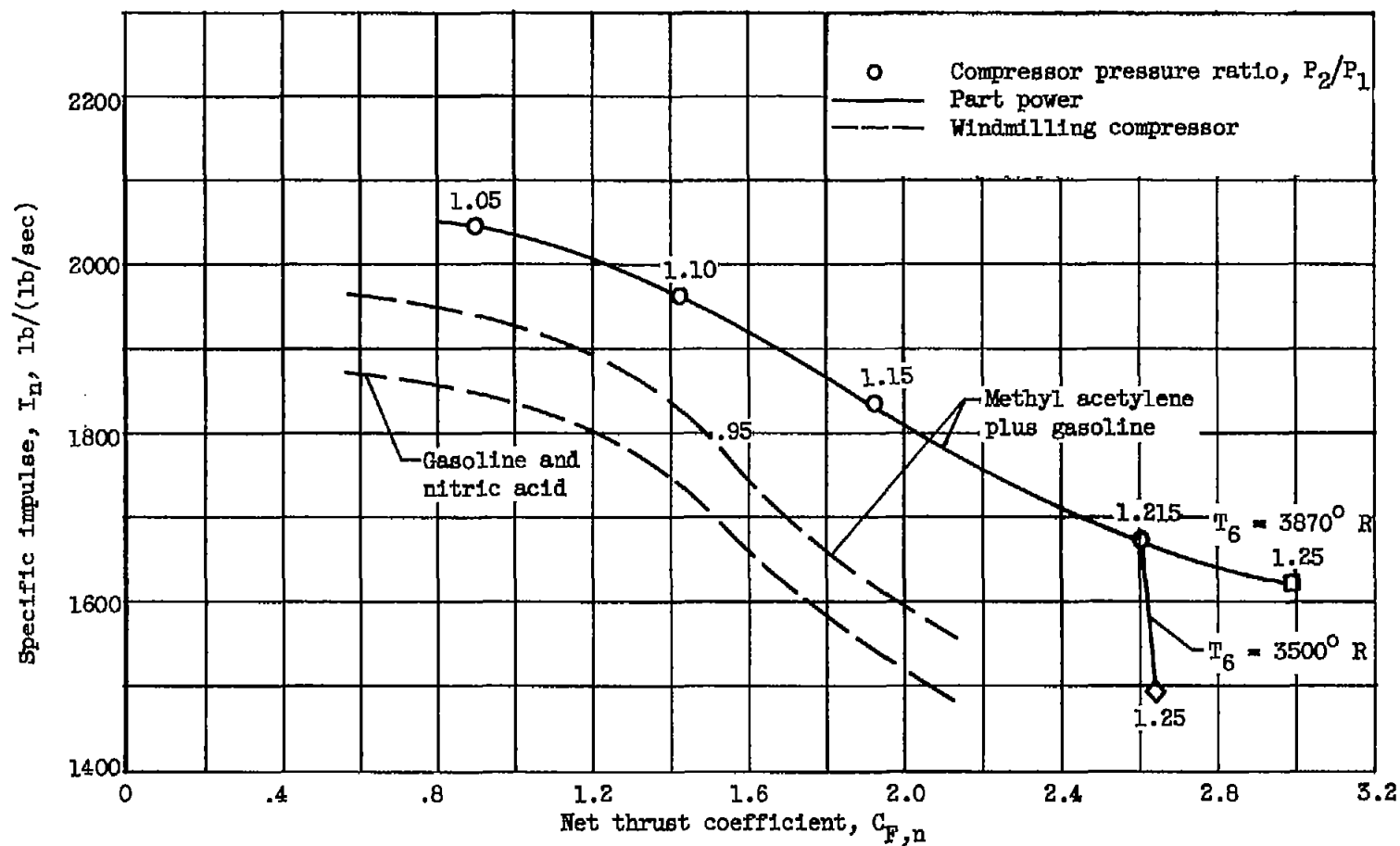
(b) Engine with two-stage compressor.

Figure 14. - Concluded. Effect of propellant type on full-power engine performance. Design flight Mach number, 2.3.



(a) With drag.

Figure 15. - Effect of propellant type on part-power performance of engine with one-stage compressor.
Design flight Mach number, 2.3; flight Mach number, 2.3.



(b) Without drag.

Figure 15. - Concluded. Effect of propellant type on part-power performance of engine with one-stage compressor. Design flight Mach number, 2.3; flight Mach number, 2.3.

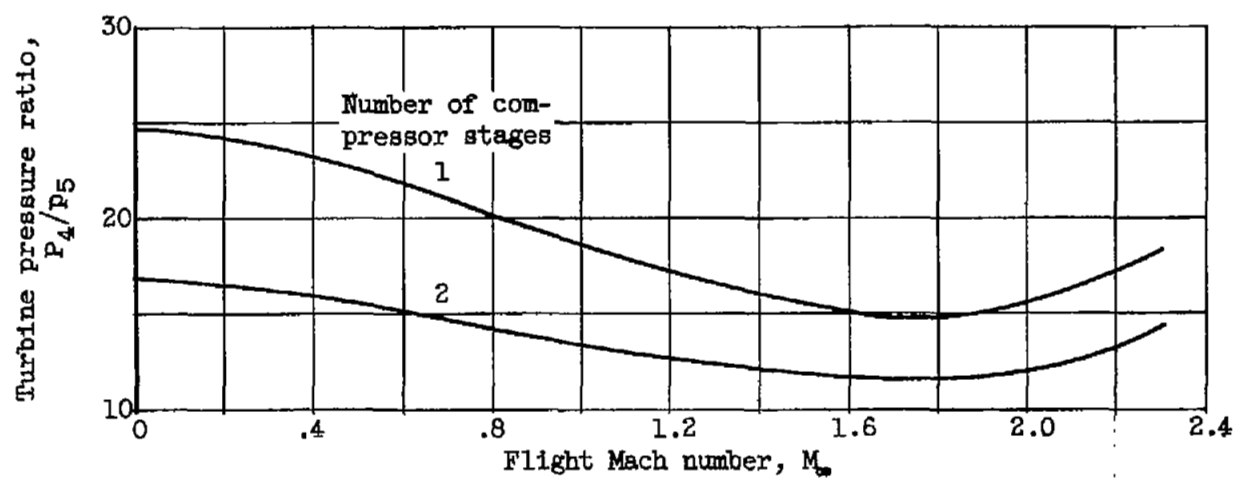


Figure 16. - Variation of turbine pressure ratio with flight Mach number.
Altitude scheduled with Mach number (fig. 7).

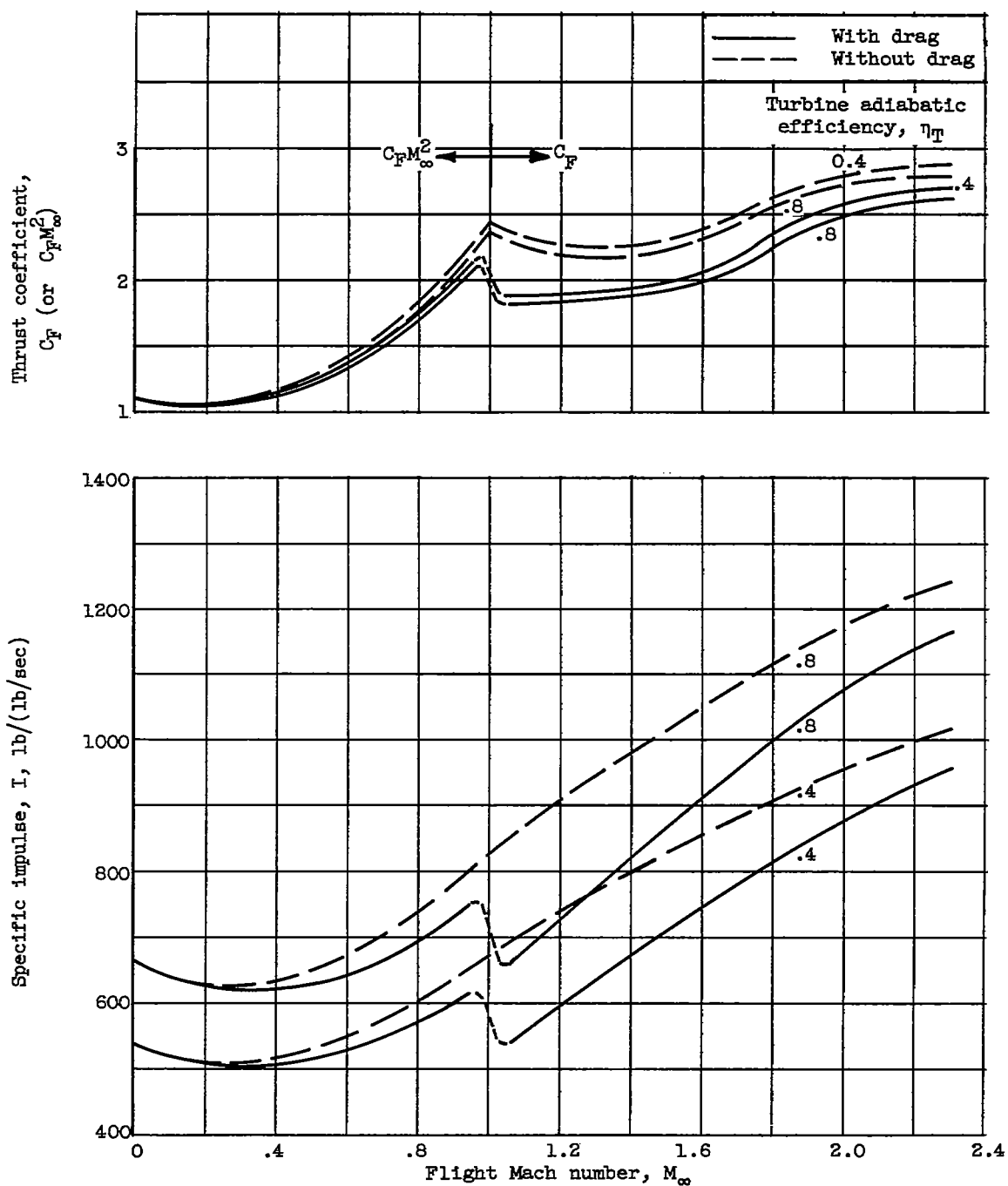
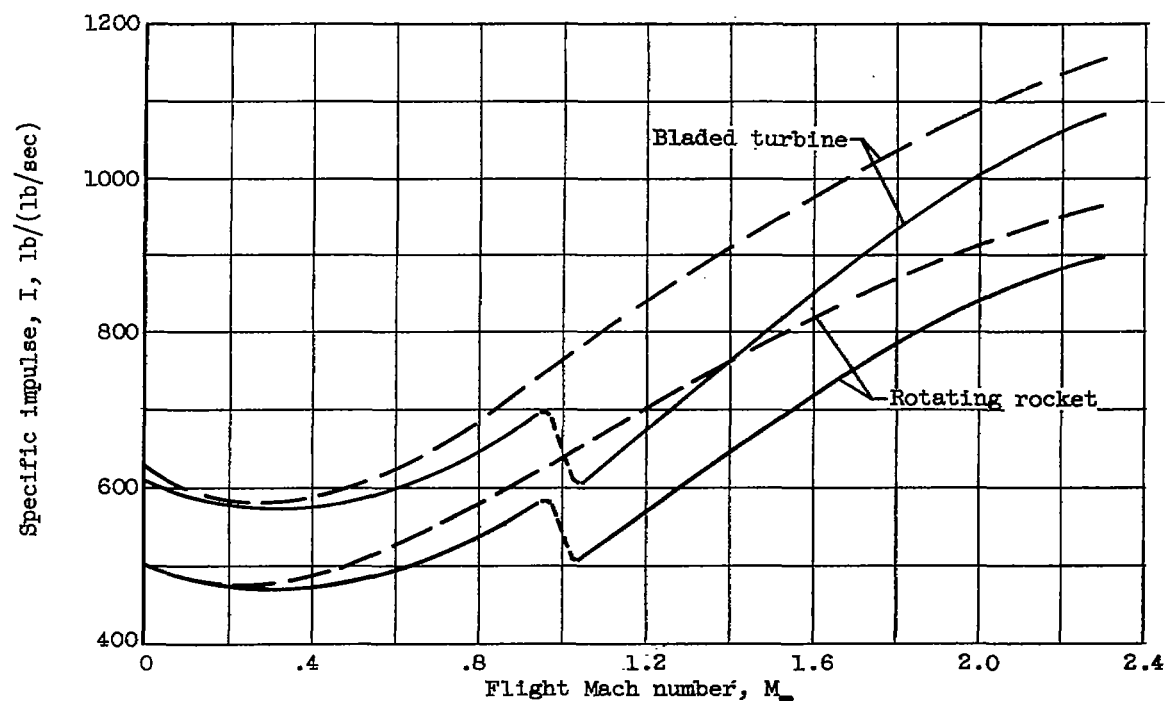
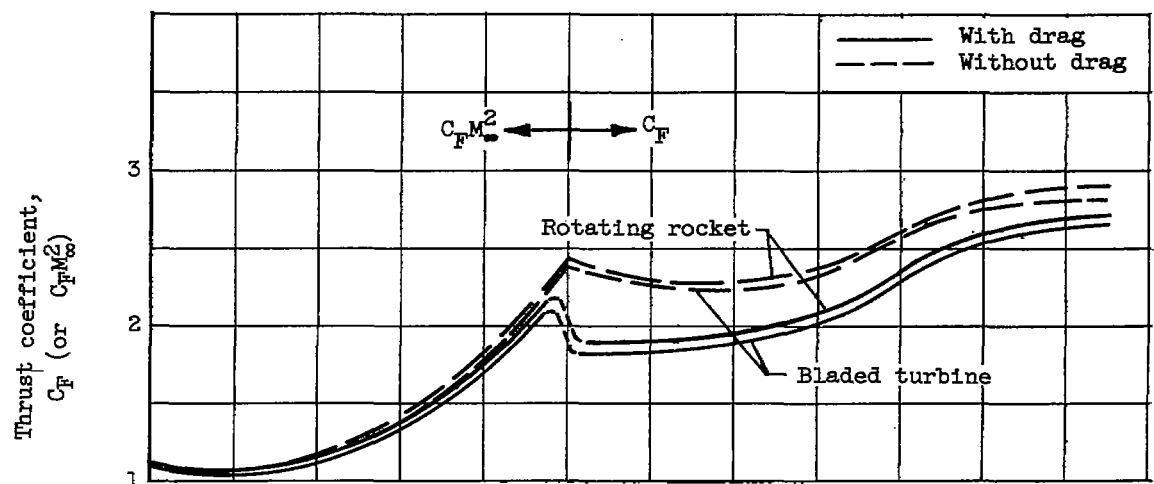
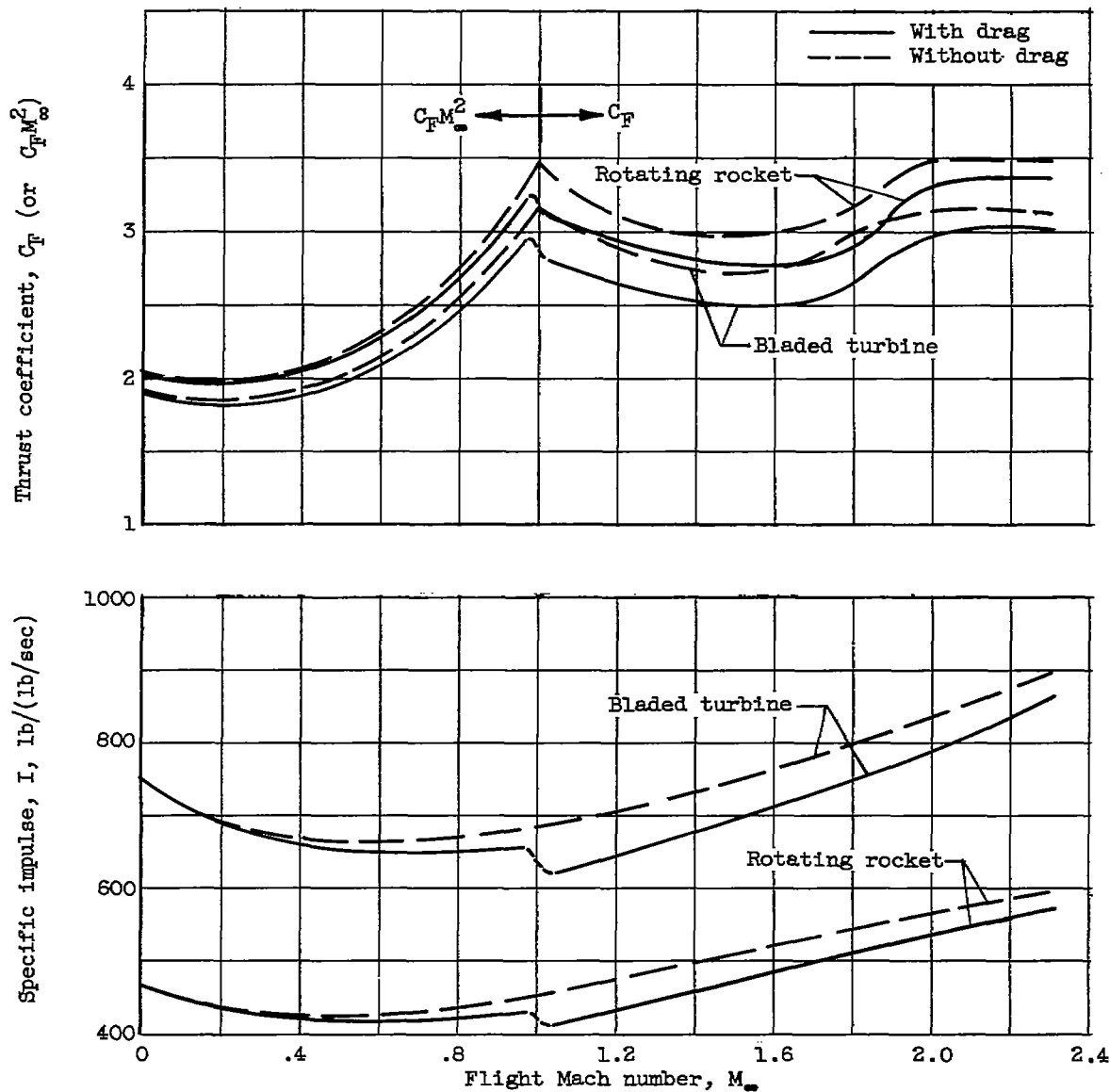


Figure 17. - Effect of turbine efficiency on full-power engine performance.
Design flight Mach number, 2.3.



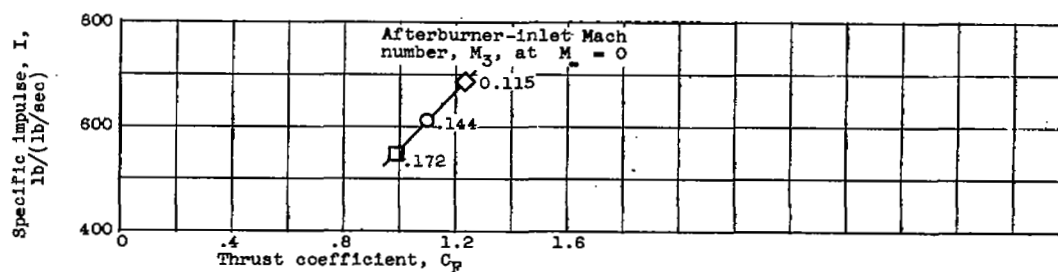
(a) Engine with one-stage compressor.

Figure 18. - Effect of turbine type on full-power engine performance.
Design flight Mach number, 2.3.

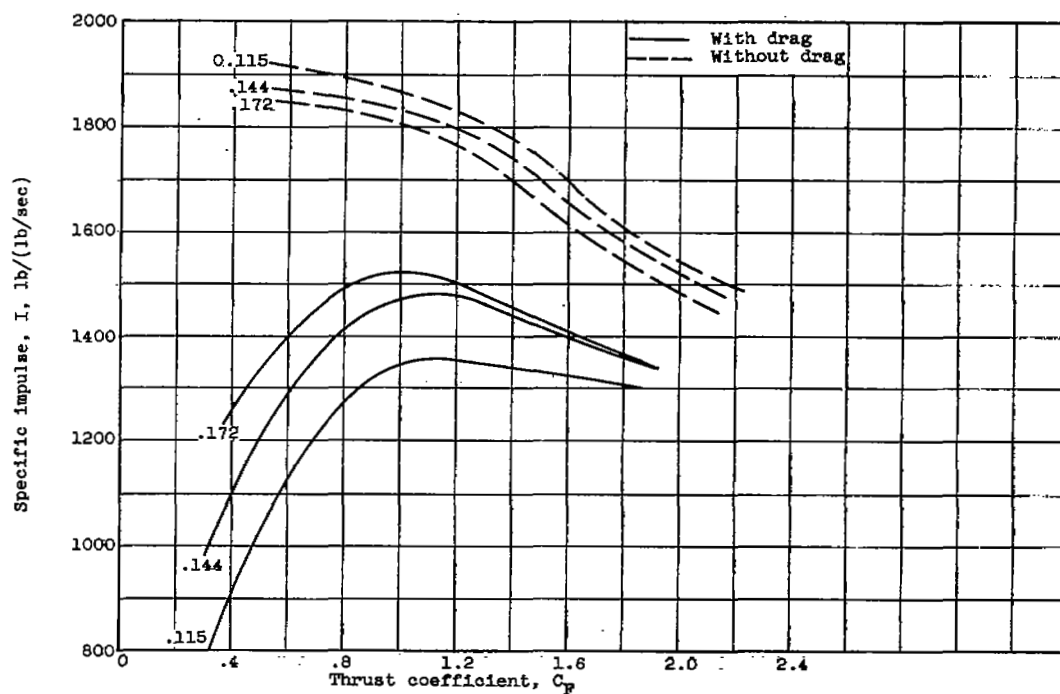


(b) Engine with two-stage compressor.

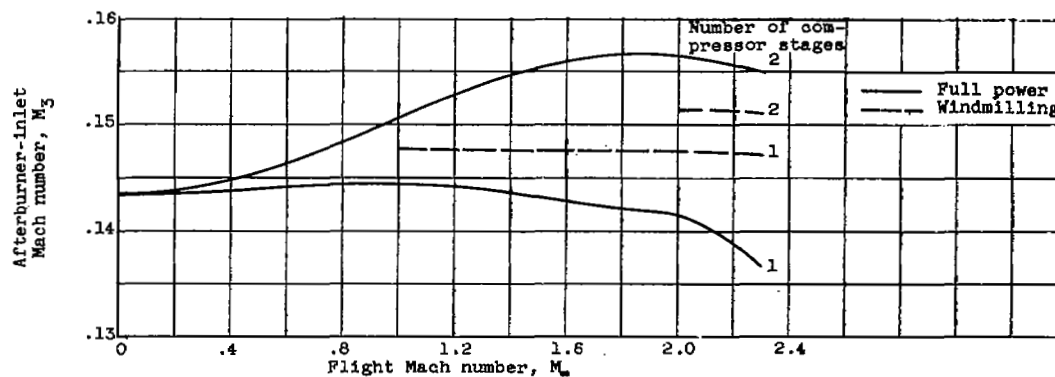
Figure 18. - Concluded. Effect of turbine type on full-power engine performance. Design flight Mach number, 2.3.



(a) Full-power operation at take-off.

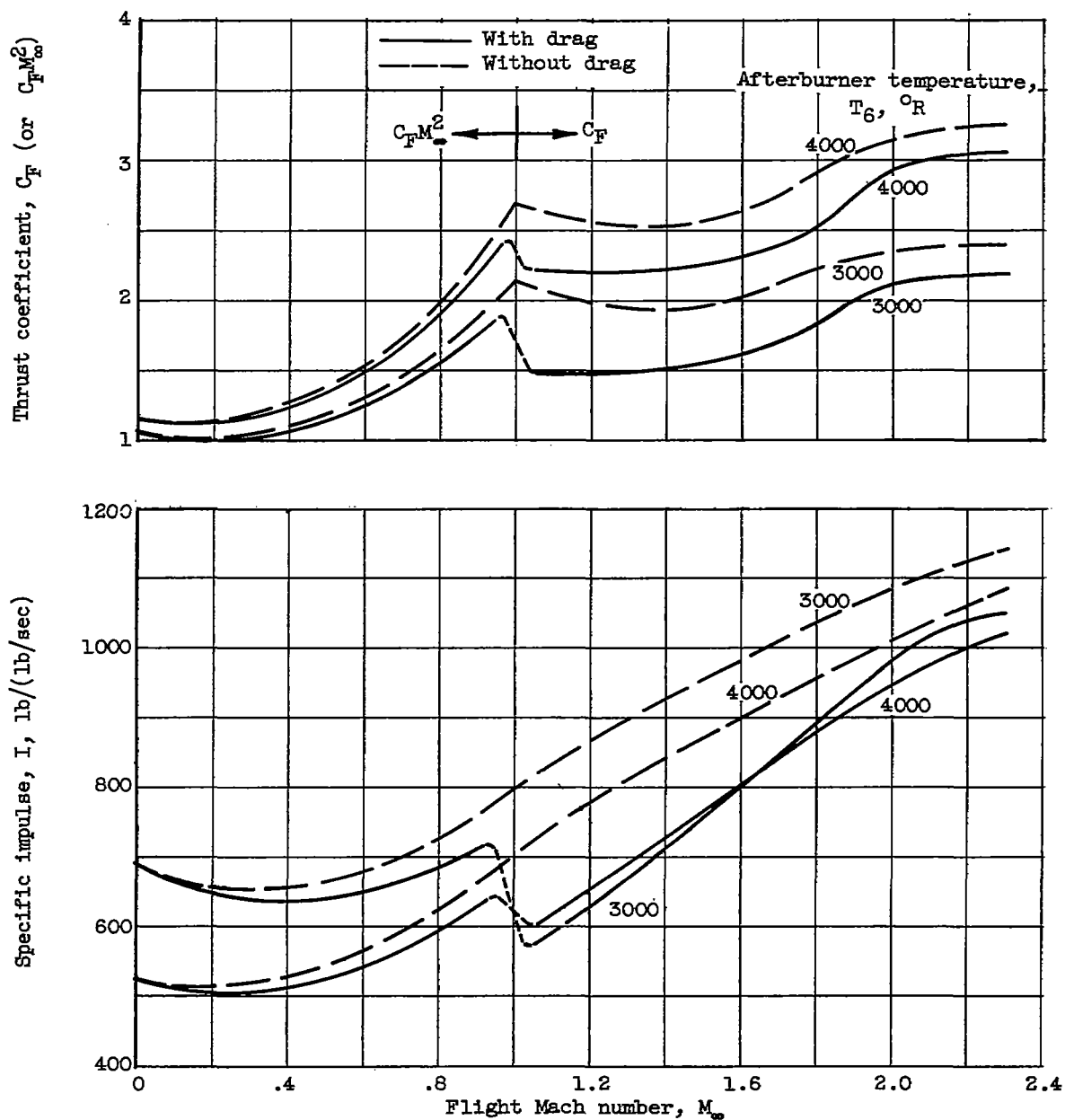


(b) Part-power operation at flight Mach number of 2.3.



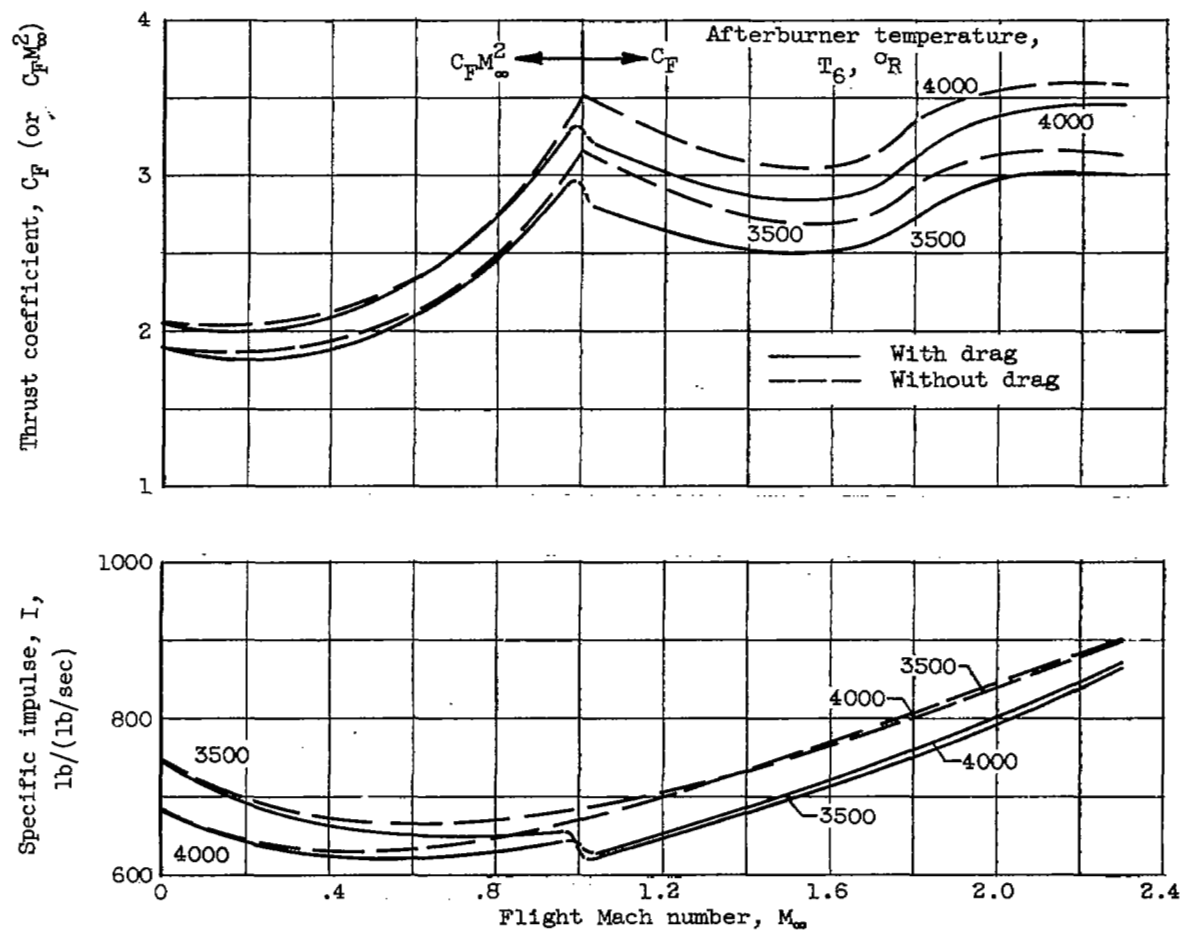
(c) Variation of inlet Mach number with flight Mach number.

Figure 19. - Effect of afterburner-inlet Mach number on engine performance. Design flight Mach number, 2.3.



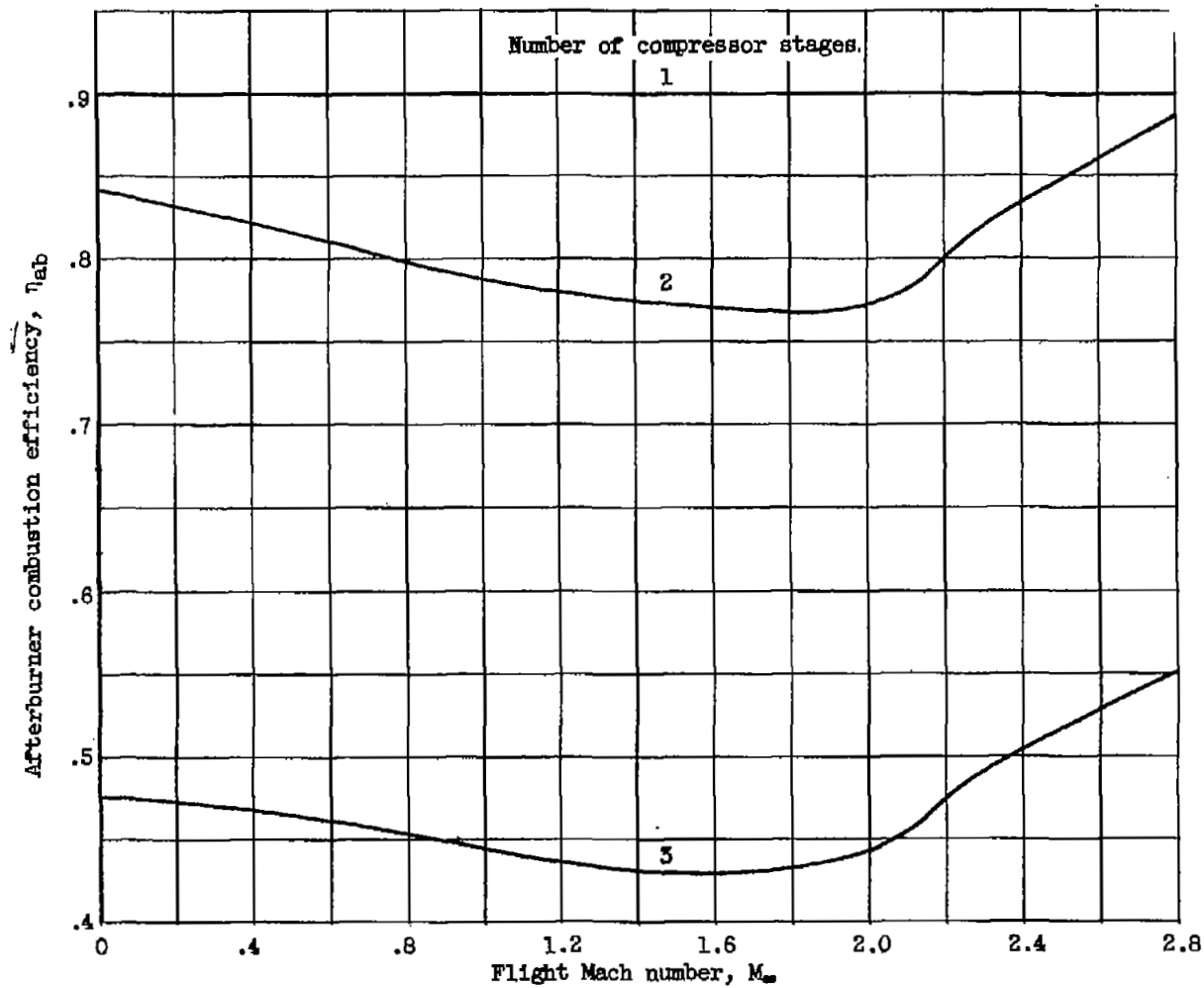
(a) Engine with one-stage compressor.

Figure 20. - Effect of afterburner temperature on full-power engine performance. Design flight Mach number, 2.3.



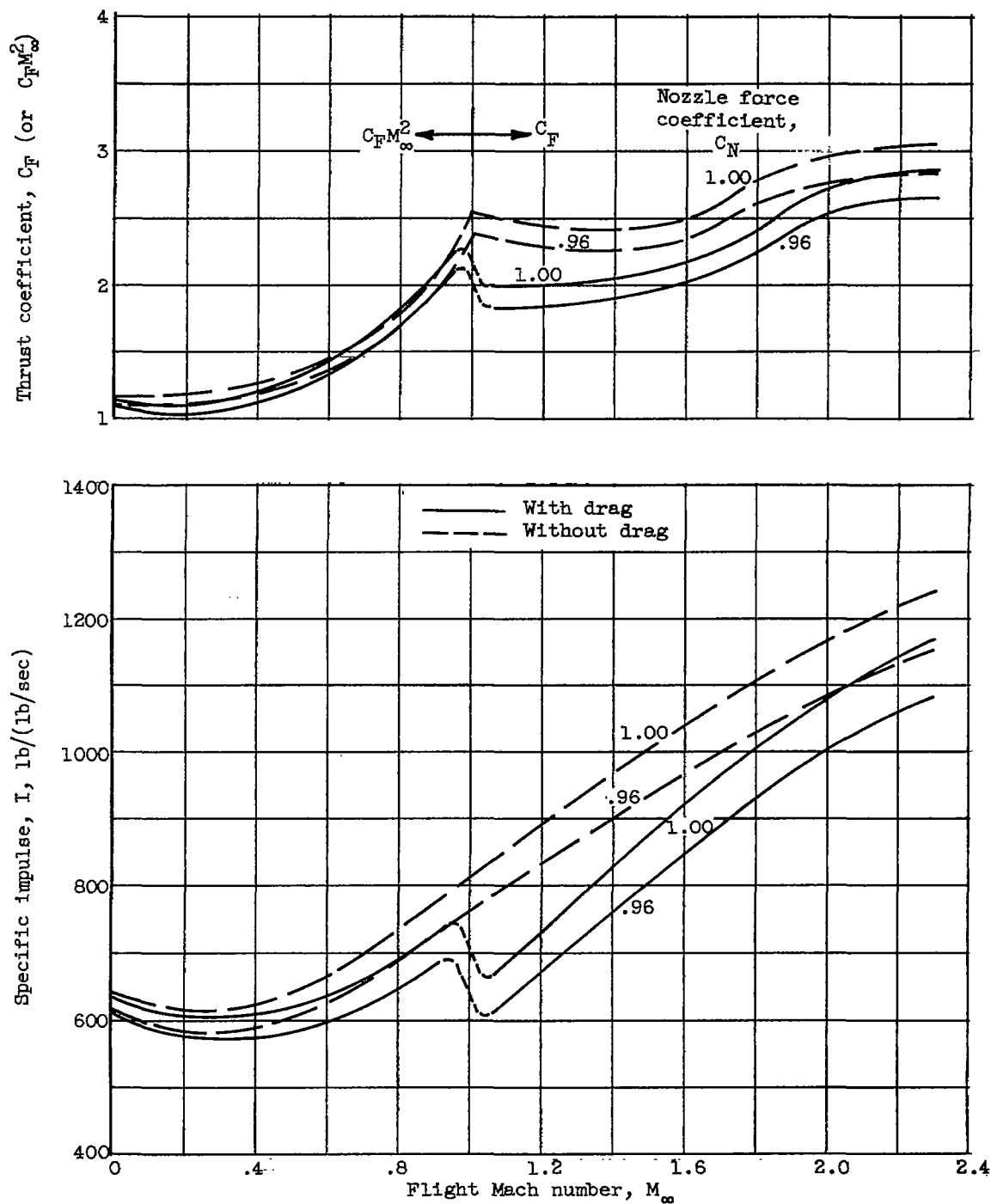
(b) Engine with two-stage compressor.

Figure 20. - Continued. Effect of afterburner temperature on full-power engine performance. Design flight Mach number, 2.3.



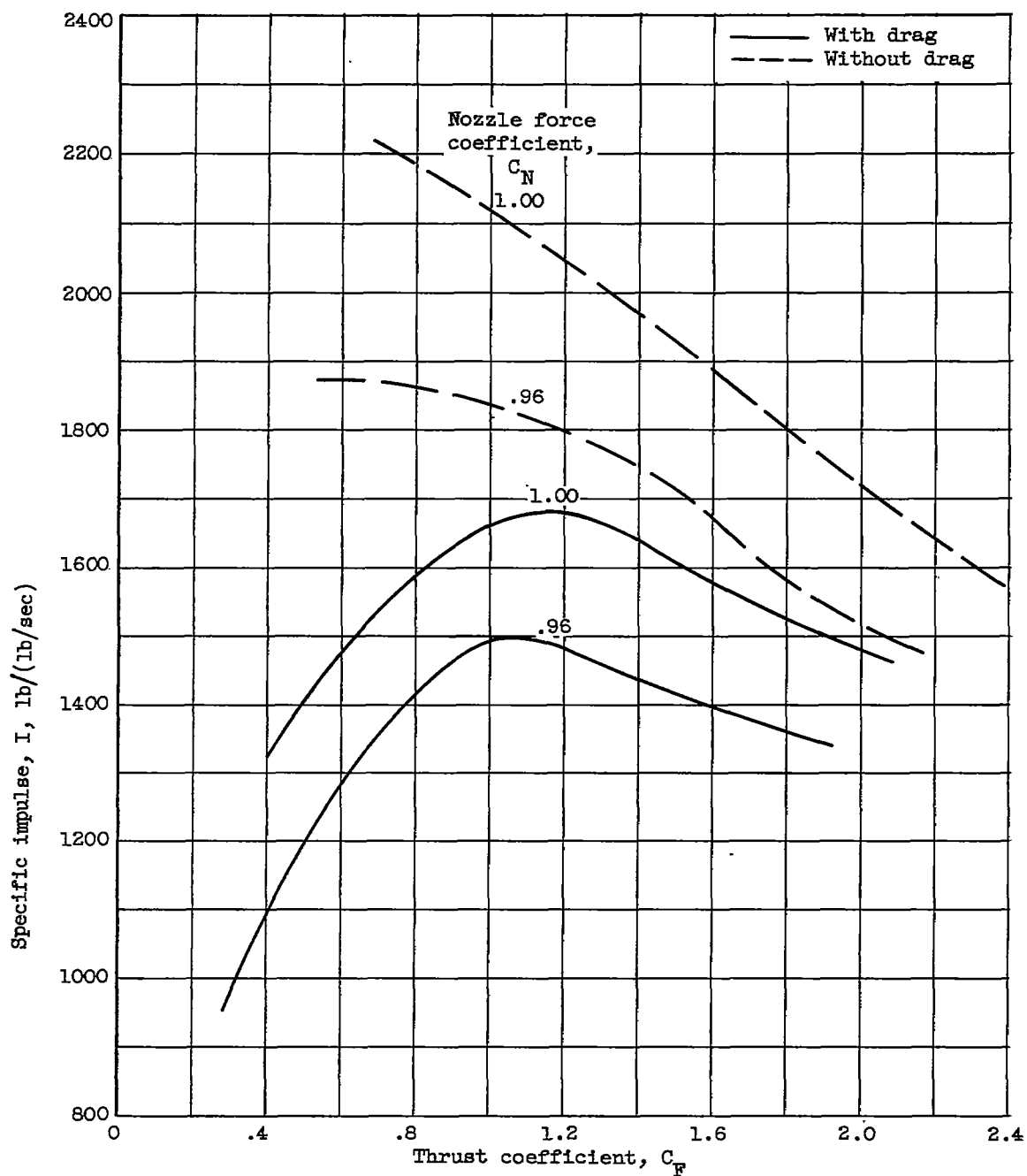
(c) Variation of effective combustion efficiency with flight Mach number. Afterburner temperature, 3500°R .

Figure 20. - Concluded. Effect of afterburner temperature on full-power engine performance. Design flight Mach number, 2.3.



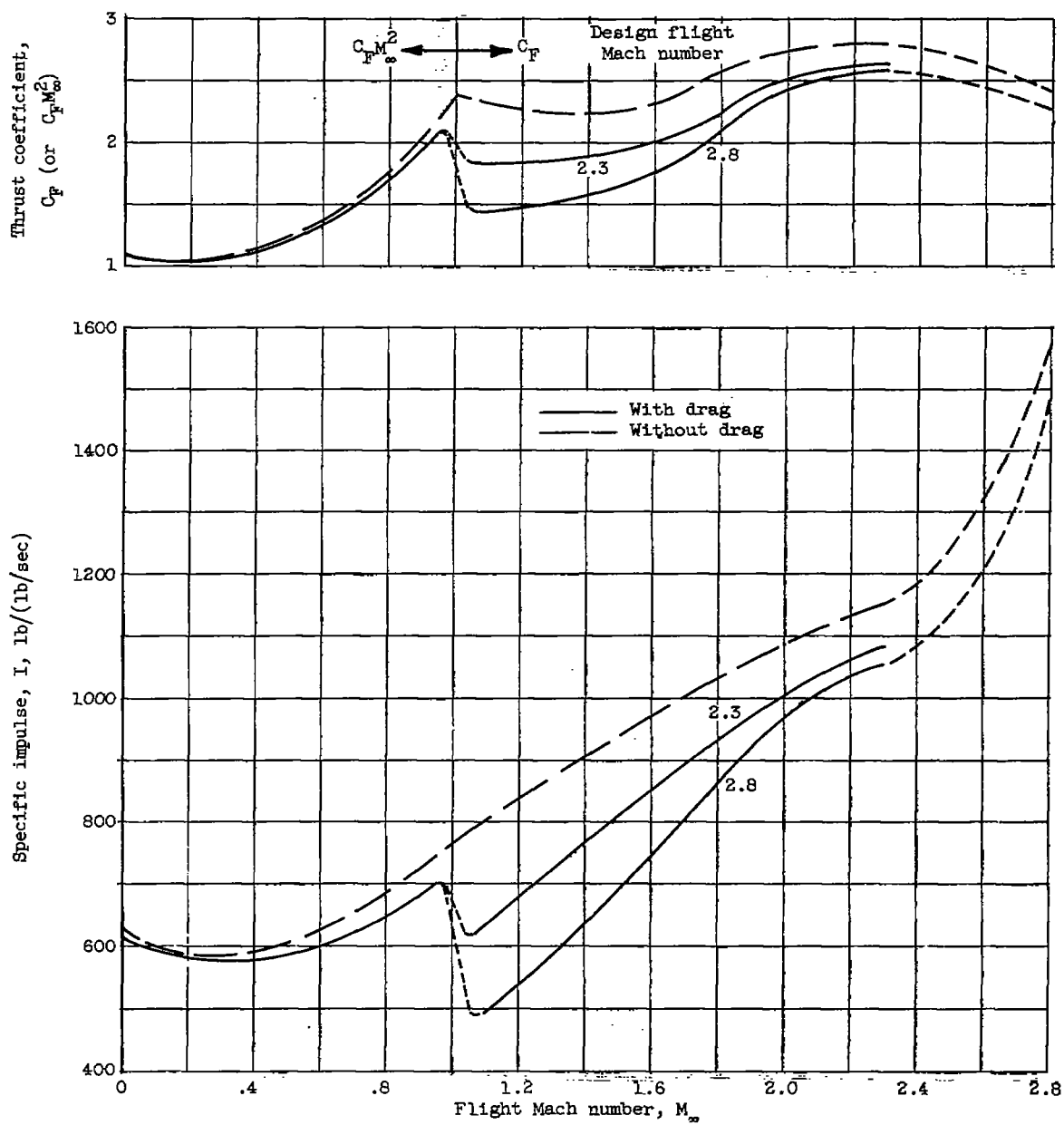
(a) Full-power operation.

Figure 21. - Effect of exhaust-nozzle force coefficient on engine performance. Design flight Mach number, 2.3.



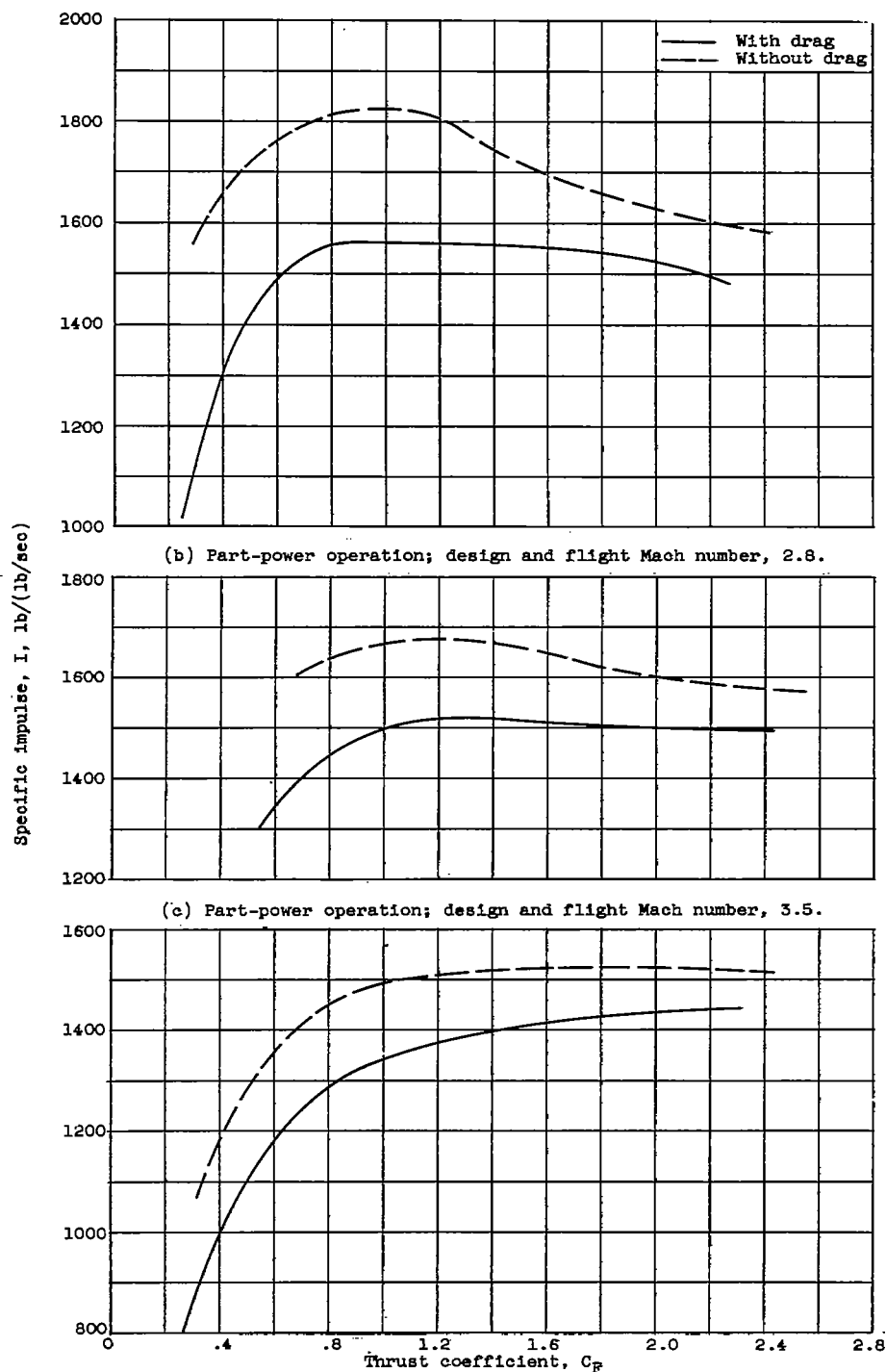
(b) Part-power operation; flight Mach number, 2.3.

Figure 21. - Concluded. Effect of exhaust-nozzle force coefficient on engine performance. Design flight Mach number, 2.3.



(a) Full-power operation.

Figure 22. - Effect of design flight Mach number on engine performance.

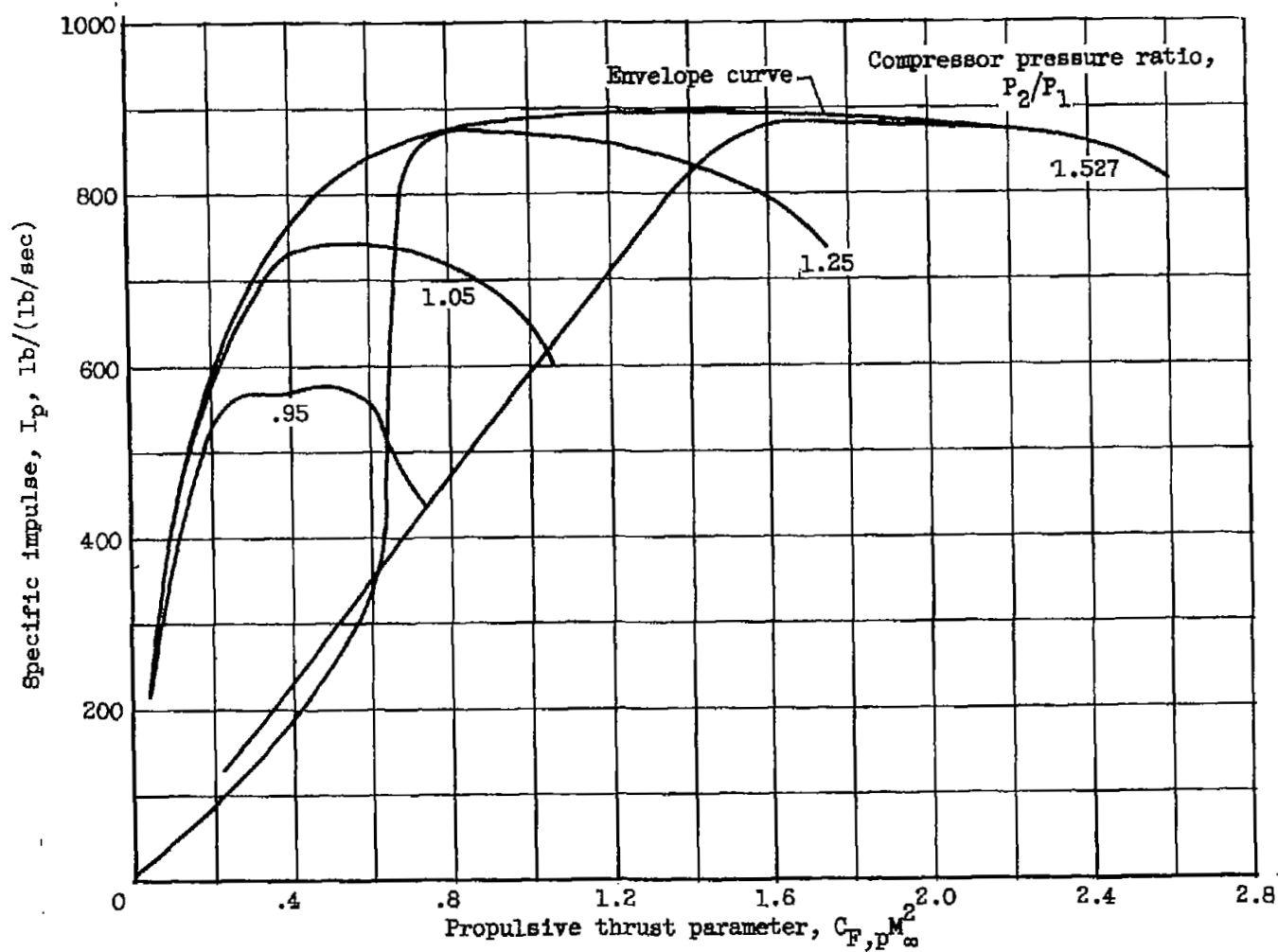


(b) Part-power operation; design and flight Mach number, 2.8.

(c) Part-power operation; design and flight Mach number, 3.5.

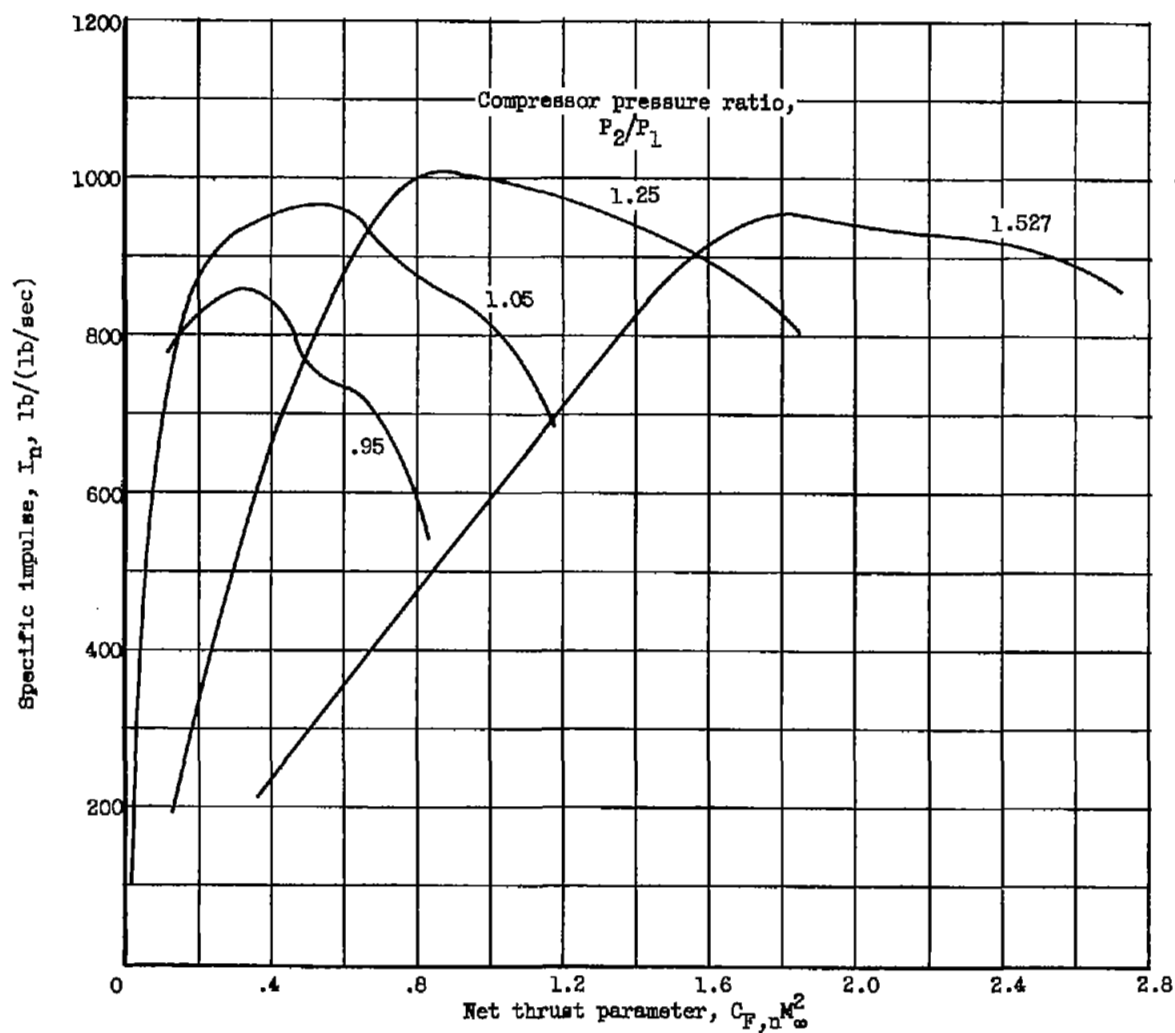
(d) Part-power operation; design and flight Mach number, 4.0.

Figure 22. - Concluded. Effect of design flight Mach number on engine performance.



(a) With drag.

Figure 23. - Effect of operating compressor pressure ratio on engine performance. Design flight Mach number, 2.3; flight Mach number, 0.9; altitude, 35,332 feet.



(b) Without drag.

Figure 23. - Concluded. Effect of operating compressor pressure ratio on engine performance. Design flight Mach number, 2.3; flight Mach number, 0.9; altitude, 35,332 feet.

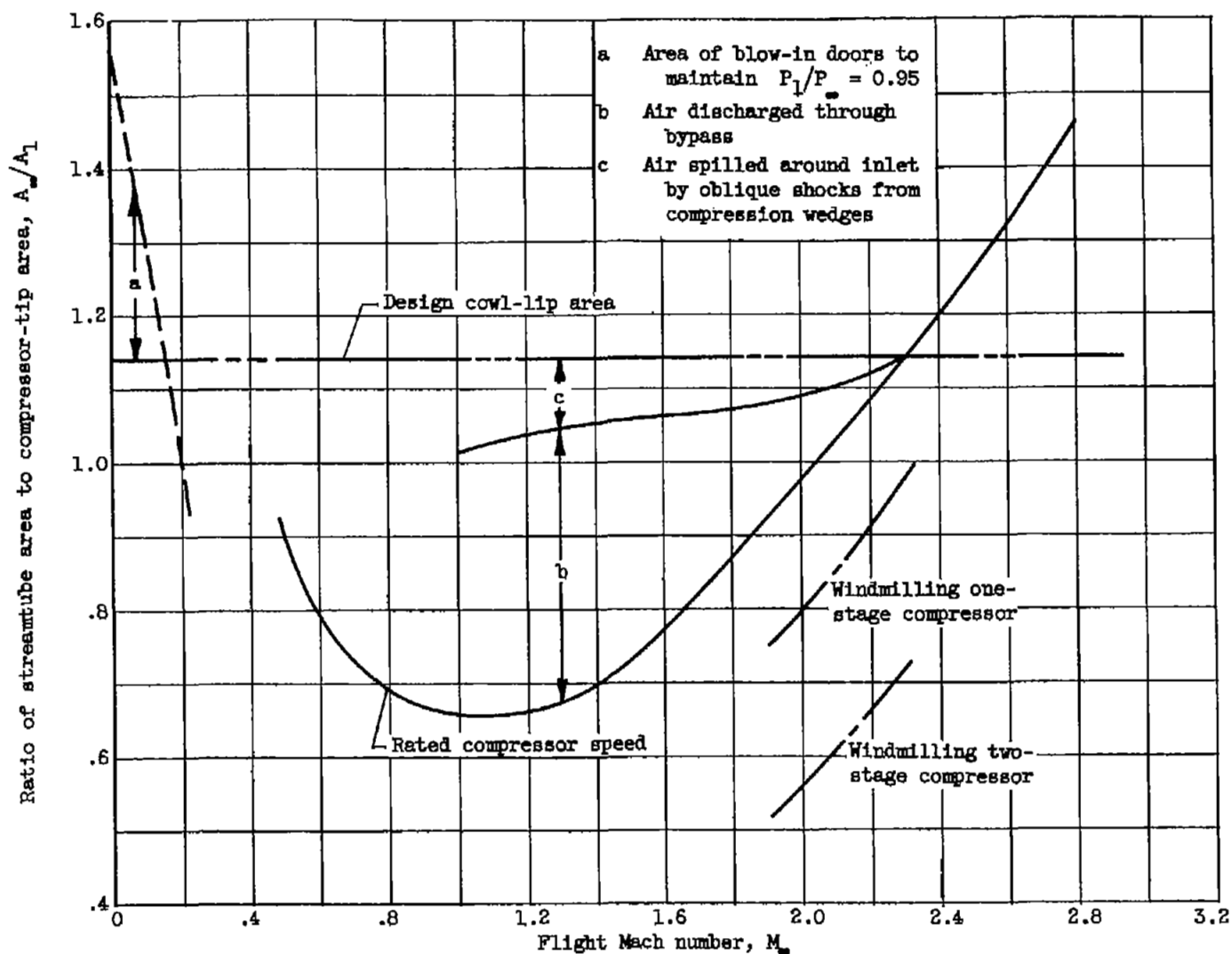


Figure 24. - Geometry variations for inlet diffuser. Design flight Mach number, 2.3.

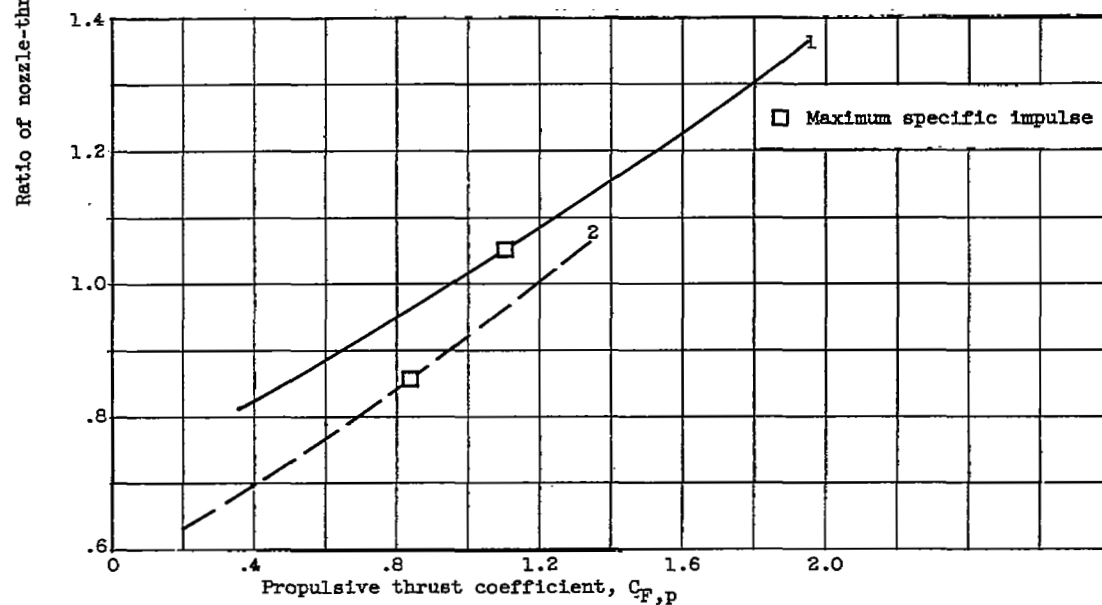
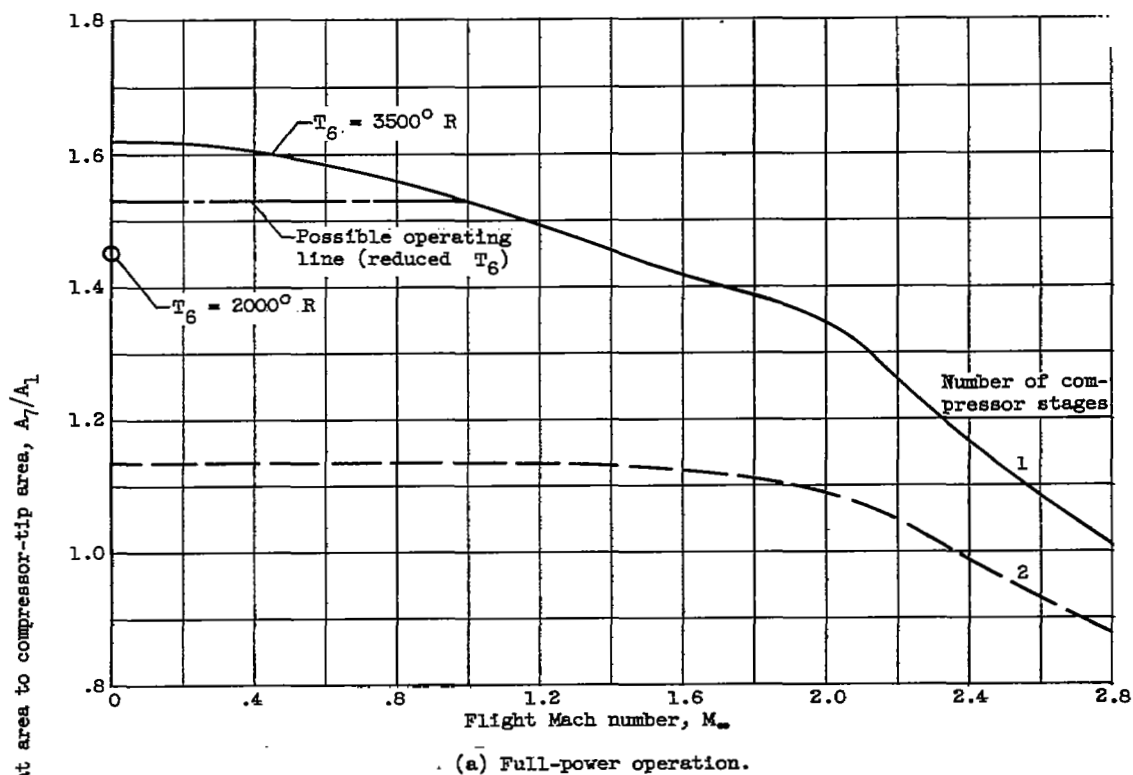


Figure 25. - Geometry variations for exhaust-nozzle throat. Design flight Mach number, 2.3.

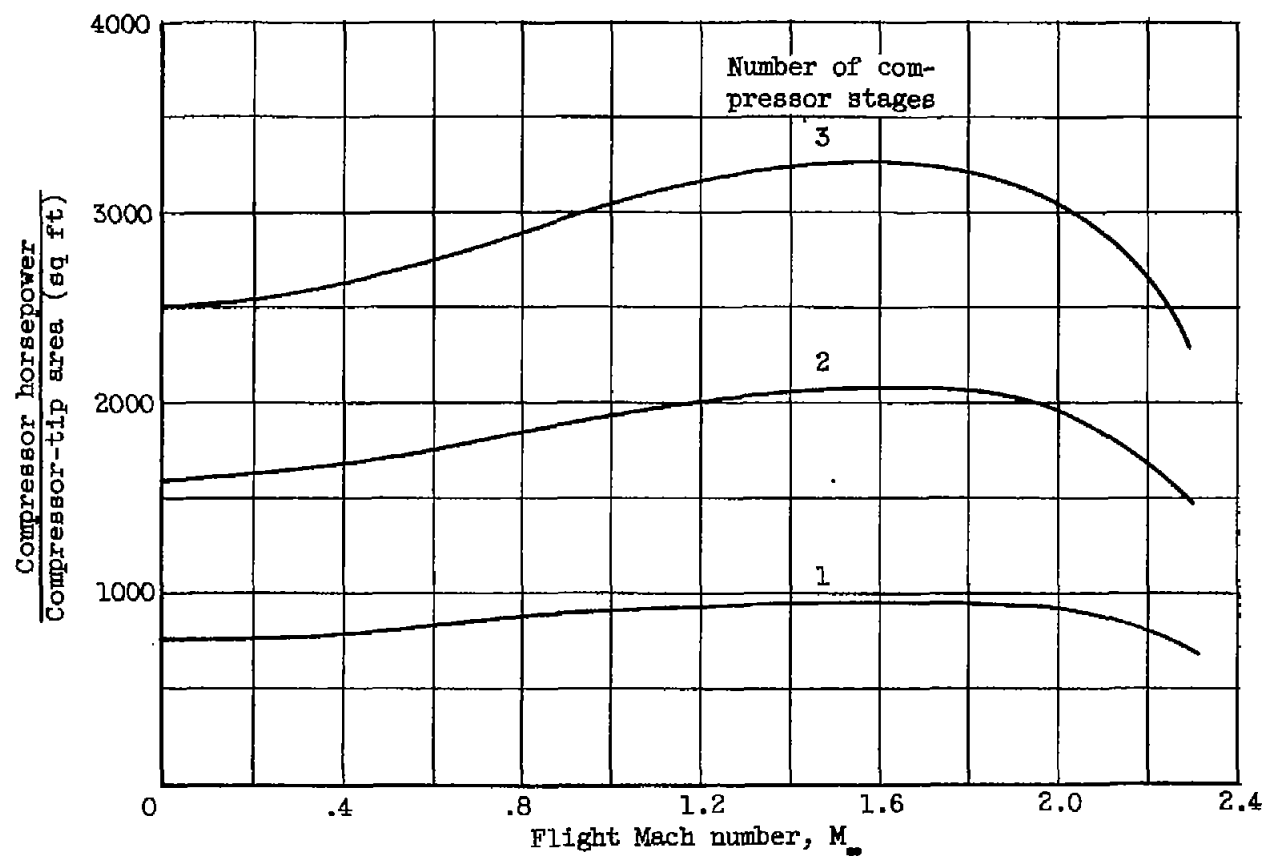


Figure 26. - Effect of flight Mach number and number of compressor stages on compressor power. Altitude scheduled with Mach number (fig. 7).

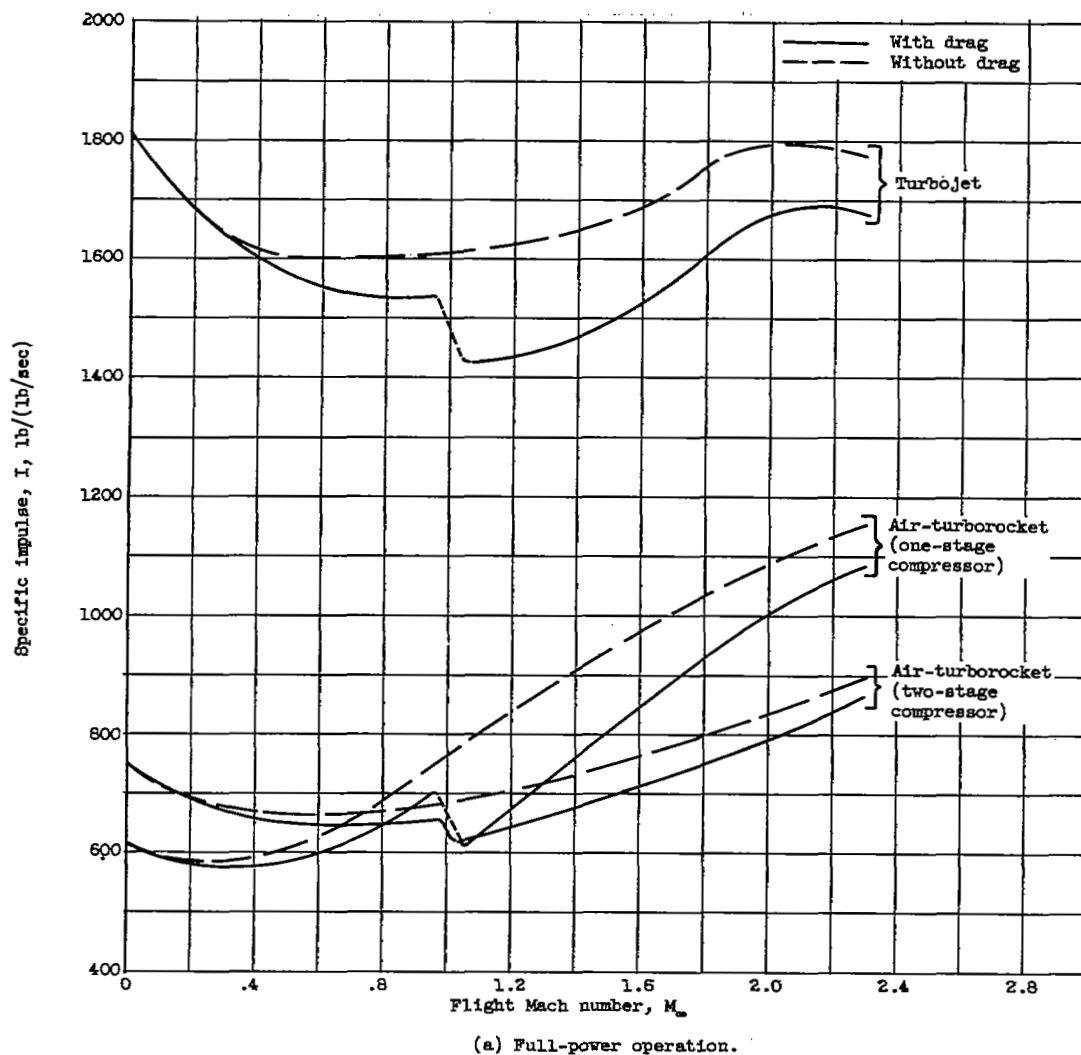
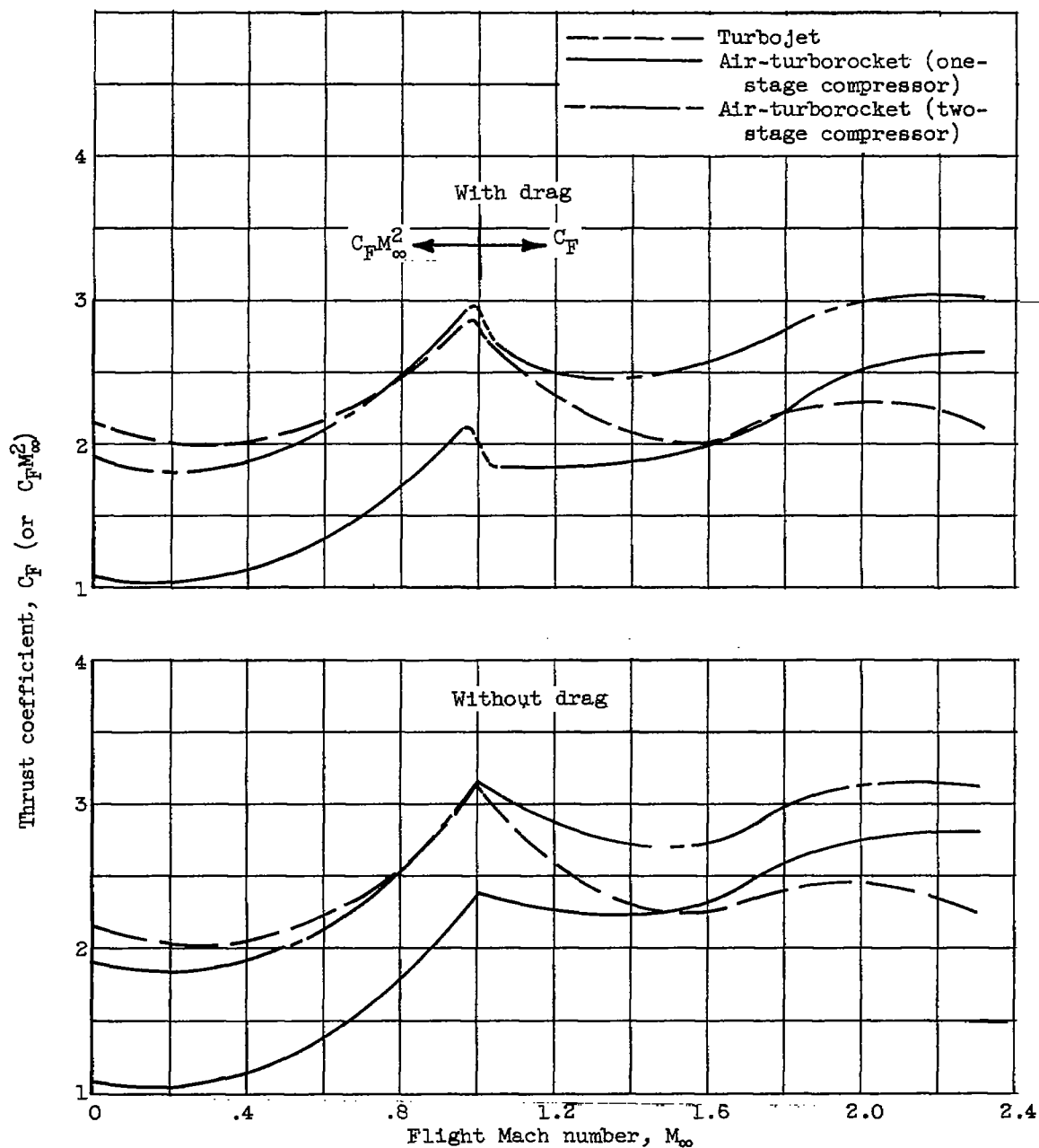
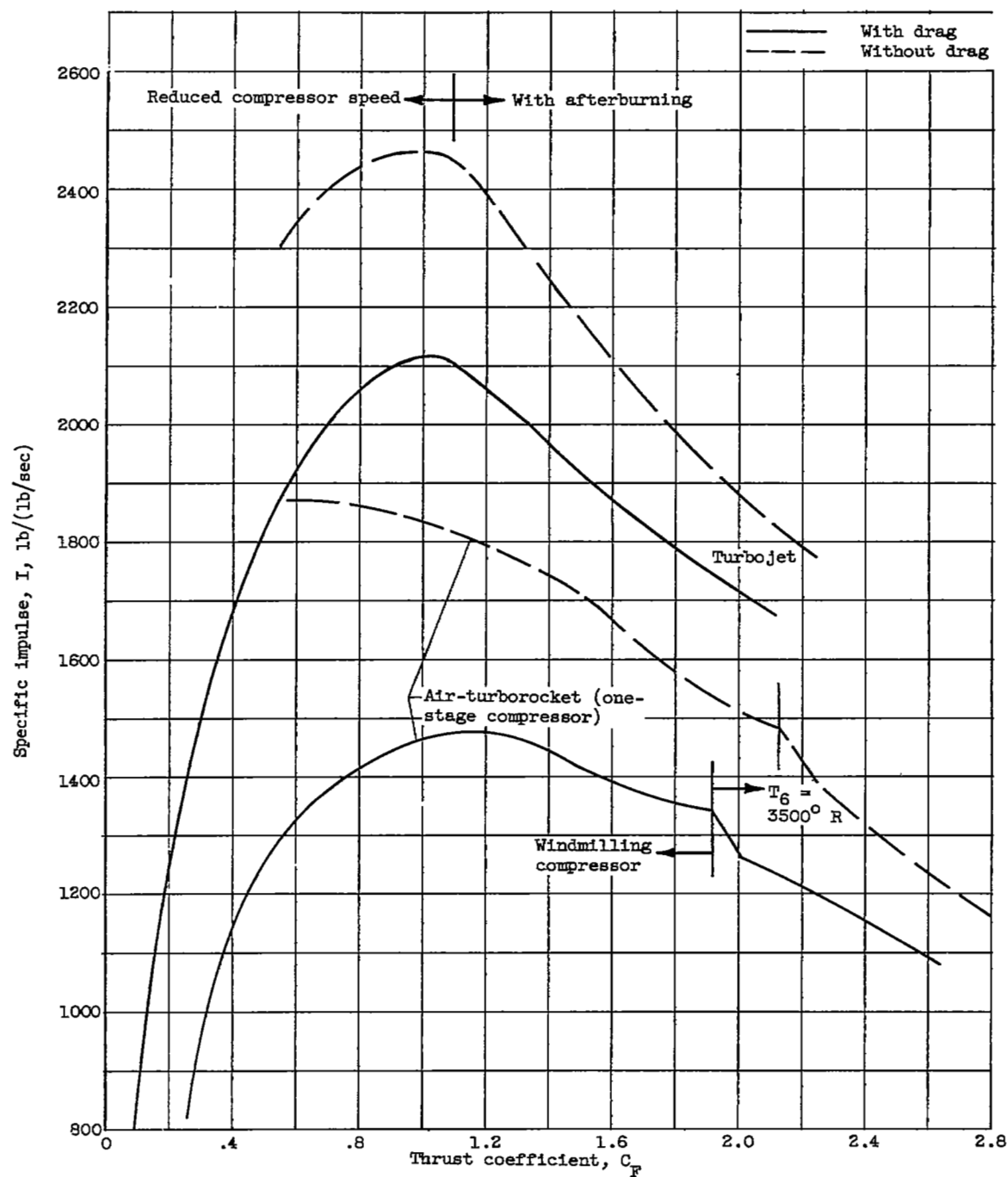


Figure 27. - Comparison of air-turborocket and turbojet-engine performance. Design flight Mach number, 2.3.



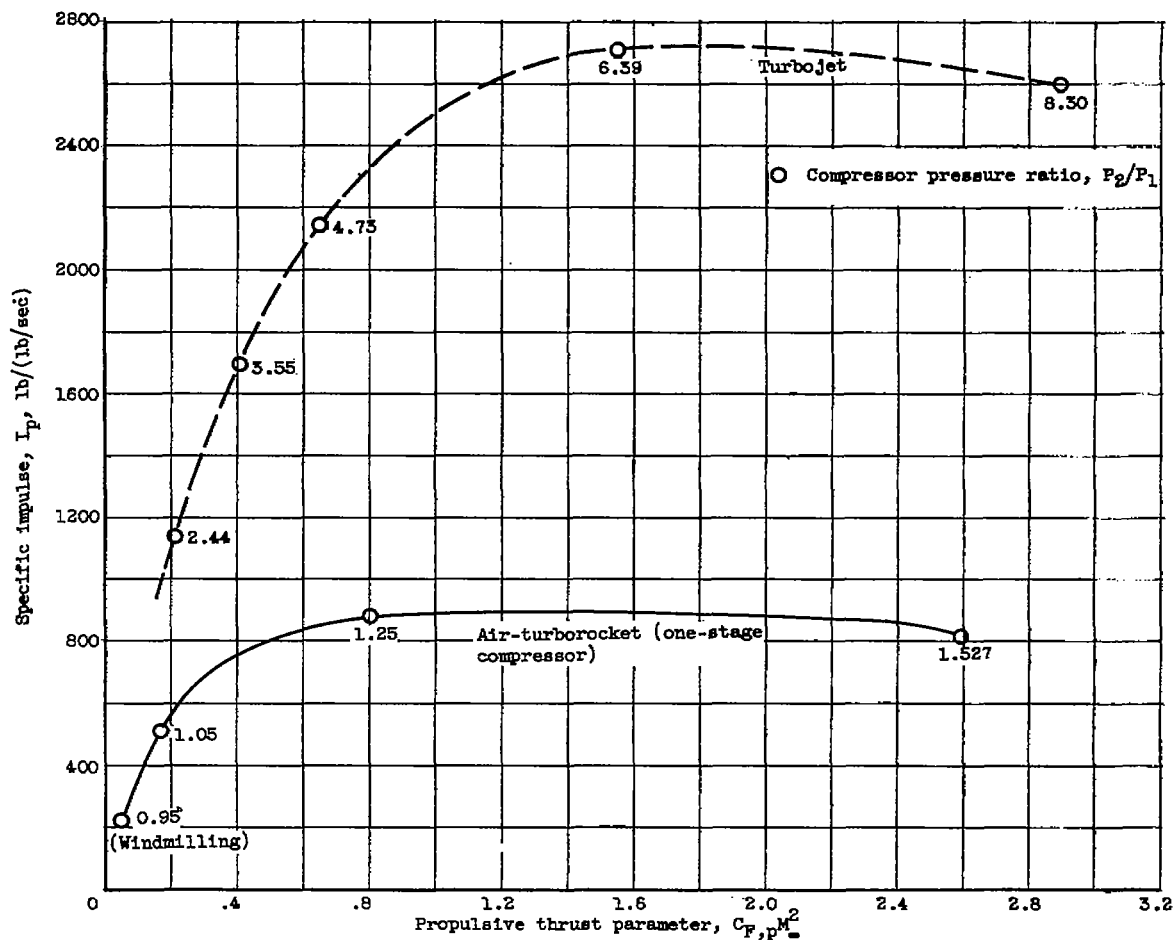
(a) Concluded. Full-power operation.

Figure 27. - Continued. Comparison of air-turborocket and turbojet-engine performance. Design flight Mach number, 2.3.



(b) Part-power operation; flight Mach number, 2.3; altitude, 46,000 feet.

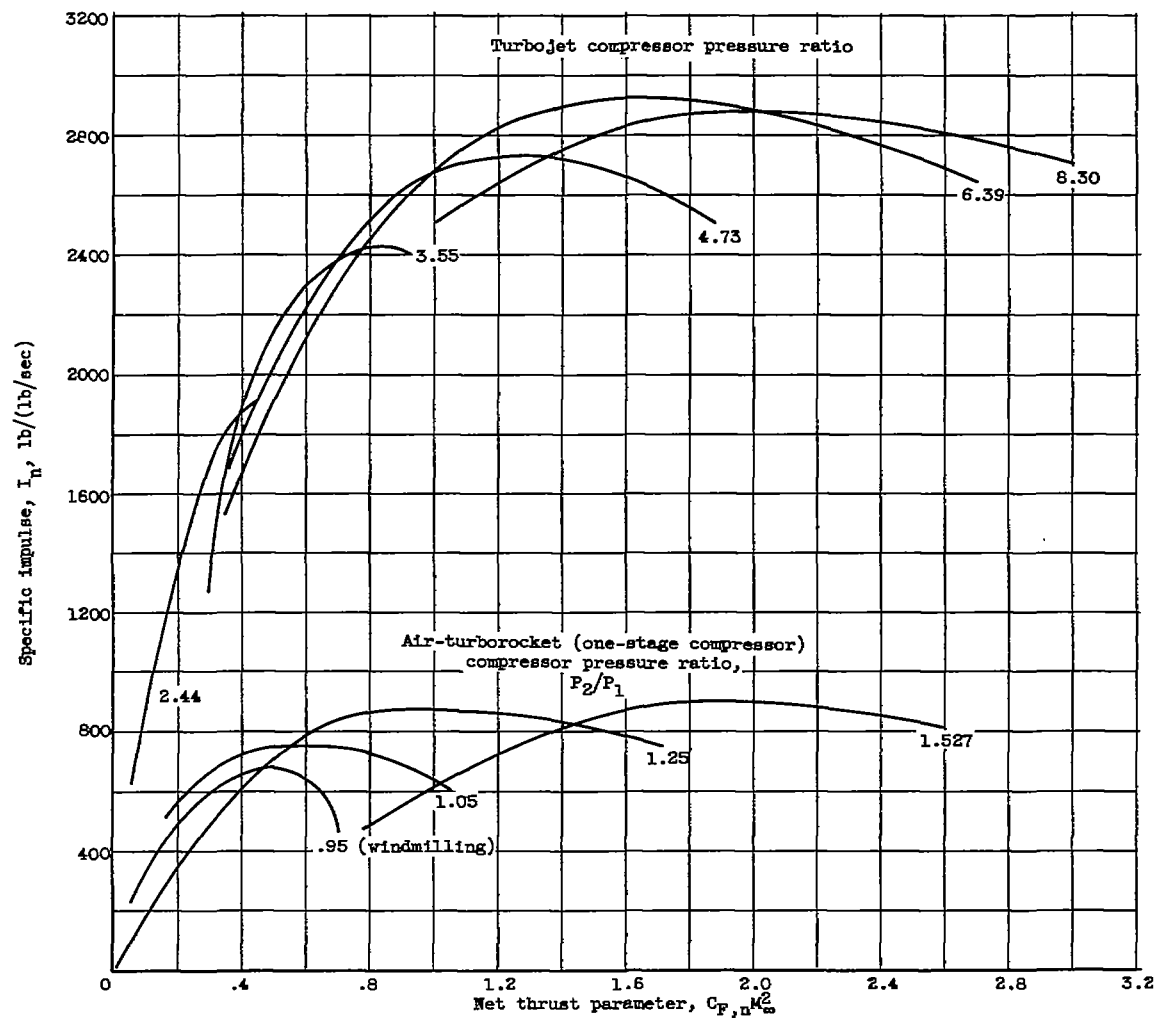
Figure 27. - Continued. Comparison of air-turborocket and turbojet-engine performance. Design flight Mach number, 2.3.



(1) With drag.

(c) Part-power operation; flight Mach number, 0.9; altitude, 35,332 feet.

Figure 27. - Continued. Comparison of air-turborocket and turbojet-engine performance. Design flight Mach number, 2.3.



(2) Without drag.

(c) Concluded. Part-power operation; flight Mach number, 0.9; altitude, 35,332 feet.

Figure 27. - Concluded. Comparison of air-turborocket and turbojet-engine performance. Design flight Mach number, 2.3.

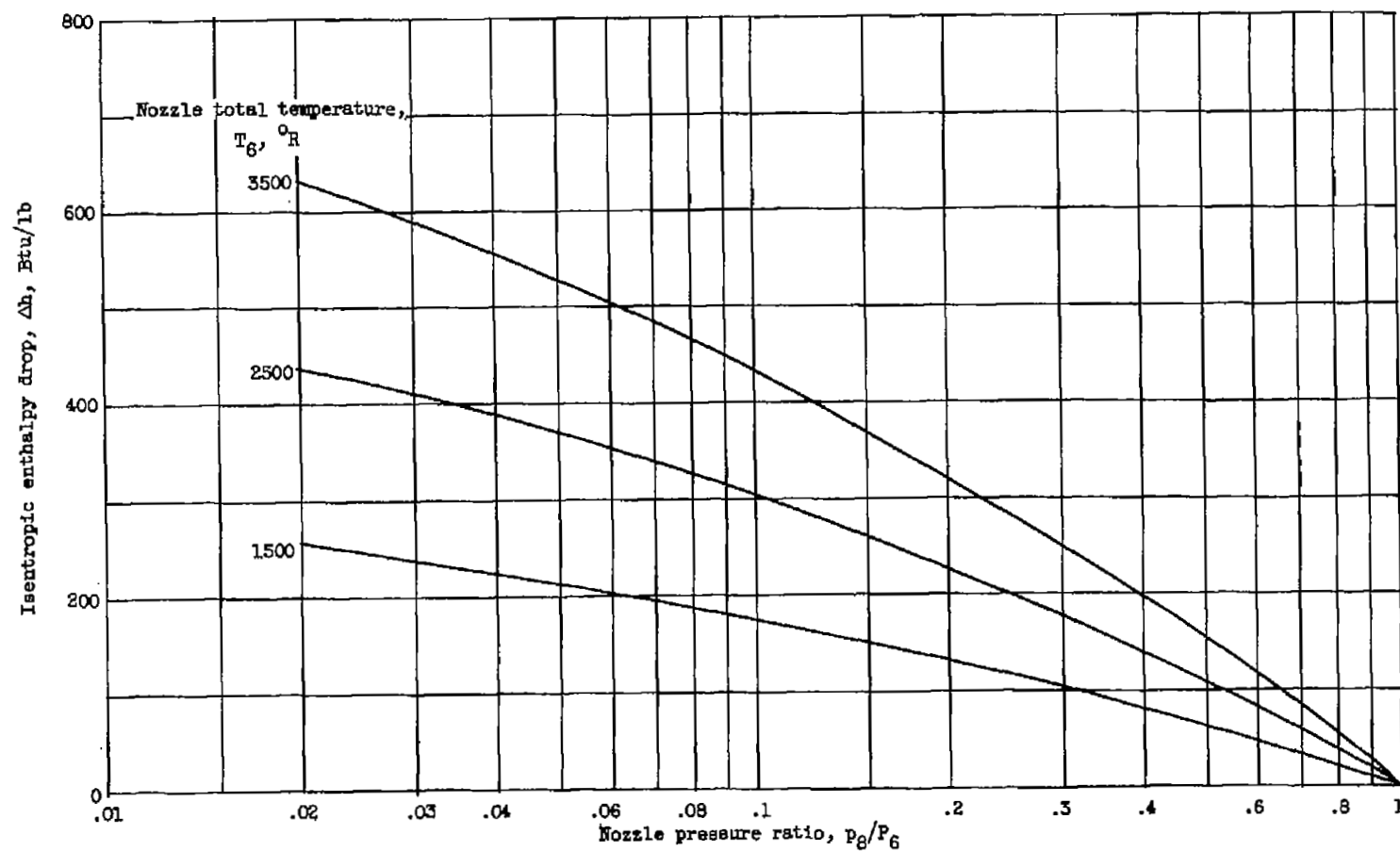


Figure 28. - Isentropic enthalpy drop of gases through exhaust nozzle.

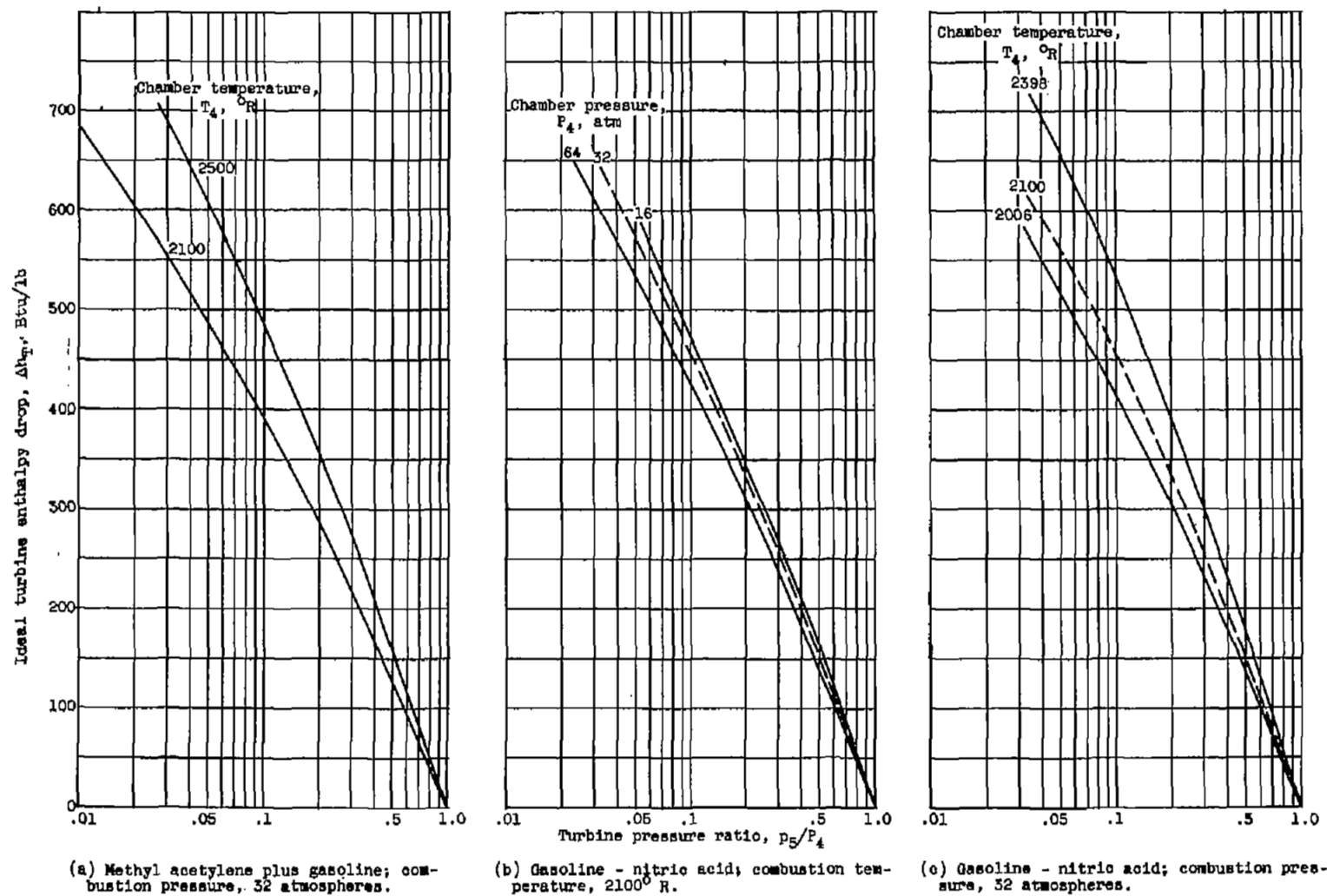


Figure 29. - Isentropic enthalpy drop of rocket gases through turbine.

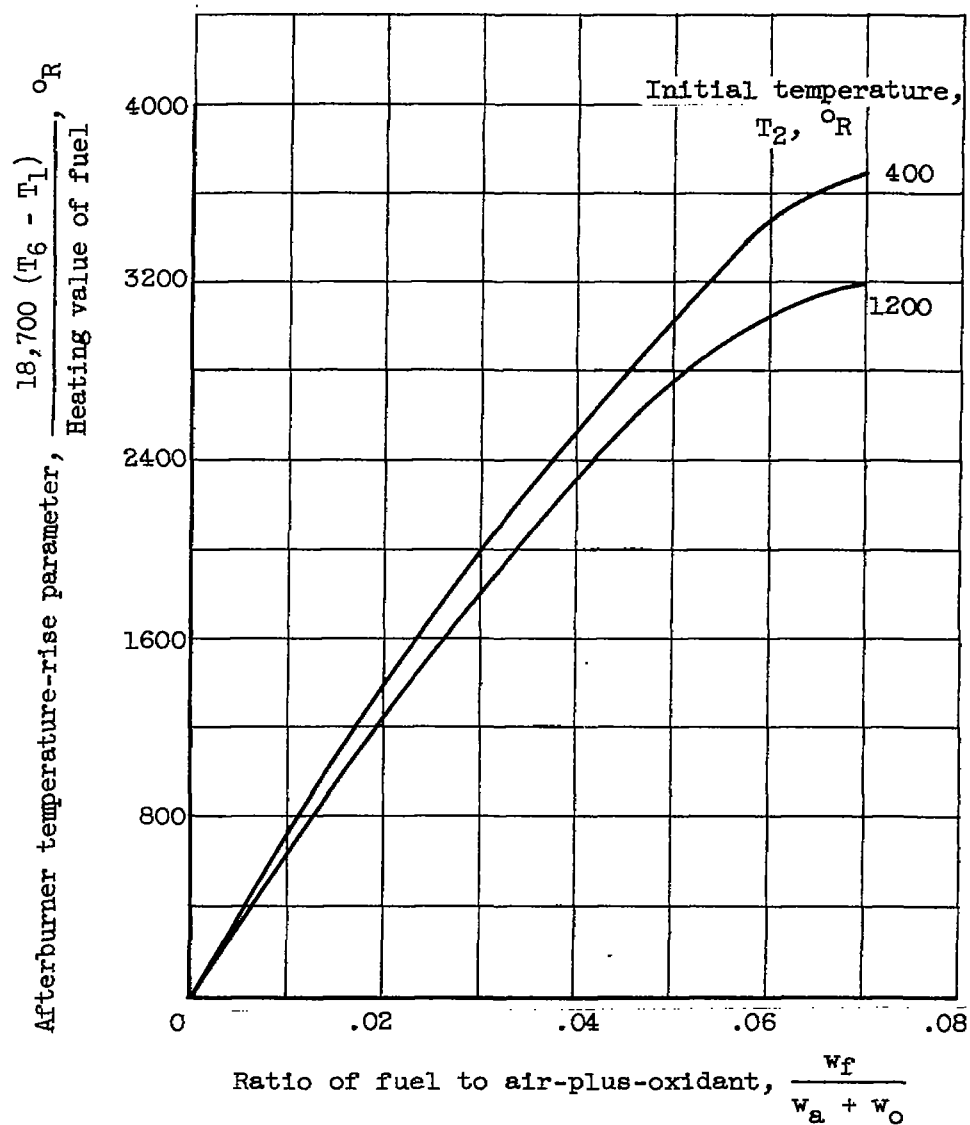
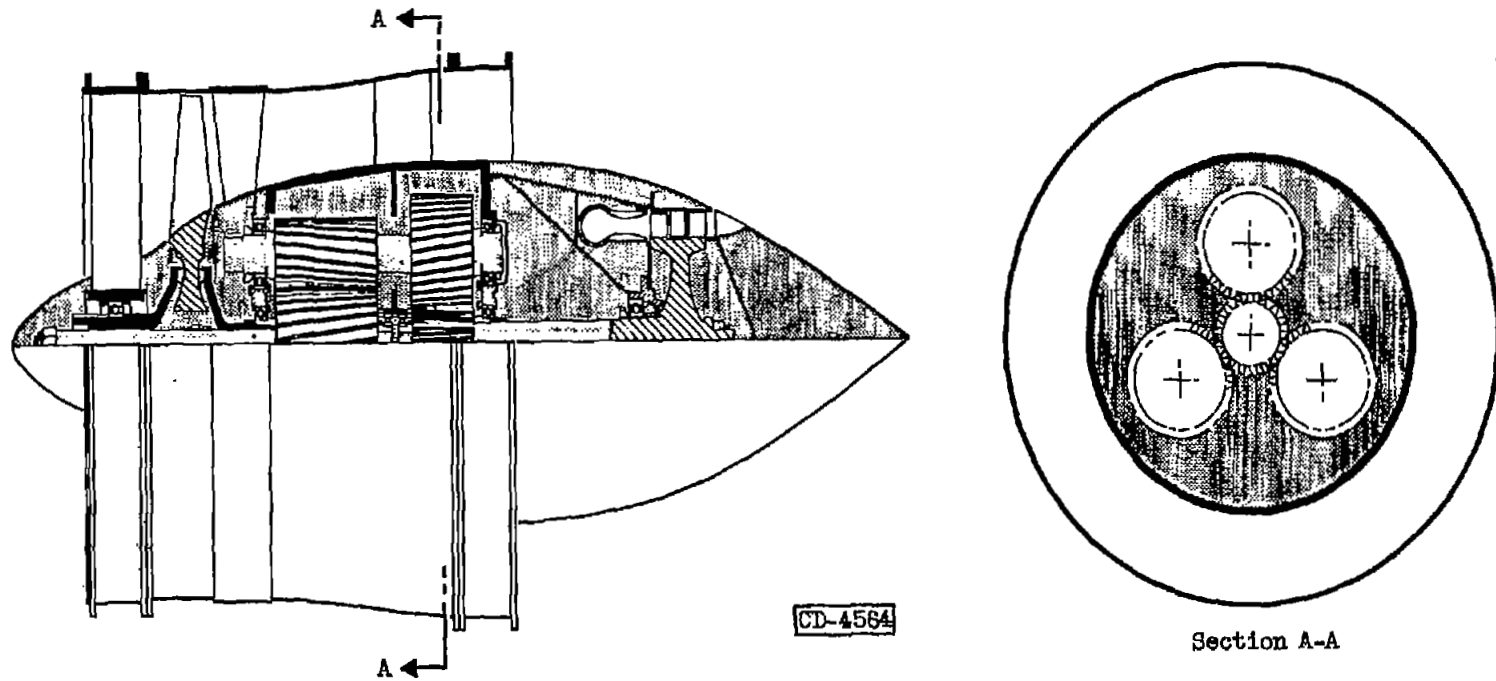
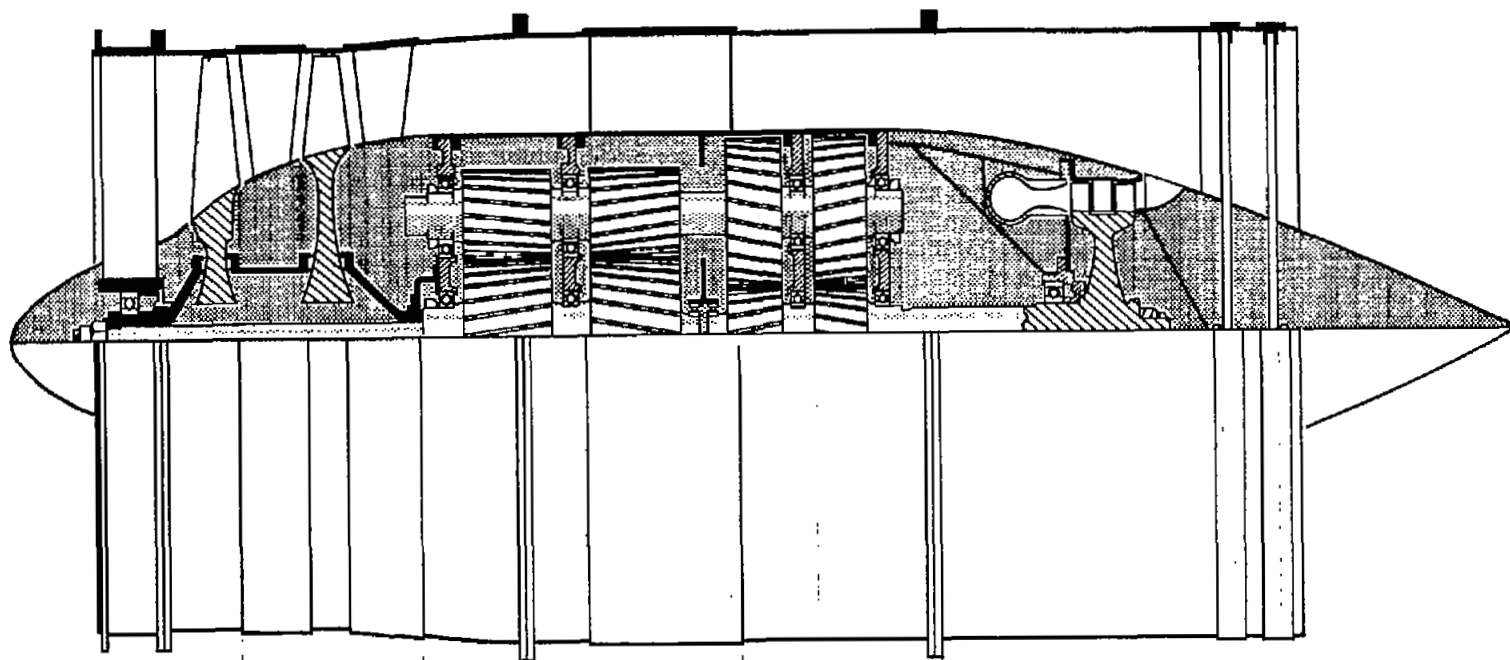


Figure 30. - Relation between afterburner temperature rise and ratio of fuel to air-plus-oxidant.



(a) Bladed turbine, one-stage compressor.

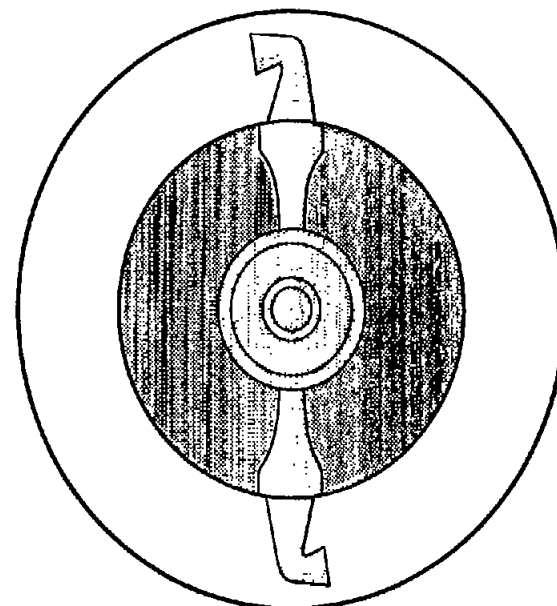
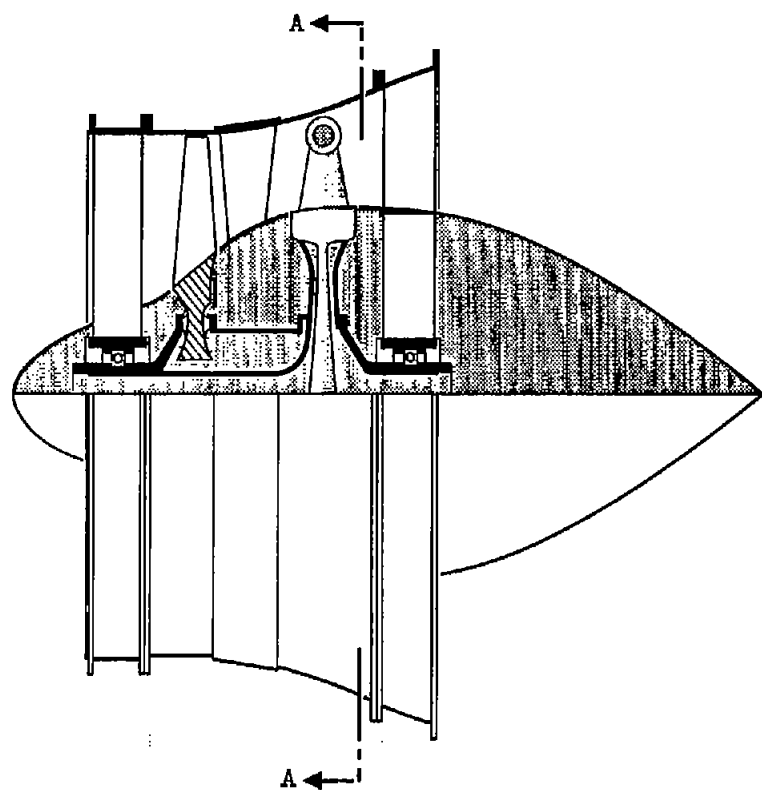
Figure 31. - Scale drawing of compressor-turbine section.



CD-4563

(b) Bladed turbine, two-stage compressor.

Figure 31. - Continued. Scale drawing of compressor-turbine section.



Section A-A

CD-4565

(c) Rotating-rocket turbine, one-stage compressor.

Figure 31. - Concluded. Scale drawing of compressor-turbine section.